

Complexation of Metal Salts with Phosphorus-Containing Poly(Arylene Ether)s

by

Elena Bonaplata Revilla

Thesis Submitted to the Faculty of the

Virginia Polytechnic Institute and State University

in partial fulfillment of the requirements for the degree of

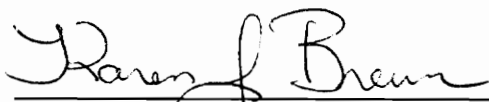
Master of Science

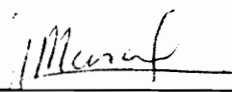
in

Chemistry (Polymer Chemistry)

APPROVED:


Dr. J. E. McGrath, Chairman


Dr. K. Brewer


Dr. H. Marand

May , 1994

Blacksburg, Virginia

LD
5655
V855
1994
R485
C.2

Complexation of Metal Salts with Phosphorus-Containing Poly(Arylene Ether)s

by

Elena Bonaplata Revilla

Committee Chairman: J. E. McGrath

Chemistry

Abstract

Poly(arylene ether phosphine oxide)s (PEPO) are a recently identified subset of an important macromolecular series which includes industrially important high performance thermoplastics, such as the polysulfones, e.g. UDEL® and polyether ketones, e.g. PEEK®, PEKK®, etc. The PEPO materials show an elevated glass transition temperature, high thermal and oxidative stability, improved solubility, and increased flame resistance. It has been demonstrated that a variety of metal salts including metals such as iron, zinc, cobalt, and copper, can be complexed at a molecular level with the phosphoryl group in films of these polymers producing novel transparent metal/polymer "composites". A procedure for obtaining homogeneous films from solutions of the metal halide complexed polymers has been developed. FTIR experiments as well as T₁ phosphorus (³¹P) NMR measurements were conducted to demonstrate the existence of metal complexation in the solid state. The effect of the chemical composition of the chain, type of metal salt, molar concentration of the metal salt, and heating cycle were investigated and found to influence properties of the films such as solubility, glass transition temperature, thermal stability, and storage modulus.

Additionally, linear poly(arylene ether phosphine oxide)s were reduced to different extents to the corresponding phosphine containing polymers. Properties such as intrinsic

One of these phosphine polymers was subsequently used in the generation of a rhodium catalyst for the hydroformylation of octene-1. The utilization of polymer-supported catalysts has important advantages such as catalyst recovery and the ease of separation of the product. The catalyst activity of the polymeric rhodium complex was studied as a function of reaction time as well as ligand to rhodium ratio. For a phosphorus/rhodium ratio of two these heterogeneous catalysts suffer in terms of reaction rate in relation to their homogeneous counterparts. However, at phosphorus/rhodium ratios of approximately eight the reaction is almost quantitative after three hours, and the selectivity is greatly improved over that of monomeric homogeneous catalysts for the same P/Rh ratio.

Acknowledgements

I take this opportunity to express my gratitude to my mentor, Professor James E. McGrath, for his support and encouragement throughout my graduate studies at Virginia Tech. My experience working with him has been greatly gratifying both intellectually and personally. I am also highly indebted to my committee members Prof. K. Brewer and Prof. H. Marand for their knowledge and advice. Special gratitude is due to Dr. A. R. Shultz for his guidance and assistance. I owe so much to the collaborative efforts of Dr. B. E. Hanson and his student Hao Ding for their help with the catalysis work, and Dr. H. Dorn for his help with the EPR and T_1 measurements. I would also like to acknowledge the invaluable assistance of Tom Glass (NMR), Steve McCartney (microscopy), Dave Gallo (intrinsic viscosity), Dr. Saikat Joardar (dynamic mechanical analysis).

I express my sincere thanks to my fellow graduate students, in and out of my research group, for their advice and comradery. I would like to acknowledge Sai Kumar Jayaraman, Gerry Meyer, Sue Mechum, Greg Lyle, Duane Priddy, Jr., Yong Joon Lee, and Venkat Sekharipuram for their help and suggestions. I would particularly like to thank Dr. Satya Srinivasan and Priya Lakshmanan not only for their critical suggestions, but also for their help in reviewing the manuscript of this thesis. Dr. M. F. Martinez (Paquita) and Priya Lakshmanan deserve special recognition for their valuable friendship. I would especially like to thank Laurie Good, Millie Ryan, Joyce C. Moser, Esther V. Brann, and Kelly P. Linkenhoker for their immeasurable assistance.

Special gratitude is due to my family for their support and encouragement, and for providing me with opportunities to succeed in life. I am especially thankful to my brother Javier Bonaplata for his reassuring kinship. Juan and Silvia Bonta, and Martin and Carmeli Leenders (my family in the United States) for their love and support. And special

thanks to Jesús Romero for being a constant source of love, encouragement, and motivation.

Table of Contents

1.0	Introduction	1
2.0	Literature Survey.....	4
2.1	Poly(Arylene Ether)s.....	4
2.1.1	General Aspects	4
2.1.2	Nucleophilic Aromatic Substitution (S_NAr).....	7
2.1.3	Poly(Arylene Ether) Synthesis via S_NAr Reaction	10
2.2	Phosphorus-Containing Polymers	14
2.2.1	Phosphorus and its Compounds.....	14
2.2.2	Flame Retardancy of Compounds Containing Phosphorus	15
2.2.3	Phosphorus-Containing Thermoplastics.....	17
2.2.4	Metal Complexation with Phosphorus Ligands.....	18
2.3	Metal-Containing Polymeric Materials.....	21
2.3.1	General Aspects	21
2.3.2	Ionic Polymers.....	21
2.3.3	Organometallic Polymers.....	22
2.3.4	Metal Doped Polymers.....	27
2.3.5	Polymer-Supported Catalysts.....	49
3.0	Experimental	52
3.1	Purification of Solvents.....	52
3.1.1	N,N-Dimethylacetamide (DMAc)	52
3.1.2	Tetrahydrofuran (THF).....	52
3.1.3	Chlorobenzene.....	53
3.1.4	Toluene	53

3.2	General Reagents.....	54
3.2.1	Potassium Carbonate.....	54
3.2.2	Iron(III)Chloride	55
3.2.3	Cobalt(II)Chloride.....	55
3.2.4	Copper(II)Chloride.....	55
3.2.5	Zinc(II)Chloride	56
3.2.6	Phenylsilane.....	56
3.2.7	Octene-1	57
3.2.8	Dicarbonylacetylacetonato rhodium (I) [Rh(acac)(CO) ₂].....	57
3.3	Preparation and Purification of Monomers.....	58
3.3.1	Bisphenol-A (Bis-A).....	58
3.3.2	4,4'-Biphenol (BP)	58
3.3.3	Bis(4-Fluorophenyl)Phenyl Phosphine Oxide (BFPPO).....	59
3.4	Synthesis of High Molecular Weight Poly(Arylene Ether Phosphine Oxide)s	60
3.5	Preparation of Metal Complexed Poly(Arylene Ether Phosphine Oxide) Films.....	62
3. 6	Synthesis of Poly(Arylene Ether Triaryl Phosphine) Ligand	64
3. 7	Catalytic Hydroformylation of Octene-1.....	65
3. 8	Characterization Methods.....	66
3.8.1	Infrared Spectroscopy	66
3.8.2	Nuclear Magnetic Resonance Studies.....	66
3.8.3	Intrinsic Viscosity	67
3.8.4	Thermogravimetric Analysis (TGA)	67
3.8.5	Differential Scanning Calorimetry (DSC)	67
3.8.6	Dynamic Mechanical Analysis (DMA).....	68

3.8.7	Gas Chromatography	68
3.8.8	Transmission Electron Microscopy (TEM) / Energy Dispersive X-Ray Analysis (EDAX).....	68
3.8.9	Electron Paramagnetic Resonance (EPR).....	68
4.0	Results and Discussion.....	69
4.1	Synthesis and Characterization of High Molecular Weight Poly(Arylene Ether Phosphine Oxide)s.....	69
4.1.1	General Introduction	69
4.1.2	Spectroscopic Analysis of Poly(Arylene Ether Phosphine Oxide)s	71
4.1.3	Thermal Characterization Data for Poly(Arylene Ether Phosphine Oxide) Thermoplastics.....	76
4.2	Composite Films Preparation and Characterization	78
4.2.1	Introduction	78
4.2.2	Solubility Characteristics of Composite Films.....	80
4.2.3	Thermal Data for Polymer-Metal Complexes	80
4.2.4	Dynamic Mechanical Analysis of Complex Films.....	91
4.2.5	FTIR Spectroscopic Studies	93
4.2.6	Phosphorus (³¹ P) NMR Studies	96
4.2.7	Microscopy Studies	104
4.3	Preparation and Characterization of Poly(Arylene Ether Triaryl Phosphine)s.....	109
4.4	Hydroformylation of Octene-1 over a Rhodium Complex of Poly(Arylene Ether Triaryl Phosphine).....	116
5.0	Conclusions	124
6.0	Suggested Future Research	127
7.0	References	128

List of Figures

Figure 2.1	Examples of Commercial Poly(Arylene Ether)s	5
Figure 2.2	Linear Step-growth Polymers. Influence of Number Average Molecular Weight ($\langle M_n \rangle$) on Properties Such as the Glass Transition Temperature	13
Figure 2.3	σ Donor- π Acceptor Bonding Model	19
Figure 2.4	Vinyllic Organometallic Monomers a) Vinyl Ferrocene b) Vinyl Ruthenocene	23
Figure 2.5	General Structure of a Phthalocyanine.....	23
Figure 2.6	Structure of Polyphthalocyaninato Metal Compound	24
Figure 2.7	Macrocyclic Metal Complex Arrangement.....	26
Figure 2.8	Dianhydrides and Diamines (Taylor and Coworkers) ⁷⁴⁻⁷⁷	29
Figure 2.9	Heteroatom Containing Diamines ⁸⁰	32
Figure 2.10	Postulated Structures of Complexes ⁸³	36
Figure 2.11	Examples of Rigid Chain Polymers Studied by Jenekhe and Coworkers ⁸⁶⁻⁸⁸	37
Figure 2.12	Poly(Amide)s Investigated 1a) Nylon 6, 1b) Nylon 11, 2) Nylon 6, 6, 3) PTMHTA ^{89,90}	39
Figure 2.13	Five-Membered Intramolecular Chelate Ring ⁹⁵	41
Figure 2.14	Octahedral Coordination around the Cobalt Center ⁹⁵	42
Figure 2.15	Proposed Structure for the CuCl_2 -Poly(Vinylpyridine) Complexes ⁹⁸	44
Figure 2.16	Proposed Structures for the NiCl_2 -Poly(4-Vinylpyridine) Complex ⁹⁸	45
Figure 2.17	Suggested Geometry for NiCl_2 -Poly(2-Vinylpyridine)	

	Complex ⁹⁸	45
Figure 2.18	Tricarbonyl(Conjugated Diene) Iron Unit	47
Figure 2.19	General Structure of Polymeric Phosphinates	47
Figure 2.20	Metal Coordinated Domex A-1 Resin.....	49
Figure 3.1	Polymer/Metal Film Composite Preparation	63
Figure 3.2	Stainless Steel Reactor used in Hydroformylation Reaction	65
Figure 4.1	Structural Repeat Units of Poly(Arylene Ether Phosphine Oxide)s	70
Figure 4.2	FTIR Spectrum of <20K> _{theo} BP-PEPO Film	72
Figure 4.3	¹ H NMR Spectrum of High Molecular Weight Bis A-PEPO in CDCl ₃ Referenced to TMS at 0 ppm(400 MHz).....	74
Figure 4.4	Phosphorus (³¹ P) NMR of Bis A-PEPO in CDCl ₃ Referenced to 85% H ₃ PO ₄ at 0 ppm (161.9 MHz)	75
Figure 4.5	Dynamic TGA Thermograms in Air of FeCl ₃ /Bis A-PEPO Composite.....	81
Figure 4.6	Dynamic TGA Thermograms in Air of CoCl ₂ /Bis A-PEPO Composite Films (10°C/min).....	82
Figure 4.7	Dynamic TGA Thermograms in Air of CuCl ₂ /Bis A-PEPO Composite Films (10°C/min).....	83
Figure 4.8	Dynamic TGA Thermograms in Air of 20 Mole % Metal Chloride/BP-PEPO Composite Films (10°C/min).....	87
Figure 4.9	DSC Traces for BP-PEPO Films (Second Scan. 10°C/minute).....	90
Figure 4.10	Dynamic Mechanical Analysis of BP-PEPO Composites (1Hz, 2.5°C/min).....	92
Figure 4.11	FTIR of 20 Mole % Metal Chloride/BP-PEPO Composite Films.....	94
Figure 4.12	Quantitative Analysis of the Decrease in the P=O Stretch	

	Intensity	95
Figure 4.13	Phosphorus (^{31}P) NMR of Bis A-PEPO/ CuCl_2 in DMAc	97
Figure 4.14	Electron Paramagnetic Resonance Spectrum of 20 Mole% CuCl_2 /BP-PEPO Film (9.55 GHz)	100
Figure 4.15	Electron Paramagnetic Resonance Spectrum of 20 Mole% FeCl_3 /BP-PEPO Film (9.55 GHz).....	100
Figure 4.16	Illustration of Inversion Recovery Method for Spin-Lattice Time Determination from Solid State ^{31}P NMR of BP-PEPO Composites Referenced to H_3PO_4 at 0 ppm (121.4 MHz).....	103
Figure 4.17	Transmission Electron Micrograph of 20 Mole % CoCl_2 Modified Films	106
Figure 4.18	Transmission Electron Micrograph of 50 Mole % CoCl_2 /BP-PEPO Composite.....	108
Figure 4.19	Proposed Mechanism for Phenylsilane Reduction of Tertiary Phosphine Oxides ¹⁵	111
Figure 4.20	^{31}P NMR Spectra Referenced to H_3PO_4 at 0 ppm (161.9 MHz) for Different Reaction Times during the Reduction of Bis A-PEPO.....	112
Figure 4.21	^1H NMR Spectrum of 70% Reduced Bis A-PEPO in CDCl_3 Referenced to TMS at 0 ppm (400 MHz).....	114
Figure 4.22	Simple Catalytic Cycle for Hydroformylation by Rhodium Catalysts ⁵⁰	118
Figure 4.23	Sample Gas Chromatogram of the Octene-1 Hydroformylation Product	120
Figure 4.24	Influence of Reaction Time on the Hydroformylation of Octene-1	121
Figure 4.25	Effect of Phosphorus/Rhodium Ratio on the Hydroformylation	

of Octene-1	122
-------------------	-----

List of Tables

Table 4.1	Solubility Characteristics of Poly(Arylene Ether Phosphine Oxide)s	70
Table 4.2	Intrinsic Viscosity of Poly(Arylene Ether Phosphine Oxide)s	71
Table 4.3	FTIR Peak Assignments for BP-PEPO Film	73
Table 4.4	Summary of Thermal Properties of Poly(Arylene Ether Phosphine Oxide)s	77
Table 4.5	Dynamic TGA Data for Bis A-PEPO Composite Films (Air. 10°C/min).....	84
Table 4.6	DSC Glass Transition Temperature Results for Bis A-PEPO Composite Films	88
Table 4.7	Chemical Shift Changes Upon Metal Salt Addition	98
Table 4.8	Line Width at Half Height Results from ³¹ P NMR Spectra of Metal Salt/Bis A-PEPO DMAc Solutions.....	98
Table 4.9	Spin-Lattice Relaxation Time Results for BP-PEPO Composites	102
Table 4.10	Thermal Properties of CoCl ₂ /BP-PEPO Composites	107
Table 4.11	Results of Phenyl Silane Reduction of 15K BisA-PEPO.....	115

List of Schemes

Scheme 2.1	Resonance Stabilization in Aryl Ethers	4
Scheme 2.2	SNAr Nucleophilic Aromatic Substitution Mechanism	8
Scheme 2.3	General Synthesis of Poly(Arylene Ether)s	12
Scheme 2.4	Synthesis of a Ladder Polymer with Copper Central Atom ⁶⁵	25
Scheme 3.1	Preparation of Bis(4-Fluorophenyl)Phenyl Phosphine Oxide	59
Scheme 3.2	Synthesis of Hydroxy Functionalized Poly(Arylene Ether Phosphine Oxide)s	61
Scheme 4.1	Phenylsilane Reduction of BisA-PEPO.....	110
Scheme 4.2	Catalyzed Hydroformylation of Octene-1	117
Scheme 4.3	<i>In Situ</i> Generation of the Active Rhodium Catalyst	117

1.0 Introduction

Poly(arylene ether)s are an important class of high performance thermoplastics. These polymers possess very attractive properties such as elevated glass transition temperature, high thermo-oxidative stability, and hydrolytic stability.¹⁻⁴ The incorporation of phosphorus functionalities in these thermoplastics, in addition to imparting flame resistance to the material, offers a potential for metal complexation.^{27,48} The present work has focused on the study of the complexation of several metal salts with phosphorus containing poly(arylene ether)s. The ultimate goal is the preparation of easily processed polymer/metal composites with novel properties (electrical, thermal, surface resistivity, permeability, ...), while maintaining the optimal characteristics of the base materials.

The literature on metal containing polymeric materials is highly extensive and diverse. The following chapter will outline several of the research efforts in this extensive area. The primary focus of this review will be doped systems in which specific interactions between the polymer and the metal are reported. The potential applications of metal modified thermoplastics are numerous and include fields such as electro-active high performance materials, extraction applications, membranes for gas separation, and catalysis.

Poly(arylene ether phosphine oxide)s (PEPO) can be synthesized via nucleophilic aromatic substitution of bis(4,4'-fluorophenyl)phenyl phosphine oxide (BFPPPO) with a series of bisphenols including bisphenol A and 4,4'-biphenol.²⁶⁻²⁸ The presence of the phosphine oxide functionality in the backbone allows for modification of these macromolecules via inorganic chemistry. The phosphine oxide group can act as an electron donor toward electron deficient metal centers and, consequently, numerous metal complexes have been reported in the literature for ligands containing this functionality.⁵⁶ We have found that a variety of metal salts including metals such as iron, zinc, cobalt, and copper, can be complexed at a molecular level with the phosphorus oxygen bond in films of poly(arylene

ether phosphine oxide) producing novel transparent metal-polymer "composites". A procedure for obtaining homogeneous films from solutions of the metal complexed polymers was developed. Employing this procedure a series of homogeneous PEPO films containing varying mole percents of anhydrous metal salts such as iron (III) chloride (FeCl_3), cobalt (II) chloride (CoCl_2), and copper (II) chloride (CuCl_2) were prepared and characterized. The properties of these materials such as solubility, thermal stability in air, and glass transition temperature were studied using a variety of experimental techniques. In addition, infrared and phosphorus (^{31}P) NMR experiments were conducted to demonstrate the existence of interactions between the metal salt and the phosphorus polymer in solution as well as in the solid state. The influence of the chemistry and concentration of metal salt, and the polymer backbone chemistry on the solubility, glass transition temperature, thermal stability, and storage modulus of the composites were investigated. Further analysis of the morphological structure of these composites was conducted using electron microscopy.

Additionally, novel poly(phosphine)s were synthesized via modification of poly(arylene ether phosphine oxide)s. Linear PEPOs were reduced to the corresponding phosphine containing polymers using phenylsilane. The reaction conditions were varied to obtain different extents of reduction. Properties such as the intrinsic viscosity, thermo-oxidative stability, and glass transition temperature of the polymeric phosphines were expected to vary with the percentage phosphine in the chain and this was demonstrated.

Non-polymeric phosphines, particularly triphenylphosphine, are used as ligands in metal complex catalysis of a wide range of organic reactions.⁵⁰ The use of polymeric phosphine/metal complexes in these catalyzed reactions would facilitate the separation of the product as well as the recovery of the catalyst. An almost completely reduced phosphine polymer was used in an attempt to generate a rhodium catalyst for the hydroformylation of octene-1. In this reaction the catalyst was generated *in situ* via the

coordination of the phosphine polymer with a rhodium precursor, $\text{Rh}(\text{acac})(\text{CO})_2$. We have investigated the ability of this rhodium-polymer complex to catalyze the hydroformylation of octene-1 at 200 psi and 120°C and in the presence of a 50:50 mixture of CO and H_2 . Two different studies were conducted to investigate the catalyst activity as a function of reaction time and with varying phosphorus to rhodium ratio, independently.

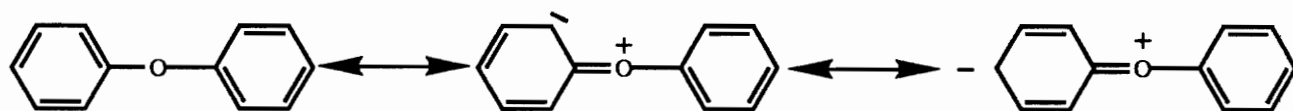
2.0 Literature Survey

2.1 Poly(Arylene Ether)s

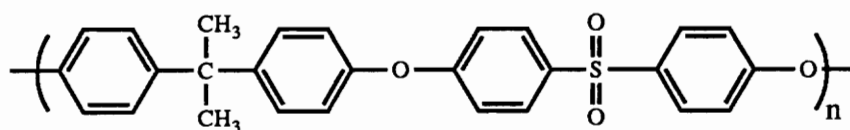
2.1.1 General Aspects

Poly(arylene ether)s belong to a class of materials known as engineering thermoplastics. This family of macromolecules are tough, rigid materials with excellent thermal stability and good mechanical and electrical properties. In addition, these polymers display excellent resistance to hydrolysis and oxidation.¹⁻⁴ By virtue of their outstanding properties some of these poly(arylene ether)s have attained commercial utility. Some examples of these include a bisphenol-A polysulfone, UDEL (Amoco); a poly(ether sulfone), Victrex; and a poly(ether ether ketone), PEEK (ICI). The structures are shown in Figure 2.1.

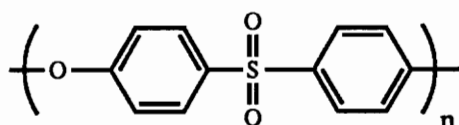
As the name implies, poly(arylene ether)s are composed of highly aromatic backbones in addition to ether linkages. Aromatic moieties such as benzene or naphthalene are known to impart thermal stability in polymeric backbones. The characteristic aryl-ether bond in poly(arylene ether)s is chemically and thermally stable. An aliphatic carbon-oxygen ether linkage has a bond strength (84.0 Kcal/mol) comparable to that of the aliphatic carbon-carbon bond (83.1 Kcal/mol). Aromatic ether linkages (Ar-O-Ar) are further stabilized through resonance as is illustrated for diphenyl ether in Scheme 2.1.⁵



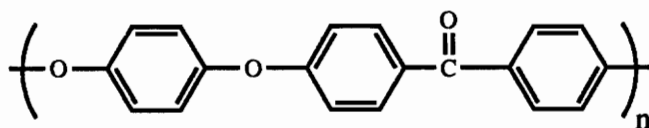
Scheme 2.1 Resonance Stabilization in Aryl Ethers



UDEL (Amoco Chemical)



VICTREX (ICI)



PEEK (ICI)

Figure 2.1 Examples of Commercial Poly(Arylene Ether)s

Compared to the C-C bond, the C-O-C linkage has a lower barrier to rotation, lower excluded volume, and decreased Van der Waals interaction forces. This results in a greater backbone mobility and, therefore, an increased flexibility of the chain. In addition, the low barrier to rotation about the aromatic ether bond provides a mechanism for energy dispersion which is believed to be the principal reason for the toughness or impact resistance observed for these materials.¹²⁹

The incorporation of other thermally stable moieties such as sulfone, ketone, or triphenyl phosphine oxide in addition to the ether group in poly(arylene ether)s has resulted in the synthesis of a wide variety of polymeric materials. The electron withdrawing character and polarity of these groups are an important factor in determining the stiffness of the chain and its ability to crystallize.⁶

Due to the increasing commercial relevance of this class of polymers, reactions leading to the preparation of poly(arylene ether)s have been studied in detail, and many alternative synthetic pathways have been developed. There are mainly three synthetic approaches employed in the preparation of poly(arylene ether)s: oxidative coupling of phenolic hydroxyl groups,^{7,8} electrophilic aromatic substitution,^{9,10} and nucleophilic aromatic substitution.^{22,24,25} Of these three methods, nucleophilic aromatic substitution is by far the most widely used, and it was the method utilized in this research. Poly(arylene ether)s have also been synthesized via nickel,¹¹ and copper coupling^{12,13} as well as silyl ether displacement.^{14,15}

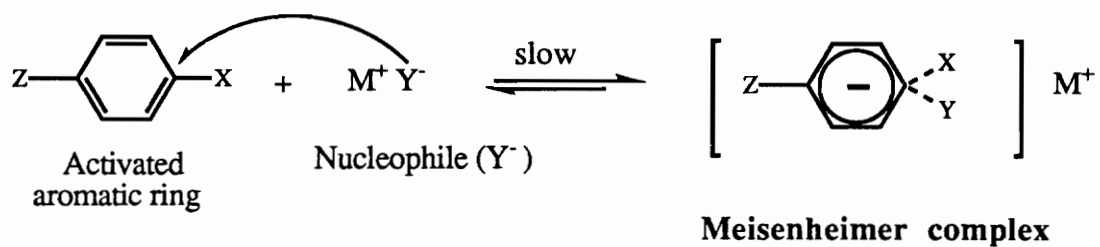
2.1.2 Nucleophilic Aromatic Substitution (S_NAr)

Nucleophilic aromatic substitution can occur via four principal mechanisms.¹⁶ The most important mechanism which operates where activating groups are present on the aromatic ring is referred to as the S_NAr mechanism (Scheme 2.2).

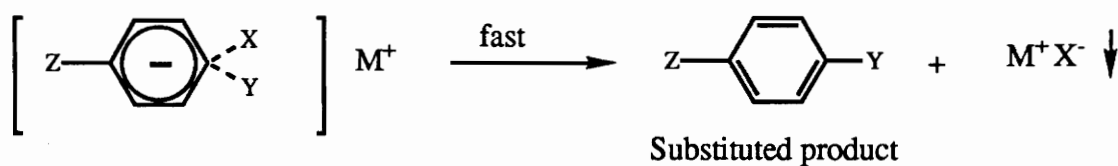
The first step is generally the rate determining step and involves the attack of the nucleophile forming a bond with the substrate. This results in the generation of a resonance stabilized intermediate (Meisenheimer complex¹⁷) followed by the departure of the leaving group. Apart from the isolation of several stable Meisenheimer salts,¹⁷ further evidence for this mechanism arrives from studies of the effects of the leaving group on the reaction rate. The order of reactivity for the halogens was found to be $F \gg Cl \geq Br \geq I$, although the carbon-fluorine bond is the strongest in that series. The rate determining step, therefore, does not involve the departure of the leaving group, and the observed order of reactivity can be explained by the better stabilization of the Meisenheimer intermediate by the highly electronegative fluorine through inductive electron withdrawing effects. Furthermore, the carbon directly attached to the fluorine will be more electrophilic and, consequently, more susceptible to nucleophilic attack.

The kinetics of the S_NAr mechanism are mainly governed by the strength of the activating group, the nucleophilicity of the attacking nucleophile, the electronegativity of the leaving group, and the reaction conditions, in particular, the solvent. Activating groups in the *ortho* and *para* positions to the leaving group accelerate the substitution reactions. The activating or deactivating ability of a variety of groups has been studied by comparison of reaction rates with *para* substituted substrates and identical nucleophiles and leaving groups. The approximate order of electron withdrawing power was found to be $NO > NO_2 > SO_2Me > CF_3 > CN > CHO > COR > COOH > Br > Cl > I > H > F > CMe_3 > Me > OMe > NMe_2 > OH > NH_2$.¹⁸ Electron withdrawing groups such as the nitro, sulfone, or ketone accelerate the nucleophilic substitution reaction by strongly stabilizing the

Step 1:



Step 2:



Z = Activating or electron withdrawing group
X = Leaving group
Y = Attacking nucleophile
M = Metal counter-cation

Scheme 2.2 S_NAr Nucleophilic Aromatic Substitution Mechanism

intermediate complex through resonance, while electron donating groups such as amine or methoxy hinder the substitution.

The reactivity of the incoming nucleophile also influences the ease of the S_NAr reaction, with the rate of the substitution reaction generally increasing with increasing nucleophile strength. The overall approximate order of nucleophilicity is $ArS^- > RO^- > R_2NH > ArO^- > OH^- > ArNH_2 > NH_3 > I^- > Br^- > Cl^- > H_2O > ROH$.¹⁹ Although nucleophilicity is generally dependent on base strength, there are some exceptions. For example, while OH^- is a stronger base than ArO^- , it is a poorer nucleophile.

We have already discussed the leaving group effect of the halides in the S_NAr reaction. The separation of the leaving group in the S_NAr mechanism is not the rate determining step, therefore, the order of leaving group ability compared to that of S_N1 or S_N2 reactions is in many cases reversed. In aromatic nucleophilic substitution it is the leaving groups which stabilize the Meisenheimer complex which promote faster reaction rates. The following leaving group trends have been observed for S_NAr substitutions: $F > NO_2 > SPh > Cl > Br \sim I > OAr > OR > SR$.^{18,20}

The reaction conditions in nucleophilic aromatic substitutions must be carefully controlled, the choice of solvent being very important. The solvent must be inert under the reaction conditions, it must dissolve both the reactants and the products (this is particularly important in polymerization reactions), and should be able to solvate counter-cations, thus, facilitating the bimolecular addition step. The most effective solvents for nucleophilic aromatic substitutions are polar aprotic solvents such as N,N-dimethylformamide (DMF), dimethylsulfoxide (DMSO), N,N-dimethylacetamide (DMAc), N-methylpyrrolidone (NMP), and sulfolane. These solvents have the ability to enhance the active concentration of the attacking nucleophile by dissociating the nucleophile-cation pair.²¹ High boiling solvents such as DMSO, DMAc, and NMP are often used in polymerization reactions

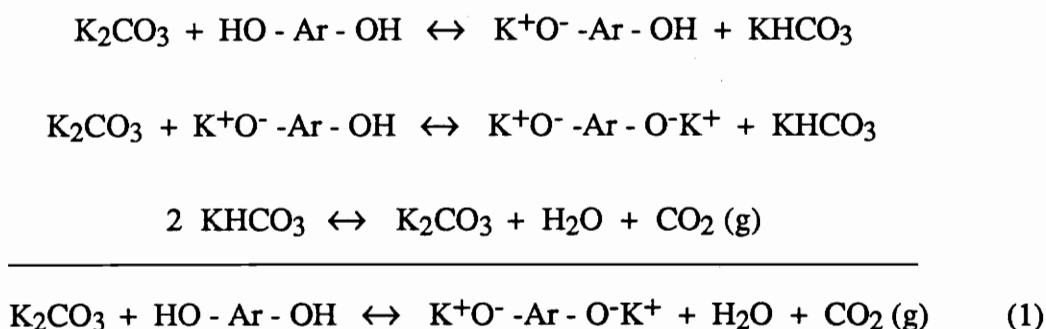
especially in the case where the nucleophile is an alkali bisphenate. In these polymerizations, high temperatures are required to dissolve the nucleophile as well as the growing polymer chain. In addition to using appropriate solvents, water must be excluded from the system. Water can act as a nucleophile in the presence of base to hydrolyze the activated substrate. Hydrolytic side reactions may prevent the synthesis of high molecular weight polymers mainly by off-setting the stoichiometry.²²

2.1.3 Poly(Arylene Ether) Synthesis Via S_NAr Reaction

Bunnett and Zahler showed that the reaction of certain activated aromatic halides with alkali metal phenates in suitable solvents proceeds via the bimolecular addition-elimination path of aromatic nucleophilic substitution and results in high yields of the corresponding aryl ethers.^{19,23} This concept was later extended to the synthesis of poly(arylene ether)s via the condensation of bisphenates with activated aromatic dihalides in polar aprotic solvents.^{22,24,25} The general reaction scheme is shown in Scheme 2.3.

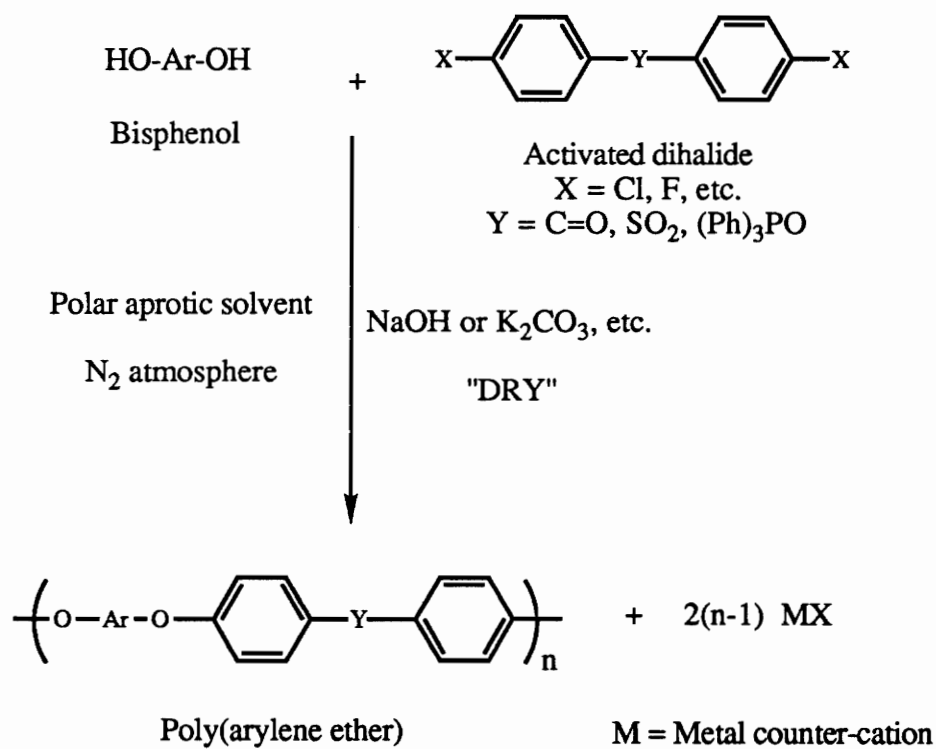
The reaction involves the formation of highly oxidizable alkali phenates, thus, the polymerization must be carried out in an inert atmosphere. The bisphenol salts of sodium and potassium are used because they are soluble in polar aprotic solvents. An excess of a strong base such as an alkali metal hydroxide in an aprotic solvent can lead to side reactions which limit the molecular weight. Weaker bases such as potassium carbonate, K_2CO_3 , are much less able to displace halogen from the activated dihalide and allow for the addition of all the reactants at the same time, whereas, sodium hydroxide must be allowed to react with the bisphenol prior to the addition of the dihalide.²⁶⁻²⁸ In both cases, water must be eliminated in a first step by azeotropic distillation, usually with a co-solvent such as toluene or chlorobenzene, and oxygen and moisture must be excluded by conducting the reaction under an inert atmosphere.

In the generation of bisphenates by K_2CO_3 one equivalent of the weak base is consumed for every equivalent of bisphenol. This is illustrated in the following reaction sequence:²⁴



This step-growth process is consistent with the principles of condensation polymerization. As such, very high purity monomers (>99.99%) and proper stoichiometry are required in order to obtain high molecular weights. In general, the effect of molecular weight on the properties such as the glass transition temperature of poly(arylene ether)s is that typical of amorphous linear polymers (Figure 2.2).

In region I, the high end group concentration and lack of molecular entanglements results in very poor properties. When the entanglements begin to form and the chain end concentration decreases (region II), the properties reach more acceptable values, and in region III they reach a plateau where large changes in molecular weight have relatively little effect on many of the properties of the material. In step-growth polymerization molecular weight control can be attained by off-setting the stoichiometry with a calculated amount of one of the difunctional reactants or by addition of a monofunctional end-capper. Both of these methods involve the application of the Carother's Equation.²⁹



Scheme 2.3 General Synthesis of Poly(Arylene Ether)s

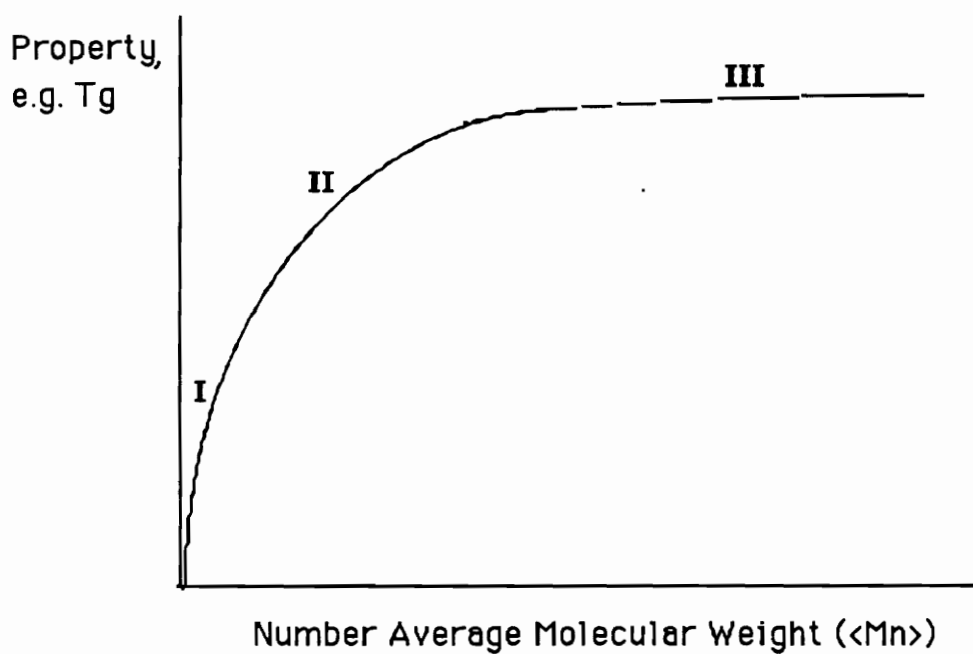


Figure 2.2 Linear Step-growth Polymers: Influence of Number Average Molecular Weight ($\langle M_n \rangle$) on Properties Such as the Glass Transition Temperature

2.2 *Phosphorus-Containing Polymers*

2.2.1 Phosphorus and its Compounds

Phosphorus is a very unique atom which can form many types of different compounds. This atom can be formally trivalent (using only three electrons) or pentavalent (using all five of its outer shell electrons). In the majority of its compounds, phosphorus is linked to three, four, or five other atoms. One, two, and six coordinated compounds are also known.³¹

The chemistry of phosphorus is very different from that of nitrogen. In the case of phosphorus the 3d atomic orbitals are readily available for bond formation since the promotional energy $3s \rightarrow 3d$ is small enough to allow for vacant d orbital bond participation. On the other hand, the promotional energy $2s \rightarrow 3d$ is too large for nitrogen, and there is no effective participation of the d orbitals in bonding. As a consequence of the contribution of higher energy d levels, phosphorus is effectively a larger atom with reduced electronegativity and more polarizability than nitrogen.

In some phosphorus compounds in addition to σ bonds, the 3p and 3d atomic orbitals of the P are used to form π -bonds. These can be of the type $p\pi(P)-p\pi(X)$; $d\pi(P)-p\pi(X)$ or $d\pi(P)-d\pi(X)$ where X is most commonly C, N, or O. The degree of d orbital contribution to the π -bond is determined by the nature of the bonded atoms or groups. Participation of the dz^2 and $d(x^2-y^2)$ orbitals is favored by electronegative substituents which increase the effective positive charge on the phosphorus. If the bonded atoms have lone pair electrons available, they can be back-donated to fill the vacant d orbitals of the phosphorus. Similarly, in transition metal complexes, filled metal d orbitals can backbond to empty phosphorus 3d orbitals. This backbonding phenomenon is stabilizing and results in

stronger bonds. The extent of π -bonding as well as π -backbonding for certain compounds is still being debated.³⁰

The strength of a given bond varies from one chemical compound to another. However, several generalizations are possible. In general, the following is found for phosphorus bonds to other atoms:³¹

- 1) P-O bonds are stronger than N-O or C-O bonds.
- 2) The P-C bond is comparable in strength to the C-C bond.
- 3) P=O bonds are much stronger than P-O, but somewhat weaker than C=O or N=O linkages.

The P-C bond is more stable than the C-C linkage in terms of resistance to oxidation and hydrolysis. The phosphoryl link is extremely strong and stable, but when the oxygen atom is involved in a bridge (P-O-C or P-O-P) it generally leads to hydrolytic instability. The most stable organophosphorus compounds are tertiary phosphine oxides. In symmetrical $R_3P=O$ type compounds the phosphoryl bond is exceptionally stable. This is believed to result from the formation of two mutually perpendicular $d\pi-p\pi$ type orbitals using two lone pairs of electrons on the oxygen atom. These overlap with two distinct d orbitals of phosphorus, resulting in the symmetry, although not the strength of a triple bond.³¹ In fact, $Ph_3P=O$ has been reported to not decompose in air below 700°C.³² Tertiary phosphines (R_3P), on the other hand, are generally very prone to oxidation in air.

2.2.2 Flame Retardancy of Compounds Containing Phosphorus

Growing interest in polymers in fields such as construction, home furnishings, and various industrial applications has created a demand for polymers with increased flame resistance. The self-extinguishing capability of phosphorus compounds has been well recognized.

Flame retardancy in polymers can be achieved by the addition of a suitable flame retardant or by incorporation of phosphorus in the polymer chain ("inherently" fire retardant polymers). Phosphorus based additives have been used for quite a long time as flame retardants, and in some cases their use has become commercially significant. The most commonly used phosphorus flame retardant additives today include chloroalkylphosphates, aryl phosphates, inorganic ammonium polyphosphates, and elemental red phosphorus. The mechanism of flame retardancy by these materials has been investigated for a series of different compounds,^{33,34} and it appears that phosphorus compounds reduce flammability of polymers by promoting char formation and inhibiting ignition.^{35,36} There are several problems associated with the use of additives. These include poor compatibility with the polymer matrix, poor processability, requirements for large quantities of additives (greater costs), generation of large amounts of volatiles, and adverse effects on the mechanical properties of the material. The incorporation of phosphorus in the polymer backbone may overcome these disadvantages. Polymers containing different forms of phosphorus such as phosphates, phosphonates, phosphines, and phosphine oxides in the side chains, the backbone of linear polymers, and in cyclic structures within the main chain have been investigated in this respect. In general, it has been found that phosphorus polymers tend to be fire retardant.³⁷⁻³⁹ The most common measure of polymer flammability is the Limiting Oxygen Index (LOI). This is a measure of the oxygen in the atmosphere surrounding the sample necessary to sustain burning in the sample under some conditions. The LOI has been found to be largely dependent on the phosphorus content as well as the chain structure, and has been related to the extent of char yield. More recently, utilization of measurements of the heat release rate, especially by cone calorimetry, has been recognized as a more reliable approach for both fundamental and diagnostic reasons.

2.2.3 Phosphorus-Containing Thermoplastics

Even though the number of phosphorus-containing organic polymers is small compared to other organic polymers, there are numerous examples of phosphorus modified macromolecules in the literature: polyphosphazenes, polyphosphonates, polyphosphites, polyphosphines, poly(phosphine oxide)s, etc. In general, these systems are hydrolytically unstable, their synthesis only results in low molecular weight oligomers, and they are mostly vinyl-like in nature. Most contain P-O and P-N linkages since these are easier to introduce into the polymer backbone than P-C bonds. The extension of phosphorus chemistry to the field of engineering thermoplastics, therefore, has been limited. The inclusion of the phosphine oxide moiety in the main chain of polymers as discussed above would result in hydrolytic and oxidative stability. Systems with main chain phosphine oxide linkage reported in the literature or in patents include polyesters,⁴⁰⁻⁴² polyimides,⁴³ polyamides,^{44,45} and some thermosetting materials.^{46,47} A relatively new class of P=O containing engineering thermoplastics, poly(arylene ether phosphine oxide)s, have been synthesized via nucleophilic aromatic substitution polymerization of aromatic bisphenols with an activated dihalide [bis(4,4'-fluorophenyl)phenyl phosphine oxide] in the presence of a slight excess of a weak base (K_2CO_3) in a polar aprotic solvent.²⁷ In addition to the outstanding thermal, oxidative, and hydrolytic stability derived from the triphenyl phosphine oxide unit as discussed above, these polymers were found to possess a number of unique characteristics:^{27,48}

- The bulky triphenyl phosphine oxide moiety rendered these materials amorphous, and enhanced their solubility.
- These polymers exhibited high glass transition temperatures (190°C-280°C).
- These materials possessed high thermo-oxidative stability (5% weight loss in air ~ 500°C)

- Phosphorus was shown to promote char formation in air, resulting in improved self-extinguishability relative to non-phosphorus containing analogous systems. Qualitative ignition tests via bunsen burner combustion showed improved self-extinguishing behavior.
- These phosphorus-containing polymers presented extremely low amounts of etching in oxygen plasma compared to other engineering polymers.

Poly(arylene ether phosphine oxide)s prepared in the manner described above were the base materials used for the present work.

2.2.4 Metal Complexation with Phosphorus Ligands

Numerous stable transition metal complexes have been prepared using phosphorus ligands. These include complexes with trialkylphosphites (i.e. $P(OR)_3$, $R = Me, Et, Bu^n, \dots$), phosphorus hydrides (PH_3 , $PHPh_2$), tertiary phosphines (i.e. PR_3 , $R = \text{alkyl or aryl}$), phosphine oxides, and polydentate tertiary organophosphines ($Ph_2P(CH_2)_nPPh_2$).⁵⁰ Much attention has been placed on P (III) ligands. These ligands exhibit pyramidal geometry, and when the metal-ligand bond is formed there is a change in the coordination of the P(III) to tetrahedral. P (III) ligands behave as Lewis bases donating the lone pair on the phosphorus to an electron deficient metal center. In addition to this σ bond, it has been postulated that charge transfer from a filled d orbital on the metal to an empty 3d orbital of the phosphorus occurs (π back-bonding).^{49,50} This σ donor- π acceptor model (Figure 2.3), however, has been widely criticized.^{51,52}

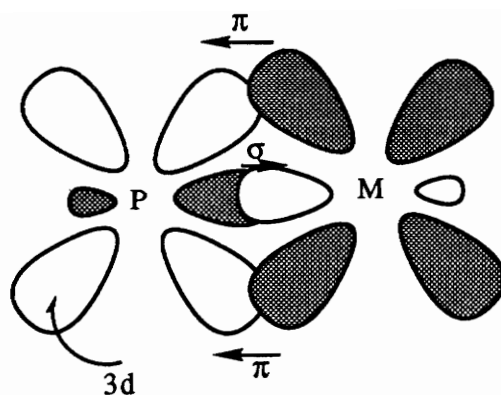


Figure 2.3 σ Donor- π Acceptor Bonding Model

Some authors have argued that the 3d orbitals of P are too high in energy and too diffuse to contribute to bonding. Alternatively, some authors propose that the σ^* orbital of the phosphorus-substituent bond accepts electrons from the d orbital of the metal.^{53,54} The nature of the phosphorus-metal bond in specific complexes of P(III) ligands is still being debated, however, it is well established that the extent to which the ligand can accept electrons from the metal is highly dependent on the substituents on the phosphorus as well as the oxidation state of the metal center.

Steric effects are another factor which plays an important role in this type of complexes. Bulky groups with large cone angles promote low coordination numbers, coordinatively unsaturated metal centers, and sometimes facile metallation. Triphenylphosphine is a very sterically hindered ligand which has become very popular and, thus, has been widely used in organometallic chemistry and homogeneous catalysis. Good reaction selectivity and activity are often obtained for catalysts derived from Ph_3P .⁵⁰ The large cone angle of this bulky ligand results in the formation of lower coordination number complexes, the generation of the less crowded isomer, and an increase in the rate of dissociation reactions. This, combined with its relatively low basicity, make triphenylphosphine an ideal ligand. Complexes such as $\text{RhH}(\text{CO})(\text{PPh}_3)$, $\text{PtH}(\text{CO})(\text{SnCl}_3(\text{PPh}_3)_2)$, $\text{RuCl}(\text{PPh}_3)_3$ and $\text{RhCO}(\text{PPh}_3)_3$ are used in a number of catalytic reactions including the decarbonylation of

aldehydes, acyl and aroyl halides, the hydrogenation of unsaturated compounds such as alkenes and alkynes, and hydroformylation of alkenes.⁵⁵

Phosphine oxides also interact with metallic compounds to form complexes. The formation of stable complexes of low molecular weight organophosphine oxides with a large variety of metals was reviewed by Karayannis and coworkers.⁵⁶ These compounds coordinate to the metal through the phosphoryl oxygen. As described earlier, the P=O bond is extremely stable having significant σ and π contributions. The σ bond (P→O) entails mainly 3s and 3p phosphorus and 2p oxygen orbitals, while the π bonding (O→P) has contributions from the 3p and 3d orbitals of the phosphorus. The stability of the P=O bond is even greater for symmetrical compounds such as triphenylphosphine oxide (Ph₃P=O). Complexes of this ligand with metals of the 3d (TiCl₆(Ph₃PO)₂, VOCl₂(Ph₃PO)₂, Co(Ph₃PO)₄(ClO₄)₂), 4d (MoPh₃PO)₃(CO)₃), and 5d (W(CO)₃Ph₃PO) transition series as well as lanthanides (NdCl₃(Ph₃PO)₃ · H₂O, Eu(NCS)₃(Ph₃PO)₃) and actinides (Th(NO₃)₄(Ph₃PO)₂) have been reported. The effect of coordination upon the P-O stretch has been studied by infrared for a large number of triaryl and trialkyl phosphine oxides.⁵⁷ The frequency of the P-O stretching mode was found to shift approximately 50 cm⁻¹ to lower values upon complete coordination.

Complexes of triphenylphosphine oxide with transition metal chlorides such as FeCl₃, CoCl₂, and CuCl₂ have also been prepared. Iron(III)chloride is a dark green or black solid that decomposes slowly at 200°C and rapidly above 300°C. Copper(II)chloride is a yellow-brown solid which is also thermally unstable above 300°C. Cobalt(II)chloride, on the other hand, is a very stable pale blue solid which decomposes above 700°C. The structure of the complexes of copper(II) and cobalt(II) chlorides with triphenylphosphine oxide ([Co(Ph₃PO)₂Cl₂] and [Cu(Ph₃PO)₂Cl₂]) has been shown to be nearly tetrahedral around the metal.^{58,59} The coordination compound with the iron(III)chloride, however, has been formulated as [Fe(Ph₃PO)₄Cl₂]⁺ [FeCl₄]⁻.⁶⁰

2.3 *Metal-Containing Polymeric Materials*

2.3.1 General Aspects

The field of metal-containing polymeric materials is very abundant and highly diverse. Our goal here is only to outline the various research areas, and review several specific examples of these systems with emphasis on those in which specific interactions between the metal and the polymer have been reported.

The different metal-containing polymers include ionomers, organometallic polymers wherein the metal is integrated into the polymer chain, doped neutral polymers, and polymer films with metal deposits. This last category refers to the less explored area of polymer film laminates in which a metal vapor is deposited onto a polymer film in an effort to increase the surface conductivity of the material. These materials are beyond the scope of this review and will not be discussed.

The motivations for introducing metals into polymer matrices vary greatly. However, the common goal is to modify the properties of the material whether it is the electrical conductivity, flammability, thermal behavior, surface resistivity, optical behavior, or mechanical properties.

2.3.2 Ionic Polymers

Ionomers are macromolecules which have an ionic group covalently attached to the backbone which is generally neutralized by a metal counterion. These systems can be prepared by the incorporation of a metal ion following the polymerization or, alternatively, by the polymerization of a metal salt polymer. An example of the preparation of this class of materials is the neutralization of partially ionized poly(methacrylic acid) with copper(II)

ions.⁶¹ Another common approach to ionic polymers is that of copolyelectrolytes. These are macromolecules with a mainly nonpolar backbone, but containing a small percent of salt units incorporated via copolymerization. The most common approach to their preparation is the copolymerization of a small amount of a functionalized vinyl monomer with a nonfunctionalized monomer followed by the conversion of the functional group to the mono- or divalent salt. Examples of these systems include salts of copolymers such as ethylene-acrylic acid, styrene-methacrylic acid, and butadiene-methacrylic acid. Among other applications, ionomers have been used in packaging and the extraction of metals from aqueous solution.

2.3.3 Organometallic Polymers

A second type of metal-containing macromolecules includes those materials in which the metal is incorporated into the polymer backbone. Systems in which units of a metallocene complex such as ferrocene, $(\eta^5\text{-C}_5\text{H}_5)_2\text{Fe}$, are connected directly or through an organic bridging group as to form a linear chain, constitute an important group of organometallic polymers. The vast majority of these systems are synthesized via the polymerization of metal-containing monomers. An example is the free radical polymerization of vinyl ferrocene or vinyl ruthenocene. The structures of these vinylic organotransition metal monomers is depicted in Figure 2.4.

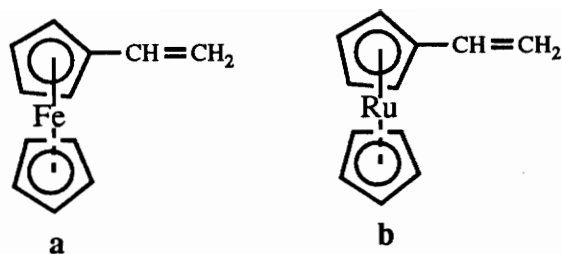


Figure 2.4 Vinylic Organometallic Monomers: a) Vinyl Ferrocene b) Vinyl Ruthenocene

Metal complexes containing macrocycles can also be polymerized. The preparation of these organometallic polymers has been extensively investigated in an attempt to synthesize organic conductors. Commercial applications of conducting polymers are numerous and are derived from the lower weight of these materials compared to metals combined with the generally more facile and less expensive processing of polymers. There is a demand for conductive polymeric materials in applications such as sheathing for electric power cable (to prevent dielectric loss between the cable and the insulating jacketing), battery components, rectifiers, sensors, switching devices, photoresist elements, etc.⁶²

The most widely used macrocycle is phthalocyanine (PcH₂), shown in Figure 2.5. Several types of polymeric assemblies have been designed using this type of monomer.^{63,64}

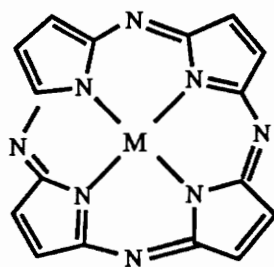


Figure 2.5 General Structure of a Phthalocyanine (M= Metal)

'Ladder' polymers can be prepared from the melt reaction of tetracyanobenzene with phthalonitrile in the presence of a metal ion such as Cu^{2+} , Fe^{2+} , Co^{2+} , or Ni^{2+} (Scheme 2.4).⁶⁵

Another mode of assembly is that of plane polymers, an example of which are polyphthalocyaninato metal compounds (Figure 2.6).⁶⁶

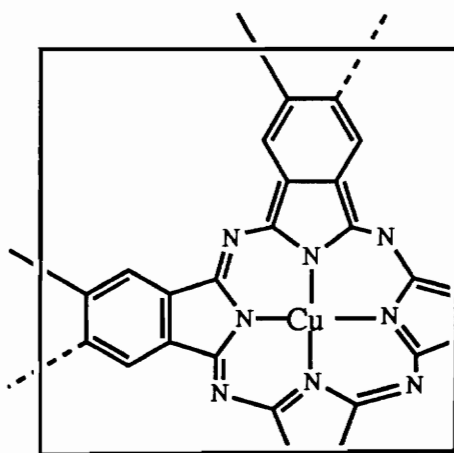
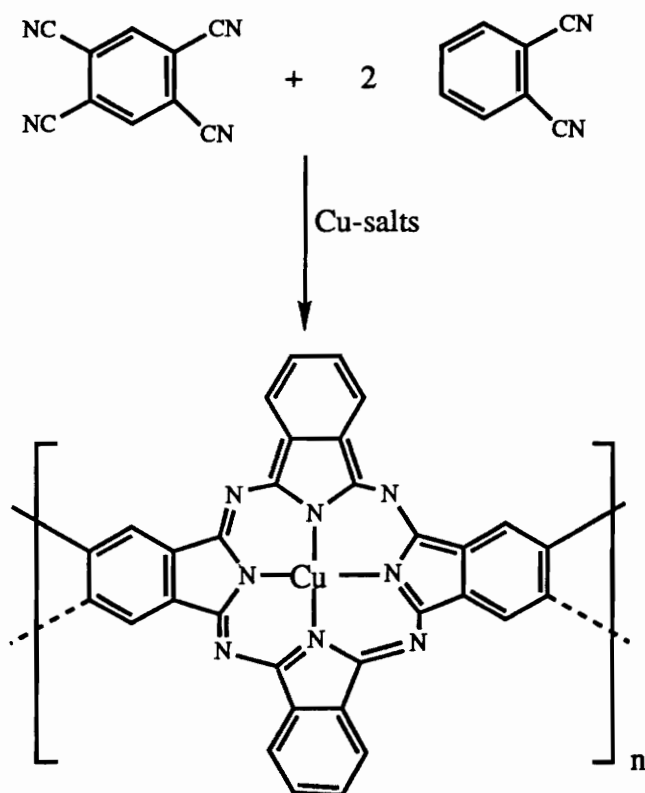


Figure 2.6 Structure of Polyphthalocyaninato Metal Compound



Scheme 2.4 Synthesis of a Ladder Polymer with Copper Central Atom⁶⁵

Yet a third possible arrangement is that of stacked metallomacrocycles in which the metal complex is planar or nearly planar. In this structural organization electron delocalization by π - π overlap of the macrocycles can be achieved. For simple metallocycles, however, crystallization seldom results in stacking. This type of architecture, on the other hand, has been made possible in bridge-stacked phthalocyanine polymers. A variety of bridging ligands including oxygen, fluorine, sulfur, and acetylene have been used.⁶⁷ Figure 2.7 illustrates the architecture of these bridged polymers.

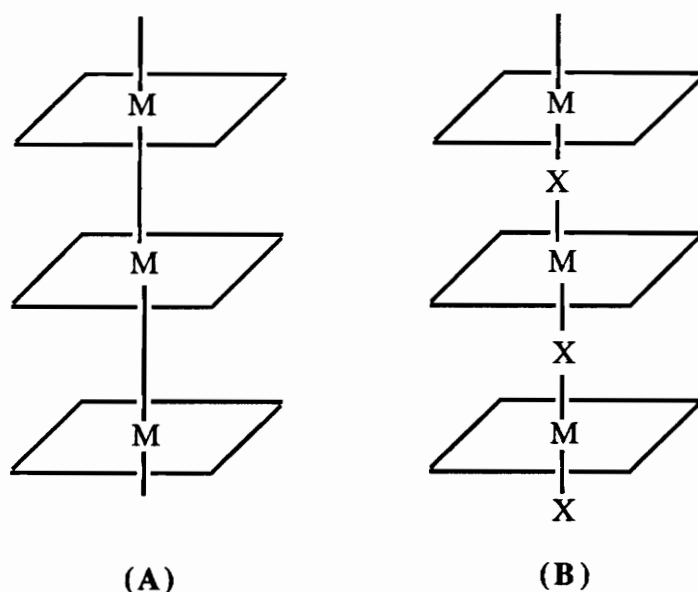
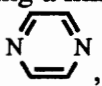
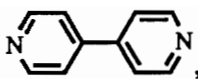


Figure 2.7 Macrocylic Metal Complex Arrangement (A) Stacked Arrangement, (B) Bridged-Stacked Arrangement.

These systems are conductive with the conduction mechanism being mainly due to π - π overlap of closely distanced stacked metallocycles with the metal ion playing a minor role. Bridging ligands containing π -electrons such as cyanide (-CN), pyrazine, , or 4,4-

bipyridine, , have also been investigated. These groups allow for electron migration from one metal center to another, and can be used with transition metals which favor octahedral coordination to construct polymers in which the main conduction channel is along the central axis of the macromolecule.⁶⁸

In general, metallocyclic polymers are found to exhibit greater conductivity than their monomeric counterparts. Moreover, halogen doping has been found to increase the conductivity of some of these systems.⁶⁷ These polymers are also unique in that they are exceedingly stable chemically as well as thermally.

2.3.4 Metal Doped Polymers

Polymer metal "doping" constitutes a very important area of research. This field includes those systems in which an inorganic filler (metal powders, iron, aluminum) is blended in with a preformed polymer. The process may be referred to as heterogeneous dispersion since the composite is formed from an insoluble blend of the two materials. Generally, the polymer is filled with a conductive material in an attempt to increase the electrical conductivity and heat transfer of the medium. The percolation theory is commonly used to describe the conductivity of systems with a conductive phase dispersed in an insulator.^{69,70} According to this theory, at a critical volume concentration of the conducting phase the composite becomes electrically conductive. The threshold is found to be dependent on the type, shape, and dimensions of the particles as well as on the interaction, if any, between the conducting species and the matrix.⁷¹ For some systems it has been observed that the formation of a continuous network of the conducting material is not required. Some authors propose that carriers can "tunnel through the insulating regions of the polymer".⁷² Fiber-like additives have been shown to decrease the critical volume loading by providing an

almost continuous path for electrons and heat. However, high loadings are generally required, and this results in very poor mechanical properties.

Organic polymers are most commonly used as thermal and electrical insulators. However, the combination of thermal and electrical conductivity with polymer properties such as flexibility, low weight, and ability to form moldable parts is becoming increasingly attractive and extensive research is being conducted in this area. Polymers with extended conjugation such as polyacetylene and polypyrrole, organometallic polymers (discussed above), and doped systems are being investigated. Materials of this type with sharply lower electrical resistance and faster heat transfer can be employed in electromagnetic interference shielding, static charge dissipation, and heat dissipation. This last property is especially important in industries such as the automotive in which greater thermal conductivity implies shorter cycle times and, therefore, reduced costs.

A more fundamentally important area than filled systems is the synthesis of metal doped polymers via processing from an initially homogeneous blend. Metal salts, metal complexes, organometallic compounds, as well as metals can be incorporated into neutral polymers in this manner. Of the metal modified neutral polymer systems, polyimides have received a great deal of attention. In 1959 Angelo⁷³ patented the addition of metal ions in the form of coordination complexes to a variety of aliphatic and aromatic polyimides. The process involved the formation of the polyamic acid, addition of the metal compound, followed by the conversion to the metal salt, metal, or metal oxide containing polyimide. Although some physical properties of these modified polyimides were reported in the patent, information about the thermal stability, glass transition temperature, state of the metal, thermal conductivity, etc. was absent. Since then, a great deal of work has been devoted to the detailed study of these systems. Taylor and coworkers have extensively investigated the incorporation of a wide variety of metals in different forms ($\text{Pd}(\text{S}(\text{CH}_3)_2)_2\text{Cl}_2$, $\text{Pt}(\text{S}(\text{CH}_3)_2)_2\text{Cl}_2$, AgNO_3 , $\text{HAuCl}_4 \cdot 3\text{H}_2\text{O}$, CoCl_2 ,...) into aromatic

polyimides.⁷⁴⁻⁷⁷ The polyimides studied were mainly derived from 3,3',4,4'-benzophenone tetracarboxylic acid dianhydride (BTDA), 1,2,4,5-benzenetetracarboxylic acid dianhydride (PMDA), and 4,4'-oxydianiline (ODA), the structures of which are shown in Figure 2.8.

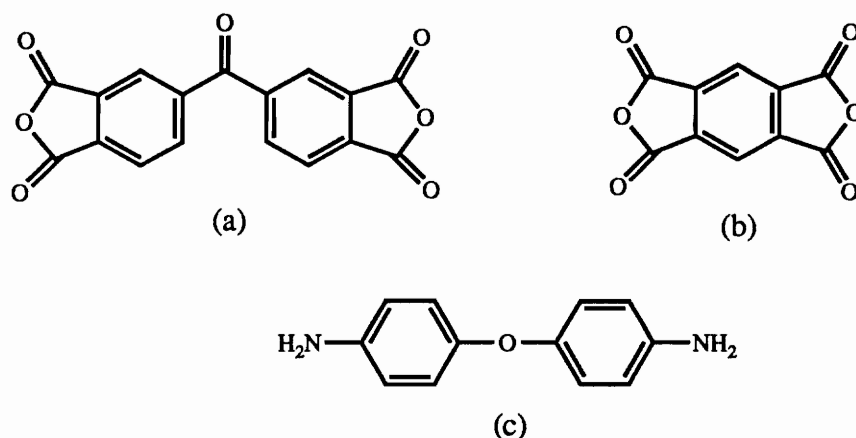


Figure 2.8 Dianhydrides and Diamines (Taylor and Coworkers):

(a) BTDA, (b) PMDA, (c) ODA⁷⁴⁻⁷⁷

The general preparation approach consisted in the synthesis of the poly(amic acid) intermediate in an aprotic polar solvent (DMAc) followed by intimate mixing of the additive in the poly(amic acid), subsequent thermal imidization, and *in situ* decomposition of the additive to the metallic state or the metal oxide generating the polyimide metal composite film. The extent of conversion of the metal salt was determined by elemental analysis, and it was observed that while some dopants were mainly converted to the metallic state (Pt, Pd, Ag, Au) others were typically converted to the metal oxide (CuO, SnO₂, Co₃O₄).

Much of this work was directed towards increasing the surface conductivity of the polyimides for potential application of these materials in aerospace and electronics

industries. In order to decrease surface resistivity, the connectivity of the dopant at the surface as well as its migration to the surface must be maximized. For this reason, the structure of the composite films was studied in detail using X-ray photoelectron spectroscopy (XPS), Auger electron spectroscopy (AES), scanning electron microscopy (SEM), and transmission electron microscopy (TEM). A structural model was proposed for the modified polyimides, according to which the films are divided into three different regions:

- 1- The bulk of the film- Predominantly polyimide with some converted or nonconverted metal additive.
- 2- A depletion zone- Oxide- or metal-rich coat 'interspersed' with polyimide.
- 3- Polymer overlayer- Surface region with predominantly polyimide and a gradient of the metal additive.

Not all these layers were found to be present in every system, and the spatial distribution of the dopant which varied for different polyimide-additive pairs was found to be highly dependent on the processing conditions. Variables such as the decomposition atmosphere (dry versus moist and air versus nitrogen) and the conversion temperature were found to affect the structure of the composite and, therefore, the surface and bulk conductivities of the material. Furthermore, in some cases different compositions were observed for the film side exposed to the curing atmosphere (air-side) and that in contact with the glass (glass-side). The thermal stability, glass transition temperature, and mechanical properties of the composites were also investigated.

Perhaps a study conducted on the modification of BTDA-ODA polyimide with a series of different metal salts best serves to illustrate the varying effects of different additives on the same system.⁷⁵ The dopants incorporated were tris(acetyl acetonato)aluminum(III) ($\text{Al}(\text{acac})_3$), tetrachloropalladate (II) (Li_2PdCl_4), silver nitrate (AgNO_3), gold iodide

(AuI₃), and tin chloride (SnCl₂ · H₂O). The incorporation of the metal additives caused an increase of 30-40°C in the glass transition of the polyimide with the exception of the tin salt for which no change in the T_g was observed compared to the unmodified polyimide. However, the increase in the softening temperature did not correlate with the metal salt content. XPS studies suggest that while some additives (Pd, Au, and Ag salts) are converted to the metallic state during the curing stage, others (Li, Al, and Sn salts) are ionic in the doped polyimide. In most cases the thermo-oxidative stability of the polyimide was not greatly affected by the dopant. Only for films containing AgNO₃ and Li₂PdCl₄ was the stability significantly reduced. The surface and volume resistivities were reduced relative to the polyimide alone only for the composites containing SnCl₂ and Li₂PdCl₄. Lastly, in terms of the mechanical properties, the tensile strength and yield strength were improved by the incorporation of the additive with the exception of the AgNO₃ system. It is apparent from this study that no generalizations can be made about the consequences of incorporating a metal salt into this aromatic polyimide. The effect of a metal salt dopant on a specific material property varies from one additive to another.

In another study, the introduction of Pd(S(CH₃)₂)₂Cl₂ into a polyimide film resulted in the formation of a metallic surface accompanied with a ten fold increase in the surface conductivity relative to the unmodified polymer.⁷⁸ Films modified with HAuCl₄ · 3H₂O presented a metallic surface underneath a polyimide layer which improved the adhesion to the metal and enhanced the barrier to mechanical abrasion.⁷⁷ Magnetic surface polyimide films were obtained by modification of BTDA-ODA poly(amic acid) with tris(acetyl acetonato)iron (III), Fe(acac)₃.⁷⁹ According to the authors, the heat treatment to form the polyimide resulted in the conversion of the iron additive on the surface to γ-Fe₂O₃ which was believed to be responsible for the observed magnetic properties. In these systems no specific interactions between the metal compound and the polymer were investigated. The polymer only served as a support to hold the additive together.

In a different study, however, polyimides containing potential coordinating groups in the backbone were employed in an attempt to obtain a regular dispersion of the metal and, therefore, enhance the bulk conductivity of the material.⁸⁰ BTDA dianhydride was reacted with several diamines and doped with a wide range of Co(II) and Co(III) additives. The heteroatom-containing diamines employed are shown in Figure 2.9. ODA was also used for comparison.

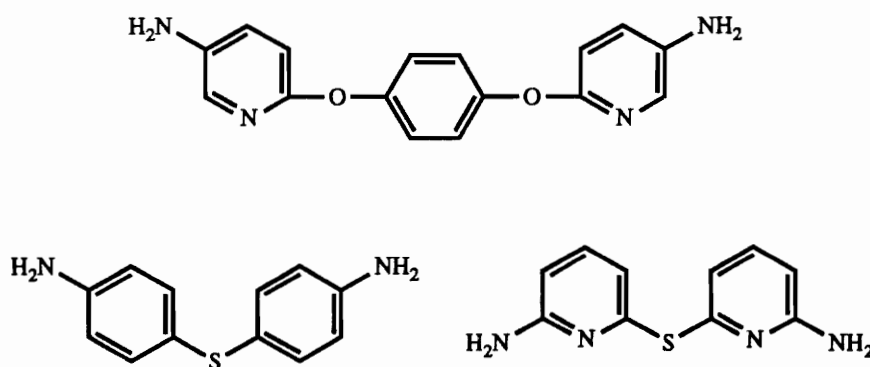


Figure 2.9 Heteroatom Containing Diamines⁸⁰

The effect of the different cobalt compounds on the glass transition temperature and the thermal stability was studied using the BTDA-ODA system. With all the additives there was an increase in the apparent softening temperature relative to the unmodified polyimide, and a decrease in the thermal decomposition temperature. It was observed that the elevation of the T_g was greater and the decomposition temperature lower for most of the bulky ligands. The same increase in the T_g and decrease in thermo-oxidative stability was found upon modification with CoCl_2 for polyimide systems prepared using a coordinating diamine. However, the increase in the glass transition temperature was not as pronounced. From XPS and Auger spectroscopy studies it appears that in the BTDA-ODA/ CoCl_2 system the majority of the cobalt migrates to the air-side surface and is converted to the

oxide (Co_3O_4), whereas, no surface migration or modification of the additive seems to take place for the coordinating polyimides. It appeared that the interaction between the metal salt and the polymer prevented the diffusion to the surface and the transformation of the additive. This interaction, however, was not demonstrated or studied.

The dispersion of metal compounds in a polymer matrix can be more effectively achieved through specific chemical interactions with the additive. Complex formation between metal compounds and a variety of macromolecules have been reported. These polymer systems include poly(amide)s, poly(vinyl pyridine)s, poly(vinyl alcohol), poly(alkylbenzimidazole)s, poly(ether)s, polyphosphines, and rigid-rod polymers such as poly(p-phenylenebenzobisthiazole). Before discussing some of these systems it is important to recognize the effect of a macromolecular ligand on the efficiency of complex formation. The ability to complex will be determined not only by the character of the ligating groups on the polymer but also by their location and distribution along the chain. If the complexing atoms are close together within the chain, a number far below the total number of groups will be used in complexation. The efficiency will also be lower if the groups are situated in the chain such that steric hindrance becomes a problem. The flexibility of the polymer chain as well as extent of cross-linking, if any, are also very important parameters. In general, the net result of using polymeric ligands is the generation of undersaturated complexes and the formation of coordination centers of different symmetries.

The concept of macromolecular complexes has often been used in an attempt to synthesize semiconductive organic polymers. Copper(II) chelates with polymers such as poly(vinyl alcohol) (PVA), poly(acrylamide) (PAAm), and poly(vinyl pyrrolidone) (PVP) have been used to prepare highly surface conducting films. Kakinoki *et al.* examined poly(acrylamide)⁸¹ chelates with copper salts including $\text{CuCl}_2 \cdot 5\text{H}_2\text{O}$, $\text{CuSO}_4 \cdot 5\text{H}_2\text{O}$, $\text{Cu}(\text{NO}_3)_2 \cdot 3\text{H}_2\text{O}$, and $\text{Cu}(\text{OOCCH}_3) \cdot \text{H}_2\text{O}$. The complexes themselves showed very

high surface resistivities ($> 10^9 \Omega \text{ cm}^{-2}$). However, when treated with iodine the surface resistivity of the chelate was highly decreased ($10^3 \Omega \text{ cm}^{-2}$). Iodine is known to form charge transfer complexes with PAAm, accordingly the conductivity increase was attributed to a combination of the metal chelate and the charge transfer complex since the PAAm-I₂ complex is not in itself conductive. The authors also succeeded in the preparation of PVA-Cu(II) chelates which again showed a large conductivity increase when modified with iodine.⁸² The resistivity was found to vary with amount of salt and iodine. Potassium hydroxide was also added to both polymer complexes in order to study the effect of ligand exchange. In the case of the PAAm system the resistivity was increased upon ⁻OH addition, whereas an increase in the conductivity was observed for the PVA complex with addition of an equimolar amount of KOH to copper(II)chloride. Other salts tested (ferric, stannic, and chromous salts) did not result in an increase of the conductivity.

Inspired by this work and in order to better understand this effect, Sumita and coworkers studied the structure of these complexes using visible and UV spectroscopy and electron spin resonance (ESR).⁸³⁻⁸⁵ In addition to the PVA-Cu(II) and PAAm-Cu(II) complexes, they studied copper chelates with poly(vinyl pyrrolidone). The polymer-Cu(II) films were prepared by the addition of OH⁻ ions. The structure of these polymer-Cu(II) chelates was found to be greatly determined by the interactions among Cu(II) ions. Here we will only describe the observations for the PVA-Cu(II) complex since similar results were obtained for the other two systems. In some cases, segregated particles due to 'coagulation' in the PVA-Cu(II) complex were observed by optical scanning microscopy. The existence of coagulation was believed to result from the crosslinking of linear chains consisting of Cu²⁺ ions bridged with OH⁻ ions and was dependent on the relative concentrations of copper ion and OH⁻ to polymer units. It was postulated that, in addition to the formation of a monomeric polymer-Cu(II) complex coordinated by four OH residues in the PVA chains

(Figure 2.10 a), polynuclear complexes with single and double bridges are formed (Figure 2.10 b-e).

When coagulation was observed, a whiteish substance appeared on the film surface upon treatment with iodine. X-ray studies showed this reaction product was γ -CuI. The appearance of high conductivity in these films was attributed to CuI formed on the film surface.

Another very interesting research area involves the solubilization in aprotic organic solvents of rigid-chain polymers containing heteroatom groups in the presence of Lewis acids (AlCl_3 , GaCl_3 , FeCl_3 , SbF_5 ...) ⁸⁶⁻⁸⁸ The structures of some of the rigid-chain polymers investigated are depicted in Figure 2.11.

These rigid-rod polymers possess excellent mechanical properties as well as thermo-oxidative stability and good chemical resistance to solvents and strong acids. The rigid conformation of these polymers results in very efficient packing of the chains and strong intermolecular van der Waals forces which account for the exceptional mechanical properties observed. However, these same structural features are responsible for the high intractability of these materials, eliminating the possibility of melt processing. These materials show no glass transition temperature below the decomposition temperature, and are only soluble in concentrated acids (i.e. methanesulfonic, trifluoromethanesulfonic, and chlorosulfonic acids).

The polymers studied contain main chain heteroatoms such as oxygen, nitrogen, phosphorus, and sulfur with nonbonding electrons (Lewis bases) which are able to donate electron density to the electron deficient metal centers to form coordination complexes. In

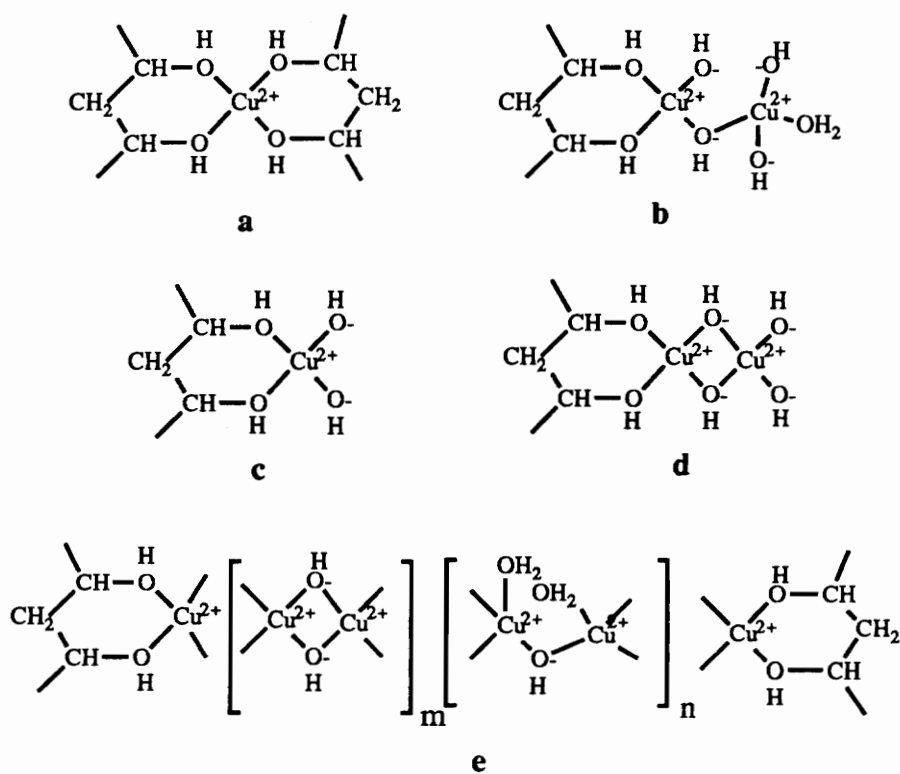


Figure 2.10 Postulated Structures of Complexes (water molecules weakly coordinated in the axial position are not depicted)⁸³

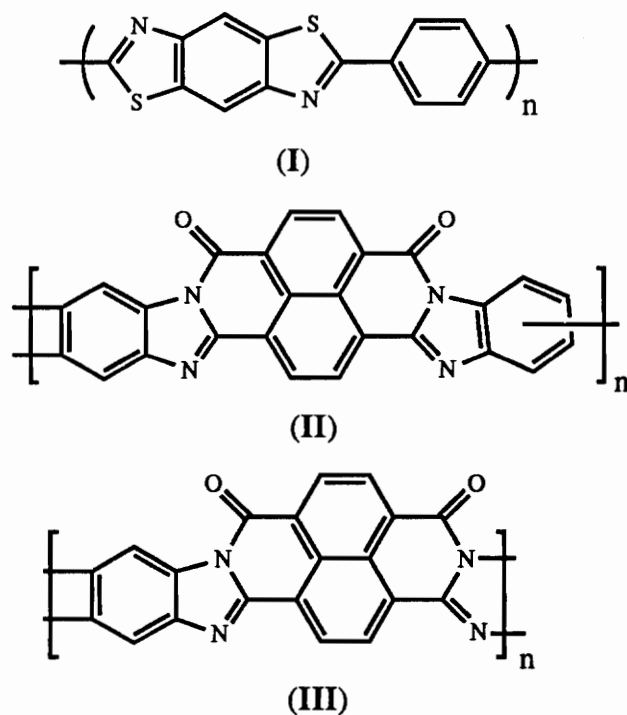


Figure 2.11 Examples of Rigid Chain Polymers Studied by Jenekhe and Coworkers:

- (I) Poly(*p*-Phenylenebenzobisthiazole), PBZT
- (II) Semiladder Poly(Benzimidazole-Benzophenanthroline), BBB
- (III) Ladder Poly(Benzimidazole-Benzophenanthroline), BBL⁸⁶⁻⁸⁸

an effort to resolve the intrinsic processing limitation of these intractable polymers, a solution of a given concentration of the metal halide in an aprotic organic solvent was added to a known weight of polymer in a moisture free atmosphere. The solution was then stirred until complete dissolution of the polymer. Stirring was conducted at room temperature or 60°C depending on the concentration of the metal solution. Of the metal salts and organic solvent combinations investigated those of FeCl₃, AlCl₃, and GaCl₃ in nitroalkanes were found to be the most effective, and dissolutions comparable to those of the polymer in methanesulfonic acid were observed. The ratio of the Lewis acid to the repeat unit of the polymer was typically varied from 0:1 to 4:1 with an increase in metal salt resulting in more efficient dissolution. Solid complexes were prepared by solution casting on a glass plate followed by solvent evaporation.

Dramatic lowerings of the glass transition temperatures of these systems were observed following complexation. The authors rationalize the depression in the T_g in terms of a disruption of the preexisting strong intermolecular forces upon complexation resulting in the separation of the chains and a corresponding increase in the free volume. These results suggest that "intermolecular forces can have a dominant influence on the glass transition temperature of polymers".

Furthermore, by immersion of the solid complexes in suitable stronger Lewis bases than the polymer ligand, decomplexation occurs with the regeneration of the pristine polymers and recovery of the T_g as well as other physical properties.

This study was also extended to other polymers with strong intermolecular forces such as poly(amide)s with N-H groups hydrogen bonded to C=O groups in adjacent chains. The complexation of GaCl₃ with several aliphatic poly(amide)s including nylon 6, nylon 11, and nylon 6,6, as well as an amorphous aromatic poly(amide), poly(trimethylhexamethyleneterephthalamide) (PTMHA) (Figure 2.12), was studied.^{89,90}

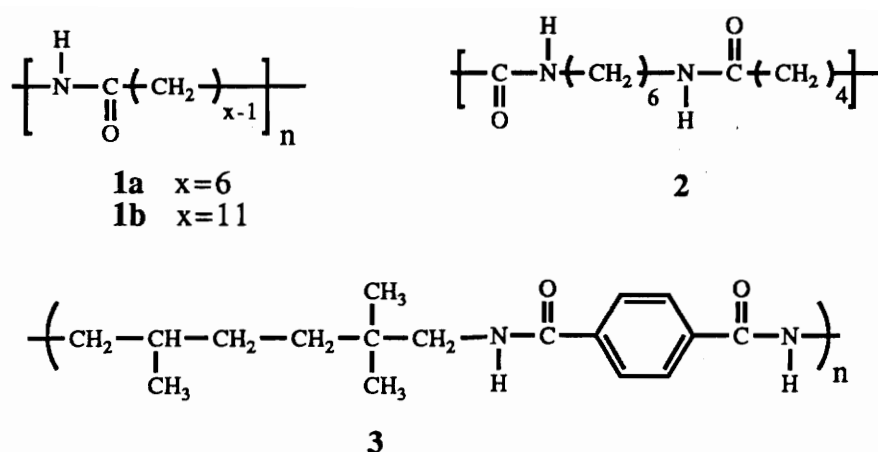


Figure 2.12 Poly(Amide)s Investigated: 1a) Nylon 6, 1b) Nylon 11, 2) Nylon 6, 6,

3) PTMHTA^{89,90}

Infrared spectroscopy studies showed a general increase of the N-H stretching frequency to higher energy accompanied by a decrease in the intensity and a broadening on Lewis acid complexation indicating the breaking of the hydrogen bonding by the formation of the coordination complex which results in the freeing of the N-H. Therefore, the electron withdrawing effect of the Lewis acid is greater than that of the N-H---O=C hydrogen bond, in accordance with the observed decrease to lower energy in the C=O bond stretch upon complex formation. Reductions in the glass transition temperatures of these poly(amide)s were also observed as a consequence of the incorporation of the metal salt. Lastly, hydrogen bonds could be reformed through decomplexation by precipitation in water or methanol.

Acierno *et al.* have investigated the complexation of unoriented nylon-6 with lithium chloride and lithium bromide.⁹¹⁻⁹³ These inorganic salts strongly depress the melting temperature and rate of crystallization of the polyamide.⁹¹ The effect of incorporation of

LiCl and LiBr (compositions varying from 0 to 7% w/w) on the melt viscosity and the glass transition temperature of a nylon-6 sample was studied. The polymer-salt composites were prepared by addition of the polymer to a methanol solution of the salt, followed by a heat treatment to remove the solvent and homogenize the components above the melting temperature. The samples were then cooled back to room temperature and stored in a moisture-free atmosphere. Initially, the addition of the salts was found to have no effect on the softening temperature of the polymer. However, strong interactions of the lithium salts with the polymer were apparent from the observed reduction of the specific volume of the molten mixture as compared to the expected value from simple additivity. Lithium chloride was especially effective at reducing the specific volume. In addition, melt viscosity in *m*-cresol at 25°C increased upon modification with the alkali metal salts. If the volume contraction were to be existent also at lower temperatures and near the glass transition temperature, it would be expected that the softening temperature would increase contrary to what was observed experimentally. Later experiments showed that the lithium salts did indeed increase the glass transition temperature of nylon-6 as long as moisture was completely excluded from the system. In the strict absence of moisture, the addition of 4% w/w LiCl resulted in a 25°C increase in the T_g of nylon-6. The earlier results were attributed to the absorption of moisture by the sample during measurements.

Complexation was also reported to bring about an increase in the glass transition temperature of several poly(ether)s in a separate study. Poly(propylene oxide) $[-(\text{CH}_2\text{CH}(\text{CH}_3)\text{O})-]$ and poly(ethylene oxide) $[-(\text{CH}_2\text{CH}_2\text{O})-]$ have been shown to complex with a number of metal compounds, e. g., NaI^{94} , ZnCl_2 and CoCl_2^{95} , and FeCl_3 .⁹⁶ Some polymer/metal salt combinations have been reported to be ionically conducting.⁹⁴ Coordination with these polymers is exceptional not only due to the presence of the oxygen ether atom (Lewis base), but also the optimal spacing of the heteroatom in the chain. A common observation for these polyethers is a substantial increase in the T_g on complexation with certain metal salts. Moacanin and Cuddihy⁹⁷ induced large increases in

the glass transition temperature of both high and low molecular weight poly(propylene oxide) with addition of lithium perchlorate to the polymer. The changes in T_g were attributed to the strong interactions between the ether atoms and the metal salt which cause a decrease in the free volume. Wetton and James⁹⁵ discovered the same trend for complexes of poly(propylene oxide) with $ZnCl_2$ and $CoCl_2$. The elevation of the softening temperature was more substantial for the composite films with $CoCl_2$. In the case of the $ZnCl_2$ coordination polymers, the authors suggest the formation of a five-membered intramolecular chelate ring which would decrease the flexibility of the chain and, consequently increase the T_g (Figure 2.13).

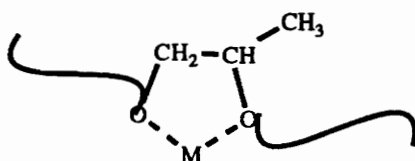


Figure 2.13 Five-Membered Intramolecular Chelate Ring⁹⁵

In the $CoCl_2$ systems intramolecular as well as intermolecular interactions via the coordination of two adjacent oxygens from three different polymer chains resulting in an octahedral geometry around the metal center would explain the greater increase in the glass transition temperature observed (Figure 2.14).

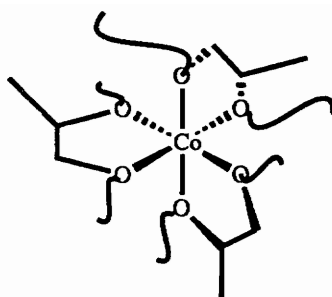


Figure 2.14 Octahedral Coordination around the Cobalt Center⁹⁵

The effect of modification of semicrystalline poly(tetramethylene glycol) with ZnCl_2 on the melting temperature and the glass transition temperature was also studied. The melting temperature was found to decrease with increasing metal salt content with the amount of crystallinity also decreasing until at 15 mole % loading the material becomes amorphous. The T_g is also seen to increase although to a lesser extent than the previously discussed systems implying weaker interactions.

The pyridine and bipyridine moieties have also been used in the preparation of coordinating polymers. The coordinative behavior of poly(4-vinylpyridine), poly(4-Vpy), and poly(2-vinylpyridine), poly(2-Vpy), towards a series of metal dichlorides (CoCl_2 , ZnCl_2 , NiCl_2 , and CuCl_2) has been investigated.⁹⁸ The solid polymer-metal chloride complexes obtained from solution were studied in terms of stoichiometry, stereochemistry of the coordinated metal ion, and intermolecular versus intramolecular complexation with the polymer chain.

Atactic poly(4-Vpy) and poly(2-Vpy) were obtained via free radical polymerization of the corresponding vinylpyridines. Isotactic polymers were also studied but will not be discussed here. The polymer-metal complexes were prepared by precipitation of a refluxed homogeneous solution of the polymer and the metal halide in ethanol (1: 1 molar ratio of polymer unit: metal), and the final stoichiometry of the complexes was determined by

elemental analysis. The coordination number and geometry of the ligand donor atoms in the coordination sphere of the metal as well as the effect of the position of the nitrogen atom in the ring (2- or 4-) were investigated. The complexes of the monomeric vinylpyridine counterparts have been extensively studied and were used for comparison with the polymeric complexes. The configurational structures of all except the $\text{Cu}(2\text{-Vpy})\text{Cl}_2$ (unstable in X-ray beam) monomer complexes were available from earlier works. In all cases, nonionic complexes are formed with the chlorine coordinated to the metal.

Due to the constraints of the polymeric ligands, as discussed in an earlier section, it was found that all the complexes had from one to two uncoordinated vinylpyridine units per metal halide. The Co(II) and Zn(II) polymeric complexes resembled those of the monomeric complexes, and their structures were assigned on the basis of color and magnetic properties in relation to the simple complexes. The blue cobalt-poly(Vpy) complexes were assigned a tetrahedral geometry. This was also the case for the white ZnCl_2 complex. On the other hand, the behavior of the Cu(II) and Ni(II) complexes did not parallel that of the monomeric analogs. Even though the determination of the structure of these polymer chelates was not conclusive, from the available observations several structures were proposed. A square-planar copper in chloride-bridged structures was suggested for the Cu(II) chelates (Figure 2.15).

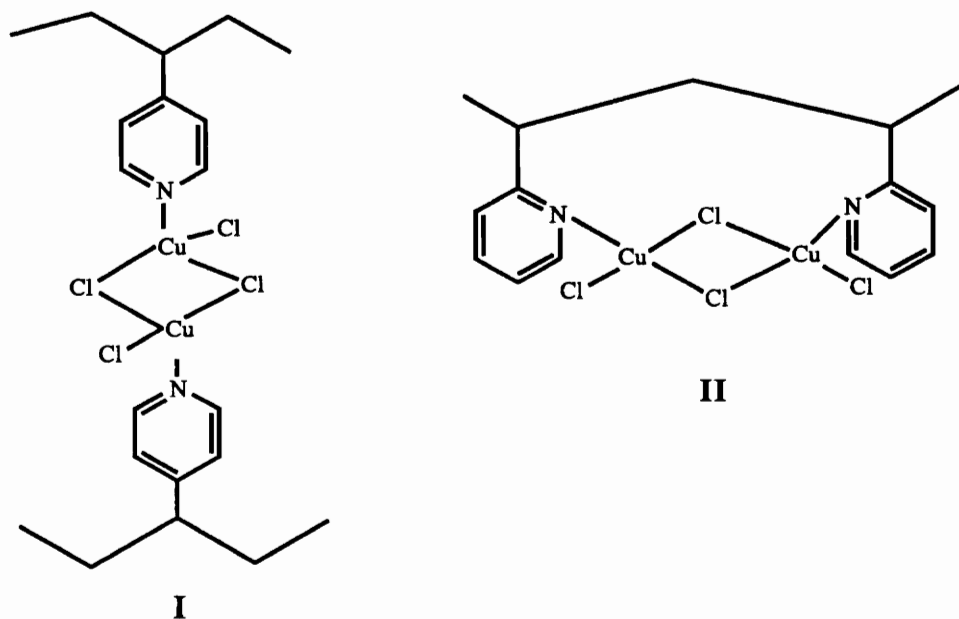


Figure 2.15 Proposed Structure for the CuCl_2 -Poly(Vinylpyridine) Complexes⁹⁸:

I. CuCl_2 -Poly(4-Vinylpyridine) Complex

II. CuCl_2 -Poly(2-Vinylpyridine) Complex

Two different forms were postulated for the Ni(II)-poly(4-Vpy) complex. These are depicted in Figure 2.16.

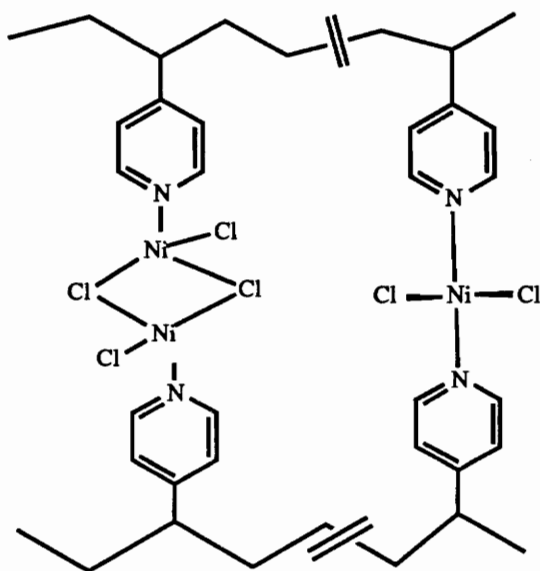


Figure 2.16 Proposed Structures for the NiCl₂-Poly(4-Vinylpyridine) Complex⁹⁸

For the atactic poly(2-Vpy) complex, on the other hand, the intramolecularly crosslinked structure shown in Figure 2.17 was proposed.

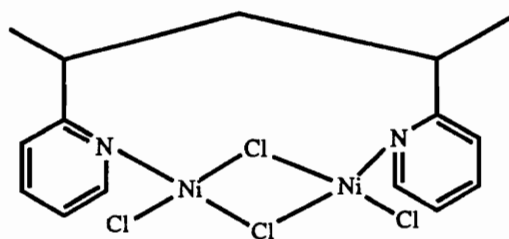
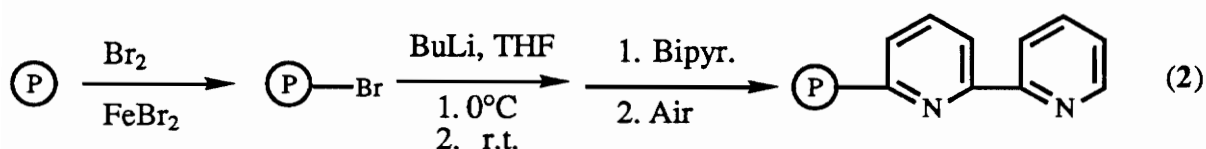


Figure 2.17 Suggested Geometry for NiCl₂-Poly(2-Vinylpyridine) Complex⁹⁸

The polymer complexes described above were all found to be crosslinked by the metal chloride. According to the authors, the network nature of these systems is consistent with the absence of a detectable glass transition temperature. Specific thermal data was not given for these systems, however, it was observed that the CuCl_2 complex was far less thermally stable than any of the other complexes.

Bipyridine which is a well known chelating agent has also been incorporated into polymer chains in an attempt to achieve specific interactions with metals. Neckers and coworkers have reported the synthesis of bipyridine attached to 2% crosslinked polystyrene (Equation 2).⁹⁹



Although the polymer ligand is easily prepared and the complexation of metals salts is remarkably simple, these systems suffer from leaching of the metal compound which limits its applications. These same authors have reported the synthesis of a bipyridine-containing polymer from 4-methyl 4'-vinylbipyridine, in addition to polymers prepared from 4-4'-diaminobipyridine for use in catalytic reactions as will be described in the next section.¹⁰⁰

There are also examples of coordination of metal compounds to unsaturated carbon double bonds in a polymer chain. Berger and Manuel studied the coordination of iron carbonyls ($\text{Fe}_3(\text{CO})_{12}$, $\text{Fe}(\text{CO})_5$) with polydienes such as *cis*-4-poly(butadiene) and showed that the polymer-metal composites prepared under a wide range of conditions contained tricarbonyl(conjugated diene) iron units (Figure 2.18) as well as uncomplexed poly(butadiene) units.¹⁰¹

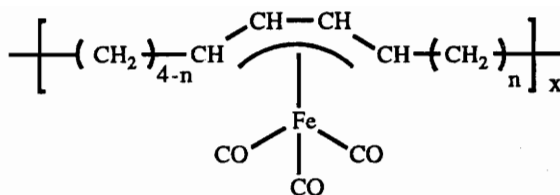


Figure 2.18 Tricarbonyl(Conjugated Diene) Iron Unit

Geometrical isomerization catalyzed by the iron carbonyl was found to compete with the complex formation reaction, with low temperature and acidic conditions favoring the isomerization.

Throughout this review the metal complex formation with synthetic organic polymers has been the primary focus. However, this type of interactions is also important in inorganic polymers as well as naturally occurring macromolecules. Doubly-bridged polymeric metal phosphinates with general structure shown in Figure 2.19 are an example of inorganic metal-containing polymers.¹⁰²

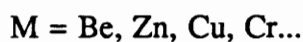
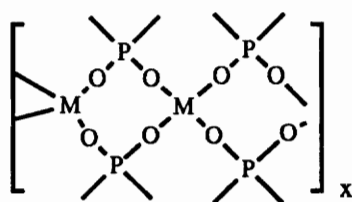
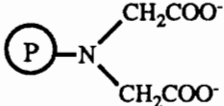
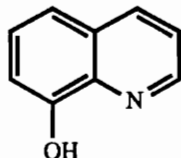


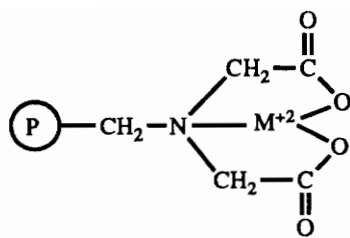
Figure 2.19 General Structure of Polymeric Phosphinates

Many other examples of metal-modified inorganic macromolecules such as polymeric sulfur, borates, and silica have been reported. Macromolecular complex formation also

takes place with naturally occurring polymers such as proteins (DNA, RNA, hemoglobin,...).¹⁰³ Furthermore, Carraher *et al.* have modified a variety of polysaccharides through coordination of metals to the hydroxyl groups in these molecules.¹⁰⁴

All the systems described above in which specific interactions or coordination between the metal compound and the polymer are present have the potential for generation of polymer films with molecularly dispersed metal particles. The possible applications for this type of materials are numerous. The uses of these materials as electro-active materials are very important and have already been discussed. Chelate-forming polymers can also be employed as ion exchange resins due to their ability to bind to metal ions in solution. Unlike conventional nonchelating ion-exchange resins in which the exchange is controlled by the relative charges and sizes of the exchanging ions, in coordinating polymers the exchange is due to the formation of strong bonds. Crosslinked functionalized polystyrenes are most frequently used for this application. Some of the functionalities which are

commonly introduced include iminodiacetic acid,  oxime,  ; and amine derivatives.¹⁰⁵ The selectivity of these resins varies with ligating group as well as conditions such as temperature, solvent, and pH. These resins are most widely used in the preconcentration of trace elements from extremely dilute solutions, removal of trace metals from seawater, selective separation of metal ions, and analytical determination of metal ions in solution. The first commercially available chelating resin was the Domex A-1 resin produced by Dow Chemical Corporation. The iminodiacetate group allows transition metals to coordinate forming five-membered rings as shown in Figure 2.20.



M = Cu(II), Ni (II), Fe(III)...

Figure 2.20 Metal Coordinated Domex A-1 Resin

Gas separation through membranes is another field in which these systems might prove useful. Since the permeation of a gas or mixture of gases through a polymer membrane takes place via a solution-diffusion process, the presence of metal in a polymer matrix can alter this process thermodynamically as well as kinetically. The solubility of the penetrant which is related to the affinity of the gas toward the membrane as well as the diffusion which is dictated by the mobility through the free volume of the film will be highly affected by the presence of metal. Different polymer-metal composites with certain metal contents will affect the permeation differently. Specific studies will determine the particular effect a given polymer/metal composite will have on the selectivity and permeability of a certain mixture of gases.

2.3.5 Polymer-Supported Catalysts

A very important application of polymer chelates involves their use as polymer-supported catalysts. The anchoring of reagents to insoluble polymer supports for solid phase synthesis was pioneered by Merrifield in the synthesis of polypeptides.¹⁰⁶ This concept was quickly extended to polymer-bound metal complexes for use in catalysis. Although homogeneous catalysts are widely used industrially, there are problems associated with the design of chemical processes that use these reagents. Generally, the high cost and toxicity

of these catalysts demand its recovery. Therefore, a separation step must be included to remove the catalyst from the product. For this reason, there is an extensive literature for the immobilization of homogeneous catalysts.¹⁰⁷⁻¹¹² Typically, polymer-bound catalysts are prepared by attaching a ligand group such as a phosphine to an organic polymer onto which the soluble metal complex is bound. Ligand-functionalized polymers can be obtained via modification of a preformed polymer, as well as via polymerization of a monomer with a pendant ligand. Phosphine-modified polystyrene is by far the most commonly used organic support, but other modified polymers such as polyvinyl chloride, soluble polysiloxanes, and polyphenylene-isophthalamide have also been described. The polymer-bound complexes can be soluble or crosslinked systems. Of the reported polymer anchors containing the phosphine ligand, only a few contain the phosphine in the polymer backbone, and those which do generally have very low molecular weights, and lack thermal as well as mechanical stability.

With a few exceptions, immobilized catalysts generally suffer compared to their homogeneous counterparts with respect to reactivity and selectivity.¹¹³ In several cases, polymer supports have been shown to enhance reaction rates relative to their homogeneous counterparts by retarding the agglomeration of the catalyst, and stabilizing reactive coordinatively unsaturated metallic sites. For instance, Pittman demonstrated a remarkable rate enhancement in the dimerization-methoxylation of butadiene to 1-methoxyocta-2, 7-diene by anchoring a palladium (0) complex onto a styrene resin with 1% divinylbenzene crosslinking.¹¹² The improved activity is attributed to site isolation, as well as the promotion of coordinative unsaturation by the polymer support. In other cases, securing the catalytic complex with a polymer anchor has resulted in a change in selectivity of the catalyst. For example, the selectivity to aldehydes in the catalyzed hydroformylation reaction of hexene-1 was enhanced by anchoring the $\text{Rh}(\text{CO})_2(\text{acac})$ complex to a styrene/divinylbenzene copolymer modified with a phosphine ligand.¹¹⁴ In a separate experiment, $\text{Pd}(\text{II})$ chloride bound to a phosphinated polystyrene was found to be more

active in the heterogeneous catalysis of the hydrogenation of a series of conjugated dienes than an analogous homogeneous catalyst.¹¹⁰ Neckers and coworkers studied the catalysis of olefin hydrogenation by a palladium(0) complex of a polyurea prepared from 4,4'-diaminobipyridine.¹⁰⁰ This catalyst system was shown to have good activity and excellent long term stability with no loss of catalytic activity after 42 successive catalytic cycles. The less hindered double bonds were reduced preferentially, and due to the polar nature of the backbone it was also observed that the hydrogenation rate increased with increasing polarity of the medium.

3.0 Experimental

3.1 Purification of Solvents

3.1.1 N,N-Dimethylacetamide (DMAc)

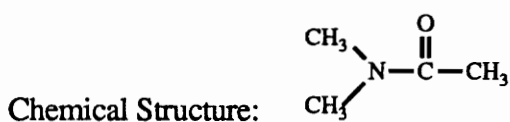
Supplier: Fisher Scientific

Molecular Formula: C_4H_9NO

Molecular Weight, g/mol: 87.14

Boiling Point, °C/mm Hg: 164/760

Density, g/cc: 0.937



Purification procedure: Sufficiently pure and dry solvent for the polycondensation reactions was obtained after stirring over calcium hydride overnight, followed by vacuum distillation at around 60°C using a vacuum aspirator. After discarding the first fraction, the constant boiling fraction was collected as a colorless liquid. Typically, DMAc was stored in a round bottom flask fitted with a rubber septum under anhydrous nitrogen pressure.

3.1.2 Tetrahydrofuran (THF)

Supplier: Fisher Scientific

Molecular Formula: C_4H_8O

Molecular Weight, g/mol: 72.11

Boiling Range, °C/mm Hg: 65-67/760

Density, g/cc: 0.886



Purification Procedure: Careful distillation of this ether solvent from sodium/benzophenone purple complexes afforded adequately dry solvent for Grignard syntheses. After discarding the first fraction, the constant boiling fraction was collected as a colorless liquid and stored under a nitrogen atmosphere in a flask sealed with a rubber septum.

3.1.3 Chlorobenzene

Supplier: Fisher Scientific

Molecular Formula: C_6H_5Cl

Molecular Weight, g/mol: 112.56

Boiling Point, °C/mm Hg: 132/760, 22/10

Specific Gravity (20°C): 1.1058 (relative to water at 4°C)



Purification Procedure: Chlorobenzene for use in the phosphine oxide reduction reactions was vacuum distilled near 35°C over calcium hydride using a vacuum aspirator. After discarding the first fraction, the constant boiling fraction was collected as a colorless liquid and stored under a nitrogen atmosphere in a flask sealed with a rubber septum.

3.1.4 Toluene

Supplier: Fisher Scientific

Molecular Formula: C_7H_8

Molecular Weight, g/mol: 92.14

Boiling Point, $^{\circ}C/mm\ Hg$: 110.6/760

Density, g/cc: 0.8669



Purification procedure: This solvent was purified by distillation under N_2 from sodium benzophenone ketyl, and stored under anhydrous conditions.

The following solvents were used as received from Fisher Scientific: methanol, acetone, diethyl ether, chloroform, and hexanes.

3.2 *General Reagents*

3.2.1 Potassium Carbonate

Supplier: Fisher Scientific

Molecular Formula: K_2CO_3

Molecular Weight, g/mol: 138.21

Melting Point, $^{\circ}C$: 891

Density, g/cc: 2.428

Purification Procedure: Potassium carbonate was used as supplied without further purification.

3.2.2 Iron(III)Chloride (98%)

Supplier: Aldrich

Molecular Formula: FeCl_3

Molecular Weight, g/mol: 162.21

Melting Point, °C: $>300^\circ\text{C}$ (decomposes)

Purification Procedure: Iron(III)chloride was used as received without further purification, and was stored under anhydrous conditions.

3.2.3 Cobalt(II)Chloride (97%)

Supplier: Aldrich

Molecular Formula: CoCl_2

Molecular Weight, g/mol: 129.84

Melting Point, °C: 735

Purification Procedure: Cobalt(II)chloride was used as received without further purification, and was stored under anhydrous conditions.

3.2.4 Copper(II)Chloride (99.999%)

Supplier: Aldrich

Molecular Formula: CuCl_2

Molecular Weight, g/mol: 134.45

Melting Point, °C: 620 (Partial degradation $> 300^\circ\text{C}$)

Density, g/cc: 3.386

Purification Procedure: Copper(II)chloride was used as received without further purification, and was stored under anhydrous conditions.

3.2.5 Zinc(II)Chloride (99.999%)

Supplier: Aldrich

Molecular Formula: ZnCl_2

Molecular Weight, g/mol: 136.28

Melting Point, °C: 293

Density, g/cc: 2.907

Purification Procedure: Zinc(II)chloride was used as received without further purification, and was stored under anhydrous conditions.

3.2.6 Phenylsilane

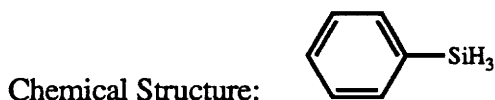
Supplier: Aldrich

Molecular Formula: $\text{C}_6\text{H}_8\text{Si}$

Molecular Weight, g/mol: 108.22

Boiling Point, °C/mm Hg: 120/760

Density, g/cc: 0.877



Purification Procedure: Phenylsilane was used as received without further purification, and was stored under N_2 pressure in anhydrous conditions.

3.2.7 Octene-1

Supplier: Aldrich

Molecular Formula: C_8H_{16}

Molecular Weight, g/mol: 112.22

Boiling Point, °C/mm Hg: 122-123/760

Density, g/cc: 0.715

Chemical Structure: 

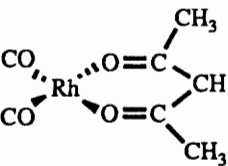
Purification Procedure: Octene-1 was used as supplied without further purification.

3.2.8 Dicarbonylacetylacetonato rhodium (I) $[Rh(acac)(CO)_2]$

Supplier: Strem Chemicals

Molecular Formula: $C_5H_7O_4Rh$

Molecular Weight, g/mol: 258.04

Chemical Structure: 

Purification Procedure: $Rh(acac)(CO)_2$ was stored under a N_2 atmosphere, and used as received to generate a hydroformylation catalyst *in situ*.

General reagents such as concentrated sulfuric acid, glacial acetic acid, magnesium turnings, and dichlorophenyl phosphine sulfide were purchased and used as obtained from Fisher Scientific. Nonane, p-bromofluorobenzene, phenylphosphonic dichloride, and sodium bicarbonate were obtained from Aldrich and used as received.

3.3 Preparation and Purification of Monomers

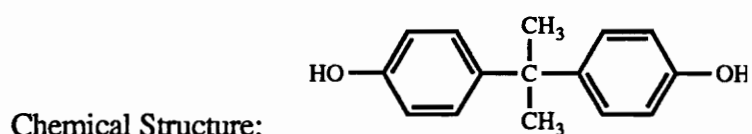
3.3.1 Bisphenol-A (Bis-A)

Supplier: Dow Chemical Company, USA

Molecular Formula: $C_{15}H_{16}O_2$

Molecular Weight, g/mol: 228.27

Melting Point, °C: 156-157



Purification Procedure: Monomer grade bisphenol-A was provided, and required no further purification. If desired, it can be recrystallized from concentrated toluene solution to afford white needles and dried under vacuum at 80°C.

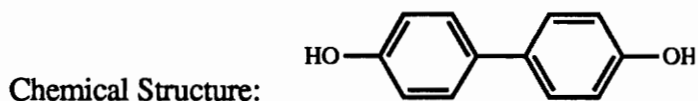
3.3.2 4,4'-Biphenol (BP)

Supplier: Aldrich

Molecular Formula: $C_{12}H_{10}O_2$

Molecular Weight, g/mol: 186.21

Melting Point, °C: 282-284



Purification Procedure: Biphenol was recrystallized from saturated deoxygenated acetone producing large white crystals, which after dried over a nitrogen flow were crushed in a mortar and pestle, and vacuum dried at 50°C.

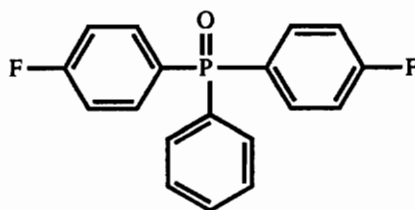
3.2.3 Bis(4-Fluorophenyl)Phenyl Phosphine Oxide (BFPPO)

Supplier: Synthesized in-house

Molecular Formula: $C_{18}H_{13}OPF_2$

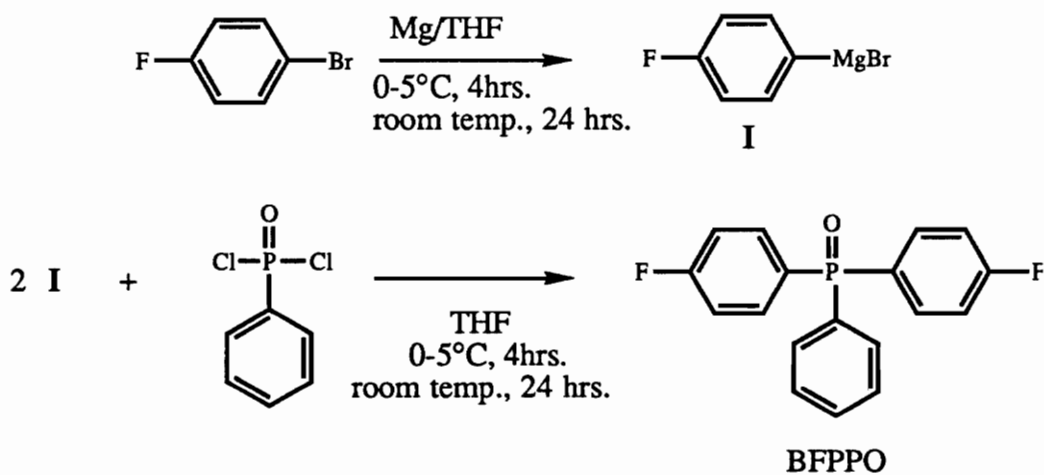
Molecular Weight, g/mol: 314.24

Melting Point, °C: 124-126



Chemical Structure:

Synthesis and Purification Procedure: Bis(4-fluorophenyl)phenyl phosphine oxide (BFPPO) was obtained and purified by a modification of known Grignard techniques as illustrated in Scheme 3.1.¹¹⁵⁻¹¹⁷



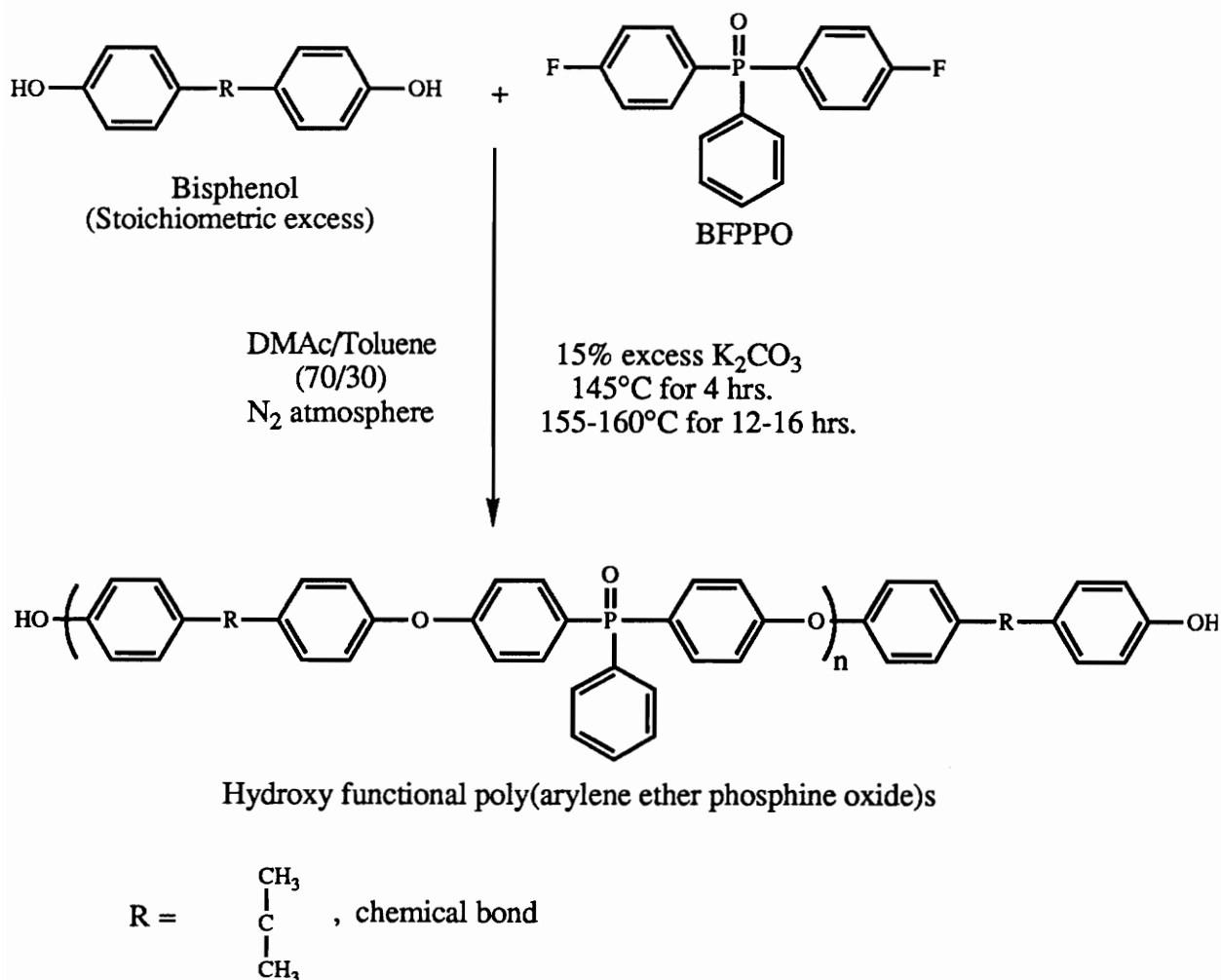
Scheme 3.1 Preparation of Bis(4-Fluorophenyl)Phenyl Phosphine Oxide

For example, 170.2g (7.0 mol) magnesium turnings (Aldrich, 99%) and 7.0 liters of dry THF were added to a flame dried 10 liter 4-neck round bottom flask fitted with and overhead stirrer, an addition funnel, and a nitrogen inlet. This solution was then cooled at or below 5°C with an ice bath, and 2165.5 g (7.0 mol) p-bromofluorobenzene (Aldrich, 99%) were added dropwise over a period of 3-4 hours. The ice bath was removed, and the solution was stirred overnight at room temperature producing a slightly cloudy gray solution. Next, 703.6 g (3.5 mol) phenylphosphonic dichloride (97%) was added dropwise at 5°C over 3-4 hours, and the mixture was stirred overnight at room temperature giving a clear yellow solution. Then, the mixture was made acidic by the addition of enough 10% aqueous sulfuric acid. Diethyl ether was employed to extract the organic from the aqueous phase. The aqueous layer was washed with ether/THF solutions. All the organic layers separated from the aqueous phase were combined, and washed thoroughly with 10% sodium bicarbonate, after which they were washed with water. The wet product could be obtained by stripping off the ether solvents. It was then dissolved in toluene, and azeotroped for several hours over activated charcoal. The dry solution is filtered through a celite pad, and allowed to stand at room temperature overnight. The large crystals produced were filtered off, dried in air, crushed with a mortar and pestle, and dried under vacuum at 70°C. Kugelrohr distillation at a pressure of one torr and 160-170°C afforded a white solid. This material can be removed from the Kugelrohr flask by melting with a heat gun, and allowing it to drip onto a sheet of teflon. Yields of about 70-80% of monomer grade crystals with melting point of 124-26°C were obtained after redistillation.

3.4 Synthesis of High Molecular Weight Poly(Arylene Ether Phosphine Oxide)s

The preparation of high molecular weight poly(arylene ether phosphine oxide)s is illustrated in Scheme 3.2. All polymers were synthesized by coreacting “AA” (bisphenol)

and “BB” (difluoride) type monomers in a typical step-growth polymerization reaction. Control of the number average molecular weight was achieved by off-setting the stoichiometry of the reaction by a calculated amount using Carother’s Equation.^{115,116}



Scheme 3.2 Synthesis of Hydroxy Functionalized Poly(Arylene Ether Phosphine Oxide)s

In a typical procedure for the preparation of high molecular weight poly(arylene ether phosphine oxide)s a 250 ml 4-necked round bottom flask equipped with a nitrogen inlet, an

overhead stirrer, a Dean-Stark trap with condenser, and a thermometer was charged with a slight excess of one of two bisphenols, bis-A or biphenol, in order to obtain phenolic endgroups and control the molecular weight, and the BFPPPO monomer. For example, 9.085 g (0.040 mol) of bis-A were weighed and combined with 12.197 g (0.039 mol) BFPPPO. The teflon beakers from which the monomers were transferred were rinsed well into the round bottom flask with DMAc, for a total volume of 100 ml (20% (w/w) solids). A 15% excess of K_2CO_3 (6.17 g, 0.045 mol) and 45 ml toluene were combined with the reaction mixture. The reaction temperature was controlled by a high temperature silicone oil bath, and a constant purge of nitrogen was maintained. After the water and toluene azeotrope formed at about 145°C, the system was allowed to dehydrate for four hours. Next, the temperature of the mixture was raised to 155-160°C and held there for a minimum of twelve hours. The resulting viscous solution was dark brown with a suspension of the white inorganic salt. It was allowed to cool until just warm, diluted with chloroform, and filtered through a Buchner funnel to remove the inorganic salts. The solution was, then, neutralized using glacial acetic acid to afford a viscous clear brown mixture. This solution was precipitated in a 80:20 methanol:water mixture using a high speed blender. The highly fibrous white material was dried in a vacuum oven at 100°C for approximately 12 hours, redissolved in chloroform, filtered, neutralized, reprecipitated in pure methanol and dried a second time under the same conditions. The resulting polymers were soluble in chloroform, methylene chloride, tetrahydrofuran, and polar aprotic solvents.

3.5 Preparation of Metal Complexed Poly(Arylene Ether Phosphine Oxide) Films

The amount of materials for a given composition of metal to polymer ratio were calculated employing the equation:

$$\frac{\text{Mass of polymer used}}{\text{MW PEPO repeat unit}} * \frac{\text{Mole \% metal}}{100} * \text{FW metal halide} = \text{g of metal halide to be used}$$

For example, for 20 mole% CoCl₂ in BP-PEPO, 1.0 g of 20,000 g/mol hydroxy endcapped BP-PEPO (molecular weight of repeat unit = 460.28 g/mol), 0.0564 g CoCl₂ (F. W. = 129.84 g/mol), and 7 ml of DMAc were used. Once calculated, the required amounts were weighed into a vial and dissolved in DMAc (~ 15 % (w/w) solids). The solution was stirred for several hours or until homogeneous, and filtered to remove any dirt particles. Under a low flow of N₂, the solutions were poured onto a silanated glass plate contained in a closed glass box (Figure 3.1).

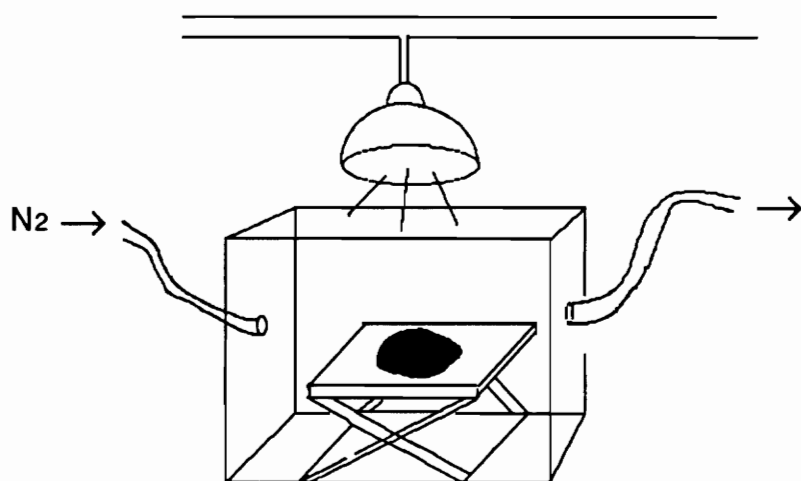


Figure 3.1 Polymer/Metal Film Composite Preparation

The solvent was slowly evaporated at 65°C using an infrared heat lamp until the film began to pull off the glass plate (12 hours). They were subsequently placed in a vacuum oven and heated to 25°C for at least two hours, after which the temperature was very slowly raised to just below the glass transition temperature of the unmodified poly(arylene ether

phosphine oxide), and maintained there for several hours in order to ensure the removal of any trapped solvent. A carbonyl resonance was not observed in the carbon-13 NMR of the films. However, thermogravimetric analysis along with mass spectroscopy would be more conclusive in establishing the complete removal of the DMAc from the films.

Using this preparation procedure the metal modified solutions afforded homogeneous, clear, tough films with colors varying from brown in the case of the iron and yellow for the copper to deep blue for the cobalt.

3. 6 Synthesis of Poly(Arylene Ether Triaryl Phosphine)

Ligand

Preformed high molecular weight bis-A based poly(arylene ether phosphine oxide)s were reduced to the corresponding phosphines to different extents using phenylsilane. The reduction was carried out in a three neck round bottom flask, and under a nitrogen atmosphere. First, the phosphine oxide containing polymer was dissolved in previously distilled chlorobenzene. At room temperature and while stirring, fresh phenylsilane was syringed dropwise into the reaction flask, and the mixture was heated slowly using an oil bath. The spontaneous evolution of hydrogen signaling the onset of the reaction was observed close to 90°C. The reduction was allowed to proceed at approximately 110°C and was monitored by ³¹P NMR until complete. An insoluble glass-like solid was occasionally observed as a byproduct. The solution was then filtered, and the polymer was precipitated by pouring the solution into a 90:10 methanol/H₂O mixture, and dried in a vacuum oven up to 150°C for 12 hours. It was subsequently redissolved in chloroform, washed with 5% HCl (aqueous), reprecipitated with hexanes, and dried once again at 150°C in a vacuum oven for 12 hours.

3. 7 Catalytic Hydroformylation of Octene-1

The catalytic reactions were carried out at 120°C in 30 ml stainless steel reaction vessels equipped with high pressure gauges (Figure 3.2).^{126,127} The ratio of the aldehyde products, n/b, was determined using gas chromatography. The catalyst was generated *in situ* by mixing a rhodium precursor, Rh(acac)(CO)₂, with the phosphine polymer. In order to ensure good reproducibility in a series of catalytic reactions, two separate stock solutions of Rh(acac)(CO)₂, 0.01M in toluene, and of the polymer, 0.100 M in toluene, were prepared. The corresponding volumes of these stock solutions were combined in the reactor at room temperature under CO, and allowed to mix for three minutes. Then, octene-1, 0.34 ml of nonane (internal standard), and toluene were added such that the octene-1/Rh molar ratio was 500 to 1, and the total volume was 2.5 ml. The reaction vessel was then closed, pressurized with CO/H₂ (1:1) gas, and placed in a silicone oil bath at 120 °C. The initial pressure at room temperature was 200 psig, and that at the reaction temperature was 230 psig. After the corresponding reaction time the vessel was removed from the bath, cooled to room temperature, and depressurized. The products were then analyzed by gas chromatography.

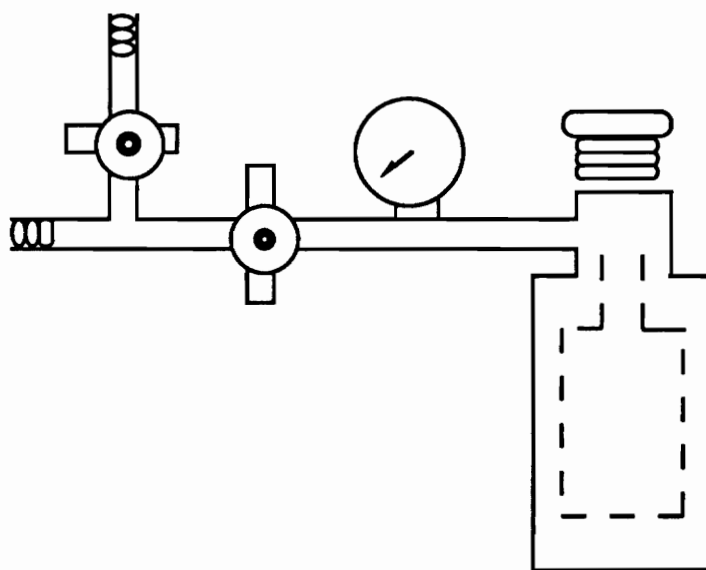


Figure 3.2 Stainless Steel Reactor used in Hydroformylation Reaction

3. 8 Characterization Methods

3.8.1 Infrared Spectroscopy

Fourier Transform infrared spectra were obtained with a Nicolet MX-1 instrument as well as a Nicolet 800. The polymer spectra were taken as very thin films on an FTIR film holder. This technique was particularly useful in confirming the complexation of the metal salts to the polymer based on the decrease of the P=O stretch peak intensity.

3.8.2 Nuclear Magnetic Resonance Studies

3.8.1.1 Proton (^1H) NMR

Proton (^1H) NMR spectra were obtained on a Varian 400 MHz instrument normally in CDCl_3 . All spectra were referenced to tetramethylsilane (TMS) at 0 ppm.

3.8.1.2 Phosphorus (^{31}P) NMR

Solution phosphorus (^{31}P) NMR spectra were also obtained on a Varian 400 MHz instrument, corresponding to a phosphorus frequency of 161.9 MHz. All spectra were referenced to 85% H_3PO_4 at 0 ppm, and dichlorophenyl phosphine sulfide was used as a standard (76.05 ppm). In most cases, a deuterated solvent was not used (^{31}P is a naturally occurring isotope), and in all cases where comparisons are made, the compounds were run in the same solvents.

Solid state phosphorus (^{31}P) NMR spectra were obtained on a Bruker MSL 300 instrument, corresponding to a phosphorus frequency of 121.4 MHz. All spectra were referenced to 85% H_3PO_4 at 0 ppm. Spin-lattice relaxation times (T_1) were measured using the inversion recovery method.

3.8.3 Intrinsic Viscosity

Intrinsic viscosities were measured at 25°C in a Cannon-Ubbelohde viscometer, generally using chloroform as a polymer solvent. Three dilute polymer solutions of low polymer concentrations were prepared. The flow time through the viscometer path-length of each of these three solutions (t) as well as that of the pure solvent (t_0) were measured. Assuming that $t / t_0 = \eta / \eta_0$, the reduced viscosity was defined as $\eta_{red} = [(\eta / \eta_0) - 1] / C_2$, and the reduced viscosity as $\eta_{inh} = 1 / C_2 \ln(\eta / \eta_0)$. Next, both η_{red} and η_{inh} were plotted against concentration. Extrapolation to zero concentration yields the intrinsic viscosity $[\eta]$.

3.8.4 Thermogravimetric Analysis (TGA)

Thermogravimetric analysis (TGA) was conducted in air or in nitrogen gas on the Perkin-Elmer 7 series thermal analysis instrument. The samples were heated to 800°C at a rate of 10°C / min. The 5 percent weight loss temperature and the percent char yield at 750°C were recorded. When comparisons were made between different samples, similar sample forms were employed. For example, films were compared with films and powders with powders.

3.8.5 Differential Scanning Calorimetry (DSC)

Differential scanning calorimetry (DSC) was performed on a Perkin-Elmer Model 7 series instrument. The samples were cold pressed, and secured in crimped aluminum pans. They were typically heated from 100°C to 300°C at a heating rate of 10°C / min, rapidly cooled to 100°C, and subsequently heated to 300°C at 10°C / min. The glass transition temperature (T_g) was recorded for the second heat.

3.8.6 Dynamic Mechanical Analysis (DMA)

Dynamic mechanical analysis (DMA) were measured on the Polymer Lab. Mark II DMTA in the bending mode, and a frequency of 1 Hz, and at a heating rate of 2.5°C per minute. Storage moduli (E') and loss tangent ($\tan \delta$) values were noted.

3.8.7 Gas Chromatography

A Varian 3300 gas chromatograph equipped with a HP1 column 25 m x 0.32 mm x 0.52 mm, and FID detector was used to analyze the catalytic reaction products. The carrier gas was He; the temperature program was from 50°C (4 min.) to 200°C (4 min.), at a heating rate of 10°C/min.

3.8.8 Transmission Electron Microscopy (TEM) / Energy Dispersive X-Ray Analysis (EDAX)

Transmission electron microscopy (TEM) and energy dispersive X-ray analysis (EDAX) were conducted on the Phillips 420T Electron Microscope. The polymer films were embedded in an epoxy resin in order to facilitate the cutting of a small film section.

3.8.9 Electron Paramagnetic Resonance (EPR)

Electron paramagnetic resonance was performed on an IBM ER 200 D-SRC instrument operating at 9.55 GHz.

4.0 Results and Discussion

4.1 Synthesis and Characterization of High Molecular Weight Poly(Arylene Ether Phosphine Oxide)s

4.1.1 General Introduction

High molecular weight 4,4'-isopropylidene diphenol (bis-A) as well as biphenol-based poly(arylene ether phosphine oxide)s (Bis A-PEPO and BP-PEPO) were synthesized via nucleophilic aromatic substitution as outlined in the experimental section. The first step in the reaction at approximately 135°C served to azeotrope off the water byproduct, whereas the second step at a higher temperature was used to drive the polymerization to very high conversions. The resulting polymers have very attractive properties such as good thermo-oxidative stability, hydrolytic stability and flame resistance, as well as the potential for metal complexation through the phosphine oxide moiety.

Linear Bis A-PEPOs (Figure 4.1 A) of theoretical number average molecular weights of 15, 20, and 30 Kg/mol and linear BP-PEPO (Figure 4.1 B) of 20 Kg/mol were synthesized and employed in this thesis. The molecular weight was controlled by addition of a calculated stoichiometric excess of the bisphenol relative to the dihalide as discussed in the experimental section. White polymers were obtained upon precipitation in a methanol/water mixture. The dry amorphous polymers were completely soluble in a variety of common solvents such as chloroform, methylene chloride, and N,N-dimethylacetamide, and the solubility characteristics of these polymers are presented in Table 4.1. As expected, the solubility of the more rigid chain BP-PEPO is somewhat limited in certain solvents relative to that of the more flexible Bis A-PEPO.

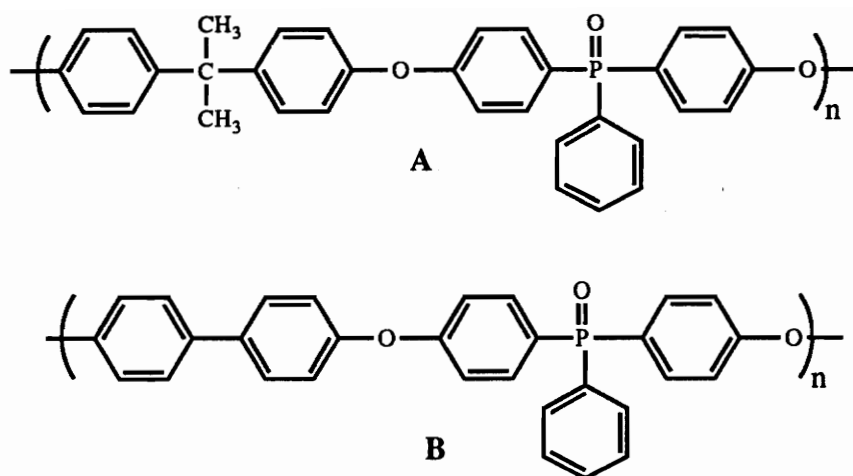


Figure 4.1 Structural Repeat Units of Poly(Arylene Ether Phosphine Oxide)s :

A) Bis A-PEPO, B) BP-PEPO

Table 4.1 Solubility Characteristics of Poly(Arylene Ether Phosphine Oxide)s

Polymer	THF	CHCl ₃	CH ₂ Cl ₂	NMP	DMAc	PhCl
Bis A-PEPO	S	S	S	S	S	S
BP-PEPO	IS	S	S	S	S	PS

S= Soluble, PS=Partially soluble, IS=Insoluble

A qualitative understanding of the molecular weight of these polymers was obtained from intrinsic viscosity measurements.¹¹⁷ The room temperature intrinsic viscosity data in chloroform and methylene chloride for these polymers is summarized in Table 4.2. The expected increase in intrinsic viscosity as a function of molecular weight was observed.

Table 4.2 Intrinsic Viscosity of Poly(Arylene Ether Phosphine Oxide)s

Polymer	<Mn> (Kg/mol)	$[\eta]_{\text{CHCl}_3}^{25^\circ\text{C}}$ (dl/g)	$[\eta]_{\text{CH}_2\text{Cl}_2}^{25^\circ\text{C}}$ (dl/g)
Bis A-PEPO	15	0.29	0.26
	20	0.36	0.30
	30	0.40	0.38
BP-PEPO	20	0.48	0.39

4.1.2 Spectroscopic Analysis of Poly(Arylene Ether Phosphine Oxide)s

The spectroscopic characteristics of these phosphine oxide containing polymers were studied using Fourier transform infrared (FTIR) and nuclear magnetic resonance. The FTIR spectrum of a thin BP-PEPO film is depicted in Figure 4.1. The principal peaks were identified and assigned according to literature references as well as those reported by C. D. Smith¹¹⁷ for the same polymers. These peak assignments are presented in Table 4.3. The phosphine oxide stretch appears at ca. 1197 cm^{-1} and will be important later in the discussion of metal complexation with these polymers.

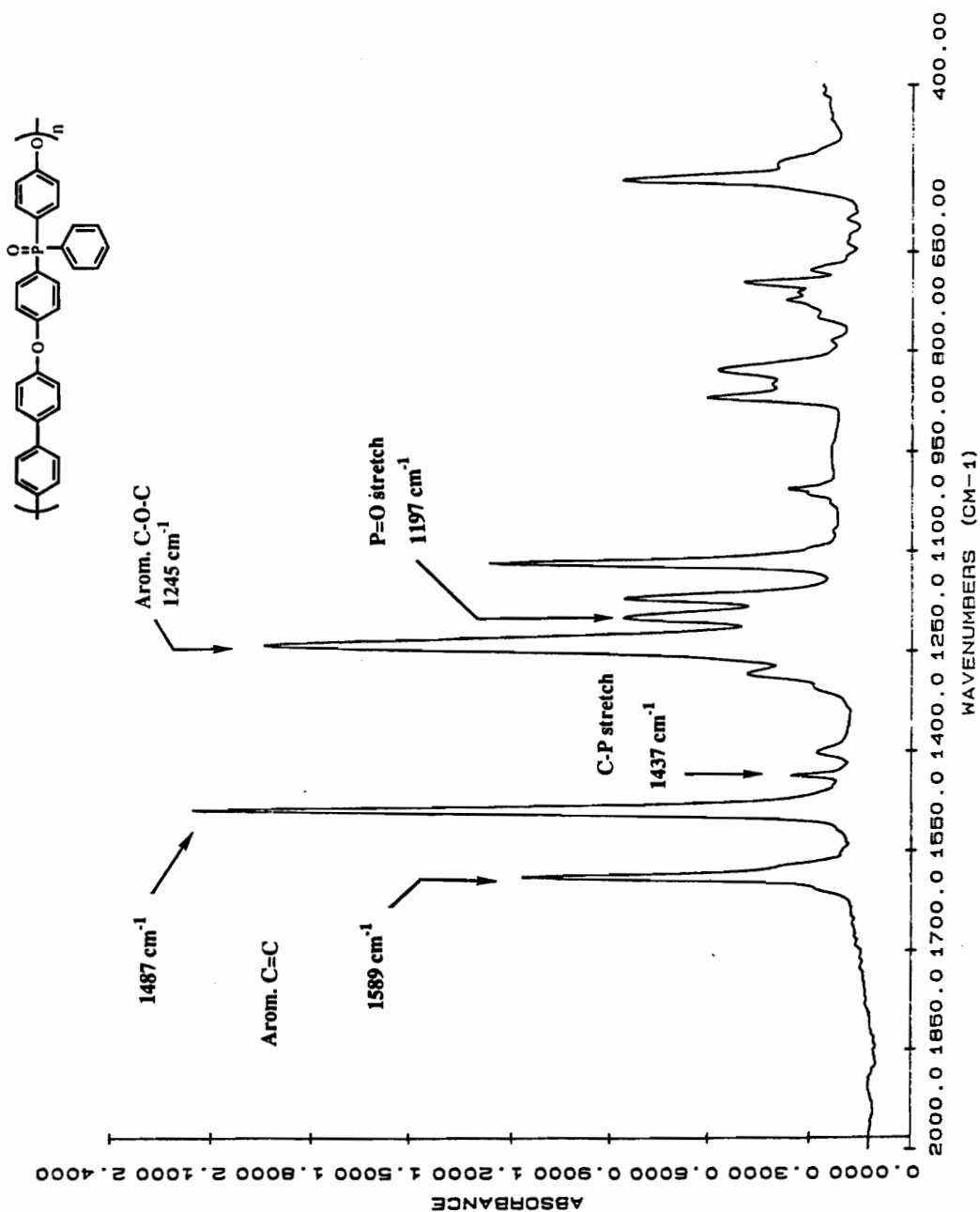


Figure 4.2 FTIR Spectrum of $\langle 20\text{K} \rangle_{\text{theo}}$ BP-PEPO Film

Table 4.3 FTIR Peak Assignments for BP-PEPO Film¹¹⁷

Peak Assignment	Wavenumber (cm ⁻¹)
Arom. C=C	1589, 1487
Arom. C-P	1437
Arom. C-O-C	1245
P=O	1197
C-P	750

A typical proton (¹H) NMR spectrum referenced to TMS at 0 ppm in CDCl₃ of a linear high molecular weight Bis A-PEPO is shown in Figure 4.3. The spectrum of these phosphine oxide polymers is complicated by the fact that the phosphorus (spin 1/2) couples with the hydrogen nuclear spin giving rise to additional splitting. The peaks have been previously identified and assigned¹¹⁷ as shown in the figure. A single peak at 29 ppm was observed in the phosphorus (³¹P) NMR of polymer solutions in deuterated chloroform as exemplified by the the spectrum of Bis A-PEPO (Figure 4.4). Solutions of this polymer in nondeuterated solvents (chlorobenzene or DMAc) resulted in a phosphine oxide chemical shift at approximately 25 ppm, when dichlorophenyl phosphine sulfide was used as a standard.

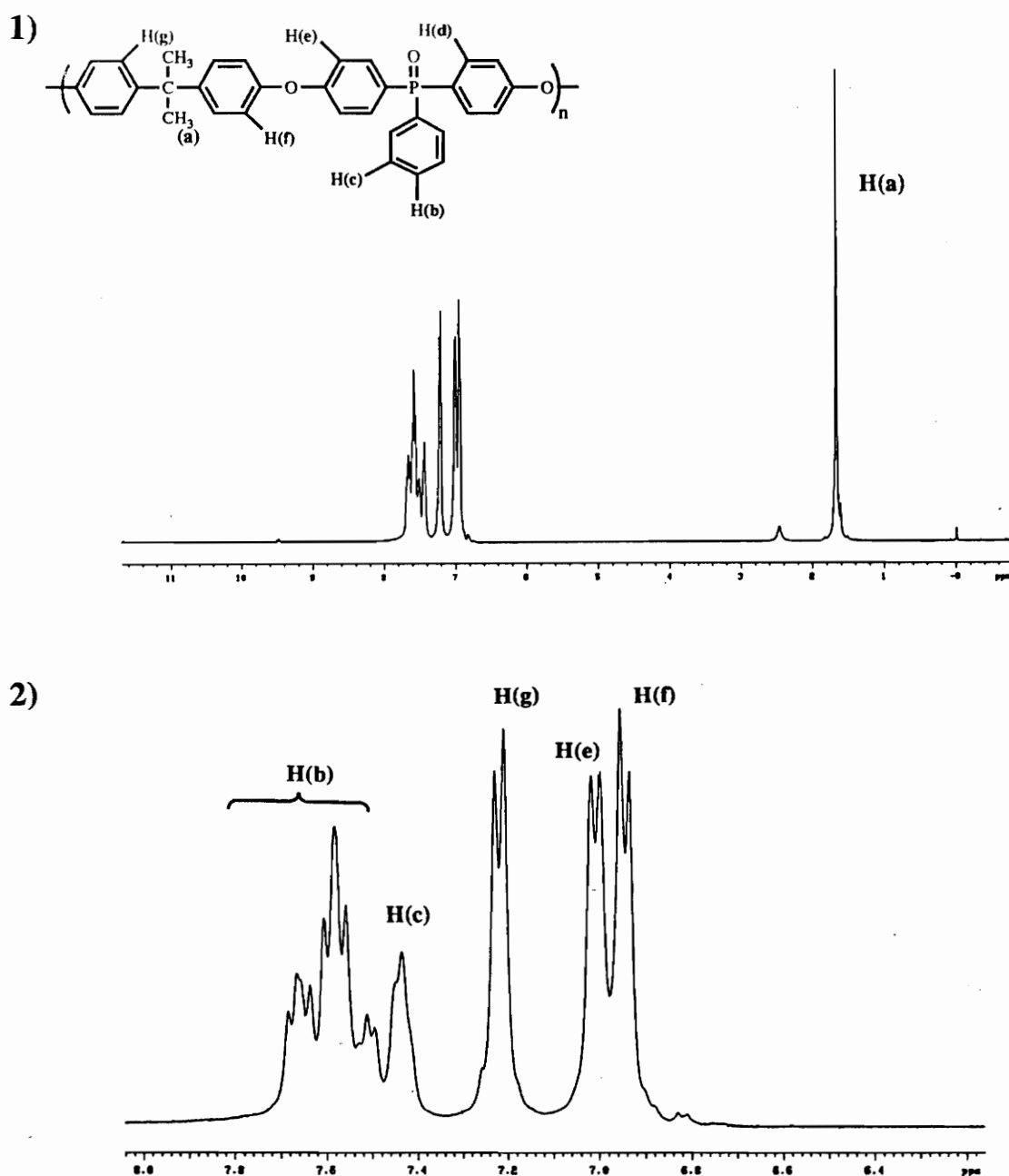


Figure 4.3 ^1H NMR Spectrum of High Molecular Weight Bis A-PEPO in CDCl_3
 Referenced to TMS at 0 ppm(400 MHz):
 1) Complete Spectrum, 2) Expanded Aromatic Region

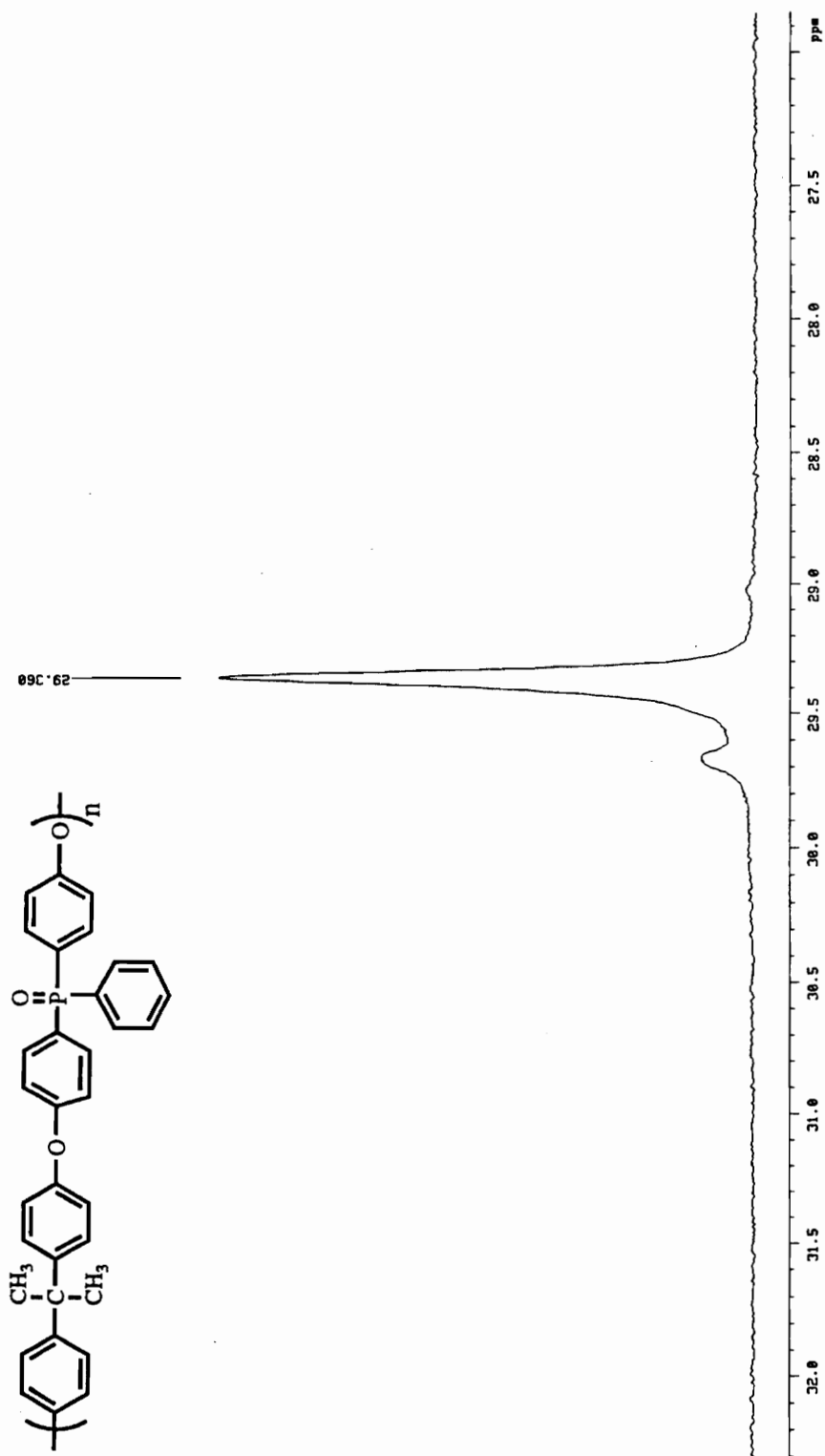


Figure 4.4 Phosphorus (^{31}P) NMR of Bis A-PEPO in CDCl_3 Referenced to 85% H_3PO_4 at 0 ppm (161.9 MHz)

4.1.3 Thermal Characterization Data for Poly(Arylene Ether Phosphine Oxide) Thermoplastics

Clear, flexible, slightly brown colored films of the Bis A and BP-PEPOs were cast from solution and their thermal properties including thermal stability and glass transition temperatures were investigated. The thermal stability of these polymers in air were determined via dynamic thermogravimetric analysis at a heating rate of 10°C/minute. The 5% weight loss of these materials is in all cases in excess of 500°C. A significant amount of char at temperatures in excess of 600°C in air were observed for these phosphine oxide polymers. As discussed in the background section, the formation of a substantial amount of char during pyrolysis has been observed for a series of phosphorus compounds as well as polymers.³⁵⁻³⁹ Char formation plays an important role in the self-extinguishing properties of these materials.

The poly(arylene ether phosphine oxide)s were all amorphous materials. Their glass transition temperatures (T_g) were determined by differential scanning calorimetry at a heating rate of 10°C/minute and are reported from the second scan after rapid cooling. The glass transition temperature of the Bis A-PEPOs increases with increasing molecular weight. For the same molecular weight (20 Kg/mol), a substantially higher T_g is observed for the BP-PEPO relative to the Bis A-PEPO. This aspect could be attributed to the greater rigidity of the biphenyl group. The glass transition data as well as the TGA results are summarized in Table 4.4.

Table 4.4 Summary of Thermal Properties of Poly(Arylene Ether Phosphine Oxide)s

Polymer	<Mn> (Kg/mol)	Tg* (°C)	5% wt. Loss (°C)**
Bis A-PEPO	15	195	490
	20	197	508
	30	201	497
BP-PEPO	20	232	518

*DSC. Second Scan. 10°C/min

**Dynamic TGA at 10°C/min

4.2 Composite Films Preparation and Characterization

4.2.1 Introduction

The formation of stable complexes of low molecular weight organophosphine oxides with a large variety of metals was reviewed by Karayannis and coworkers.⁵⁶ Preliminary studies conducted in our laboratories by C. D. Smith demonstrated the potential for complexation of poly(arylene ether phosphine oxide)s with a number of metal salts.¹¹⁷ A series of composite films were prepared in order to further investigate the metal coordination capabilities of these phosphine oxide containing macromolecules. The films were prepared from DMAc solutions of various metal salts (FeCl_3 , CoCl_2 , and CuCl_2) as described in the experimental section. The salts were initially anhydrous and were stored in a dry box in sealed containers. However, due to the hygroscopic nature of these metal compounds, some amount of water was sorbed during the weighing process. Homogeneous solutions could be easily prepared using DMAc since it is a good solvent for both the transition metal salt and the polymer. Chloroform could not be used since the salts were insoluble in this solvent and immediate gelation took place upon addition of the metal compound to a chloroform solution of the polymer. The amide solvent prevents gel formation presumably by interacting with the metal chlorides and, therefore, hindering the coordination with the polymer. In fact, complexes of DMAc with triphenylphosphine oxide have been previously reported.^{118,119}

Comparative studies were conducted on 20 Kg/mol PEPO films containing varying amounts of the different metal chlorides. Bis A-PEPO films comprising 0-20 mole % (based on the repeat unit molecular weight, 502.55 g/mol) of FeCl_3 , CoCl_2 , or CuCl_2 were prepared in order to investigate the variation in properties such as solubility, thermal stability, and glass transition temperature with the type and content of metal salt.

Additionally, BP-PEPO composite films with an equal loading of the metal salts (20 mole %) were prepared to study the influence of polymer backbone chemistry.

The procedure outlined in the experimental section for film casting and drying is crucial for obtaining homogeneous films. In an attempt to reduce the extent of metal halide decomposition during drying a nitrogen flow or vacuum atmosphere were employed. It was important to remove the solvent slowly to prevent the formation of bubbles and to dry the films close to the glass transition temperature of the base polymer, as even small traces of solvent can interfere with the complexation. The rate of drying was found to be important in terms of the agglomeration of the metal salt. Two BP-PEPO films containing an equal loading of the cobalt salt were dried under the same conditions but at different rates, one at a relatively fast rate and the other at a very slow rate. At the very slow heating rate, diffusion of the metal halide was visually observed by a dark blue ring forming around the contour of the film. At the fast rate the formation of bubbles became a problem. Consequently, an intermediate drying rate was found to be optimum for these systems as described in the experimental procedure. The extent of metal salt aggregation is also expected to depend on the glass transition temperature of matrix. The extent of diffusion of the metal salt during the drying process may also be a function of the polymer structure.

In general, the films prepared from solution were homogeneous, clear, and tough with colors varying from brown in the case of the iron and yellow for the copper to deep blue for the cobalt. Only in several of the copper Bis A-PEPO films were heterogeneities visually observed. During the drying process the iron modified systems changed colors from an initial dark yellow to a dark brown upon heat treatment. Even though an attempt was made to provide an inert drying atmosphere, the formation of iron oxide on the surface of the films is a plausible explanation for this change in coloration.

4.2.2 Solubility Characteristics of Composite Films

The films containing from 0 to 15 mole % of the metal salts all redissolved in DMAc, N-methylpyrrolidone, and chloroform at ambient temperature. However, when 20 mole % of any of the three salts was incorporated the room temperature solubility was limited to amide solvents.

The BP-PEPO films modified with 20 mole % of the different salts were extracted with refluxing chloroform. The cobalt and the copper films disintegrated after several hours. On the other hand, after a period of three days the ferric chloride film still retained over 35% of its initial dry weight. The presence of a "gel fraction" indicates the existence of strong interchain complexation for the iron system and perhaps a weaker interaction in the case of the cobalt and copper films. Nonetheless, these "crosslinks" must be reversible since the composites can be redissolved in amide solvents that are able to enter the coordination sphere of the metal, disrupting the structure of the polymeric complex.

4.2.3 Thermal Data for Polymer-Metal Complexes

The effect of metal salt incorporation on the thermal stability in air and in nitrogen as well as the glass transition temperature of the poly(arylene ether phosphine oxide)s was also investigated. It has been generally reported that for filled systems where interactions between the additive and the polymer are absent, doping has detrimental effects on the thermal stability of the material. Therefore, it is important to study whether the same effect is observed for the phosphine oxide systems in which specific interactions were attempted.

Shown in Figures 4.5, 4.6, and 4.7 are the dynamic TGA thermograms in air at 10°C/minute of the FeCl₃, CoCl₂, and CuCl₂/ Bis A-PEPO composite films, respectively. The 5 % weight loss temperatures and the char yields at 750°C for these systems are tabulated in Table 4.5.

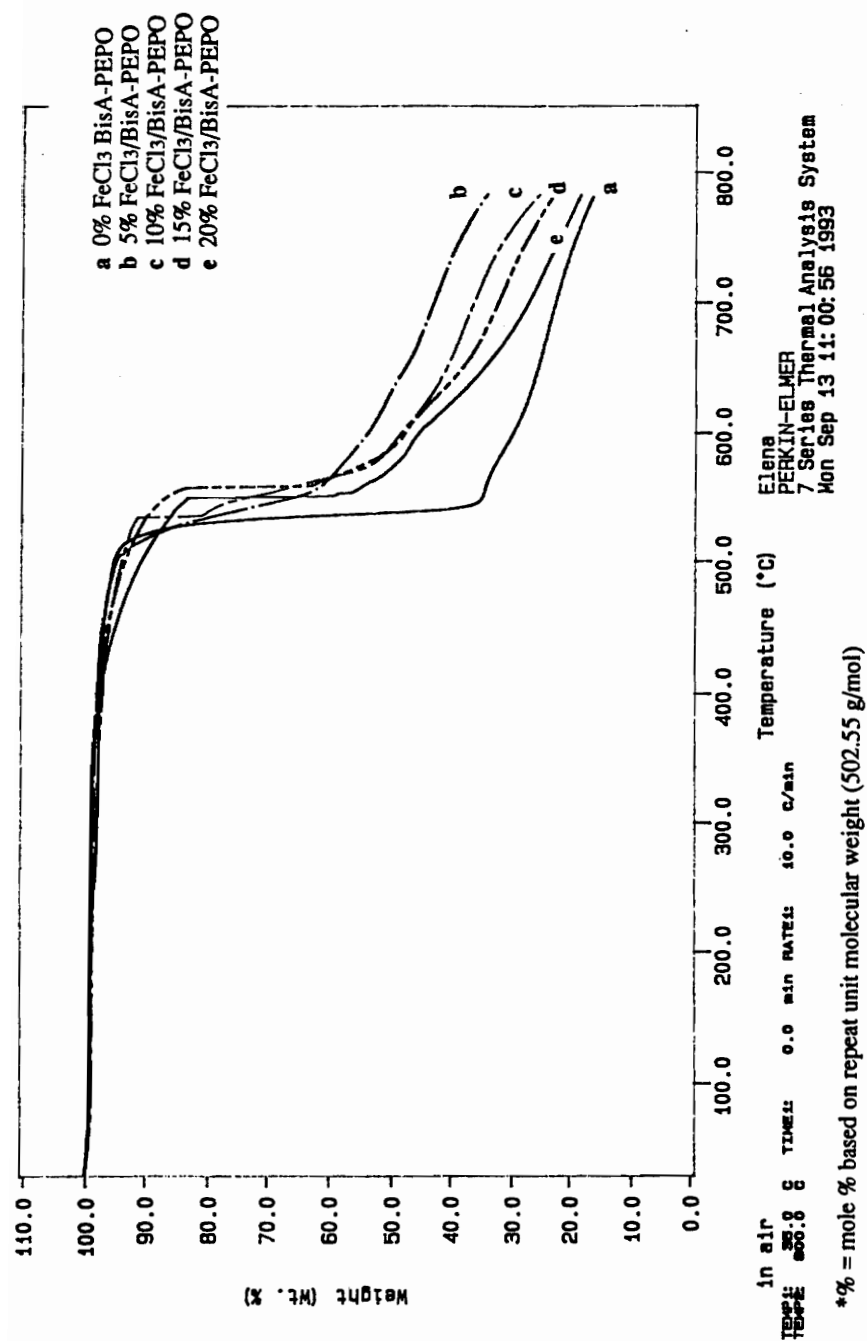


Figure 4.5 Dynamic TGA Thermograms in Air of FeCl₃/Bis A-PEPO Composite Films (10°C/min)

(The different metal salt concentrations are indicated in the figure)

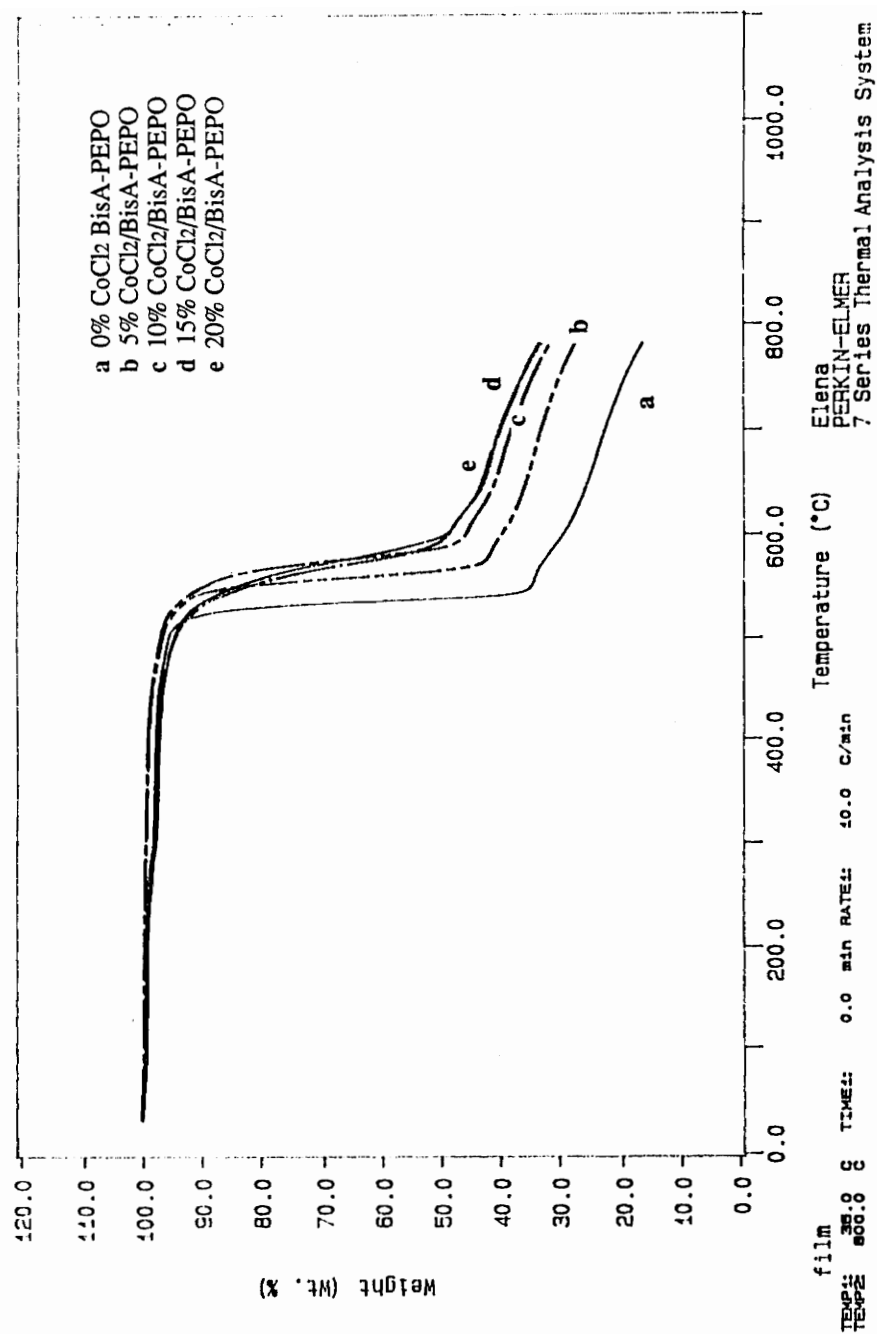


Figure 4.6 Dynamic TGA Thermograms in Air of CoCl₂/Bis A-PEPO Composite Films (10°C/min)

(% = mole % based on the repeat unit molecular weight, 502.55 g/mol)

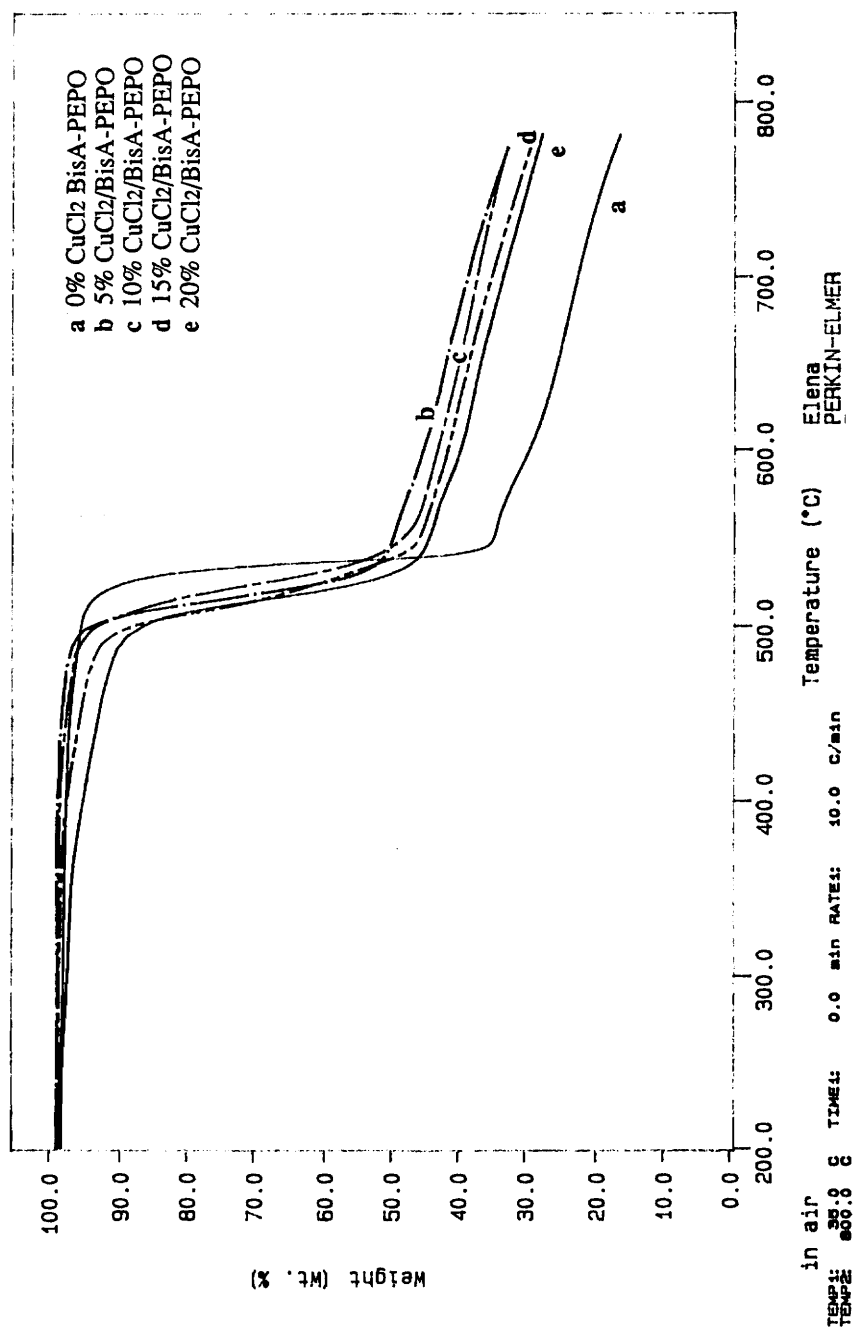


Figure 4.7 Dynamic TGA Thermograms in Air of CuCl₂/Bis A-PEPO Composite Films (10°C/min)

(% = mole % based on the repeat unit molecular weight, 502.55 g/mol)

Table 4.5 Dynamic TGA Data for Bis A-PEPO Composite Films (Air. 10°C/min)

Metal Salt	Mole* % Salt	Weight % Salt	5 %wt. Loss Temperature (°C)	% Char at 750°C ±10%
FeCl ₃	0	0	508	19
	5	1.6	503	39
	10	3.2	487	31
	15	4.8	481	27
	20	6.5	454	22
CoCl ₂	0	0	508	19
	5	1.3	523	30
	10	2.6	530	35
	15	3.9	494	37
	20	5.1	495	37
CuCl ₂	0	0	508	19
	5	1.3	498	35
	10	2.7	494	35
	15	4.2	464	31
	20	5.4	406	30

*Based on the repeat unit molecular weight, 502.55 g/mol

The thermo-oxidative stability in terms of the 5 % weight loss temperature of the FeCl_3 films decreases relative to the unmodified Bis A-PEPO polymer with increasing metal content. In the case of the CoCl_2 complexes the 5 and 10% films show a higher 5 % weight loss temperature relative to the unmodified Bis A-PEPO. However, the 5 % weight loss of the 15 and 20 mole % films were evidenced at lower temperatures in comparison to the base polymer (It is suspected that the latter behavior could possibly be influenced by a small amount of residual solvent. In fact, as will be discussed later, the incorporation of 20 mole % CoCl_2 resulted in an enhancement of the thermal stability of the unmodified BP-PEPO film. Additionally, the relevance of these aspects in relation to the trends observed in the glass transition temperatures will be discussed later in this section. The copper modified films show the greatest lowering in thermal stability relative to the base polymer.

It needs to be noted that Fe(III) chloride and Cu(II) chloride decompose above 300°C , whereas, Co(II) chloride is stable to very high temperatures. Hence, the observed lowering of the thermal stabilities in the composite films may result from a combination of partial decomposition of the salts, and the influence of metal complexation.

Similar trends in thermal stabilities were observed in nitrogen. The temperature of onset of decomposition was always higher in the inert nitrogen atmosphere. This suggests that oxygen accelerates the decomposition of the polymeric complexes, as would be expected.

The char yields at 750°C of the complexes are in all cases higher than that of the unmodified polymer. It is seen from Table 4.5 that the enhanced char yields in the metal modified films, in almost all cases, exceed the amounts of metal salt initially present in the films. Thus, the increase in the char yields cannot be attributed solely to the weight of the metal salt.

From an analysis of the TGA data one can also obtain trends in char yield percentages as a function of varying mole percent incorporation of a given metal salt. In the case of the

cobalt films, the char yield increases with increasing metal salt concentration. In contrast, in the copper and iron films the opposite trend is observed. A detailed study of the mechanism of decomposition of these complexes would be required to explain these data, and is beyond the scope of this study.

The dynamic TGA thermograms at 10°C/minute in air of the 20 mole % metal chloride/BP-PEPO composites are shown in Figure 4.8. The thermo-oxidative stability of these metal complexed films was also found to depend on the chemistry of the metal salt. The 5 % weight loss temperature of unmodified BP-PEPO was increased by the incorporation of either FeCl₃ or CoCl₂, and decreased by the addition of CuCl₂. In contrast, in the case of Bis A-PEPO the 5 % weight loss temperature was increased by the incorporation of CoCl₂, and decreased by the addition of FeCl₃ or CuCl₂.

In general, the thermal stabilities of the metal modified polymers are influenced by the backbone structure of the polymer, the chemistry of the metal salt, and their relative concentrations.

The glass transition temperatures of the metal complexed films were also found to depend on the metal salt, its content, and the structure of the polymer matrix. The glass transition temperatures were measured by differential scanning calorimetry (DSC) and from dynamic mechanical analysis (Discussed in the next section). The values obtained for the Bis A-PEPO composite films are tabulated on the next page (Table 4.6). The glass transition temperatures of the Fe(III) chloride films gradually increase as a function of metal halide concentration. An increase in the T_g was also observed for the 5 and 10 mole % Co(II) chloride films. However, upon loading of 15 and 20 mole % of this salt, the T_g is depressed relative to the base material; this phenomenon is not understood. All the Cu(II) chloride films exhibit a lowering of the glass transition temperature in comparison to the unmodified material.

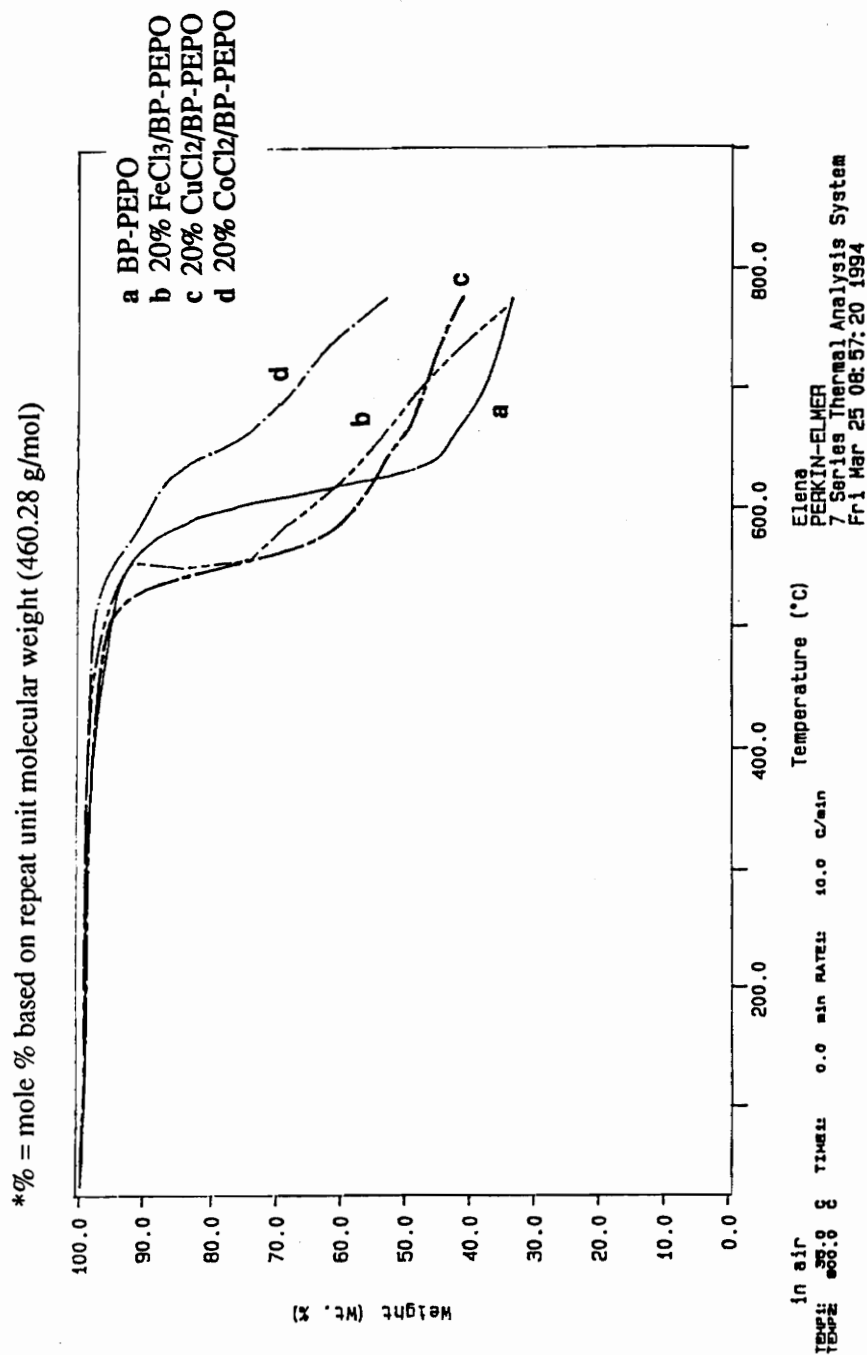


Figure 4.8 Dynamic TGA Thermograms in Air of 20 Mole % * Metal Chloride/BP-PEPO Composite Films

Table 4.6 DSC Glass Transition Temperature Results for Bis A-PEPO (20K)
Composite Films

Metal Salt	Mole % Salt*	Tg** (°C)
None	----	197
FeCl ₃	5	197
	10	198
	15	212
	20	215
CoCl ₂	5	203
	10	210
	15	203
	20	201
CuCl ₂	5	190
	10	198
	15	193
	20	190

*Based on the repeat unit molecular weight, 502.55 g/mol

**Second scan. 10°C/min

An increase in the glass transition temperature such as that evidenced for FeCl₃/Bis A-PEPO composites, strongly suggests the existence of strong interactions between the metal salt and the polymer which cause a reduction in the free volume and/or a decrease in the flexibility of the chains. The complexation with CuCl₂, on the other hand, leads to a depression of the T_g of the Bis A-PEPO film. However, interchain complexation is suggested by the much higher rubbery state modulus as seen in the dynamic mechanical spectra in section 4.2.4. The observed depression of the glass transition temperature could possibly result from the combination of a decrease in the intermolecular forces as a result of complexation, and a plasticizer effect by uncomplexed metal salt. The complexation behavior of the CoCl₂ salt is suggested to be similar to that of the FeCl₃. The lower T_{gs} observed for the higher CoCl₂ concentration films may result from the presence of residual solvent. This aspect was discussed in relation to the thermal stability of the composites, and is in agreement with the trends observed for the BP-PEPO films discussed below.

The glass transition temperatures of the 20 mole % metal chloride/BP-PEPO composites in relation to that of the unmodified film are presented in Figure 4.9. An increase in the T_g is observed for the FeCl₃ and CoCl₂ modified films, whereas, a depression is experienced as a result of CuCl₂ modification. These trends in T_{gs} are influenced by factors including crosslinking through complexation, enhanced chain rigidity, decrease of preexisting intermolecular forces, and plasticizer effects.

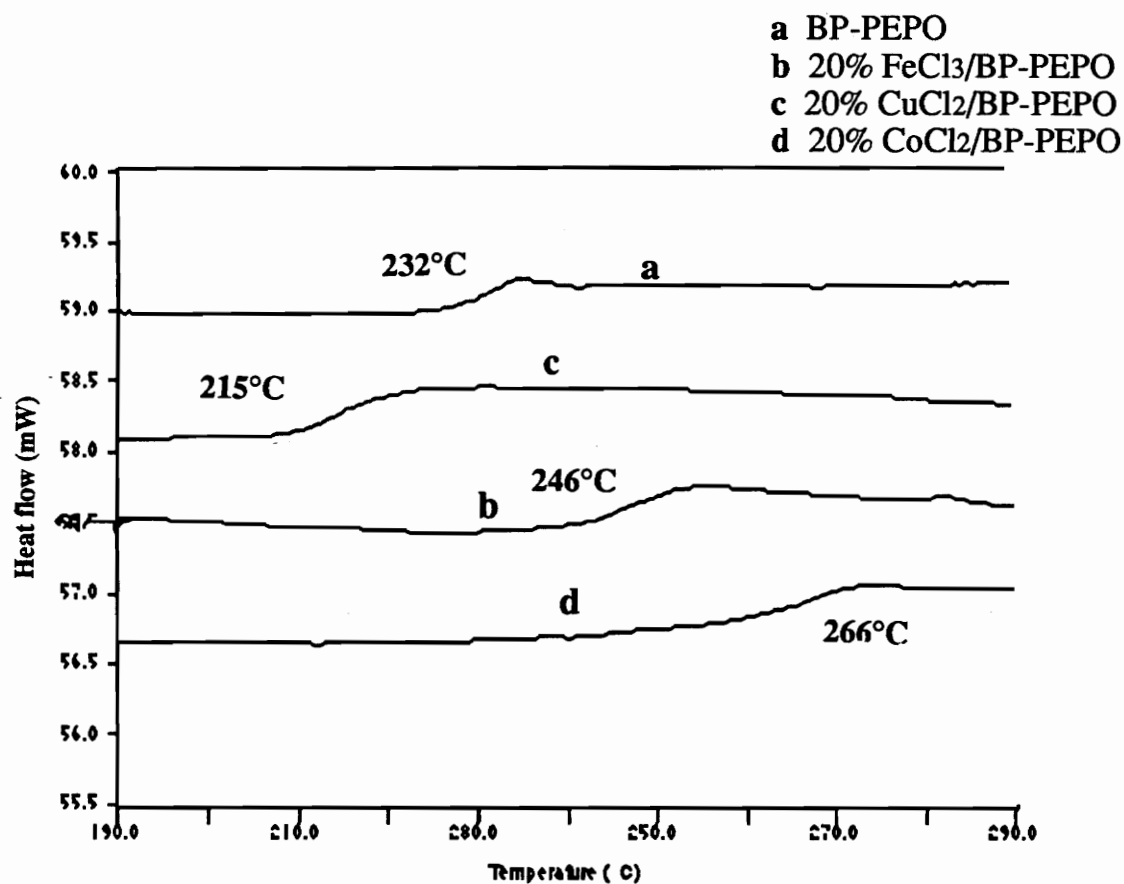


Figure 4.9 DSC Traces for BP-PEPO Films (Second Scan, 10°C/minute)

(% = mole % based on repeat unit molecular weight, 460.28 g/mol)

4.2.4 Dynamic Mechanical Analysis of Complex Films

The mechanical properties of the metal salt-BP-PEPO complexes were investigated using dynamic mechanical analysis (DMA) in the bending mode. The behavior of the 20 mole % metal chloride BP-PEPO films along with that of the unmodified polymer film are shown in Figure 4.10.

The metal salt modified films show substantially improved modulus relative to the base polymer. The storage modulus of the unmodified BP-PEPO film decreases gradually with increasing temperature and loses its mechanical integrity at T_g or slightly above. On the other hand, the metal salt systems exhibit a retention of the storage modulus well beyond the glass transition temperature. In fact, the storage modulus of the CoCl_2 film remains essentially unchanged through the glass transition. This behavior is highly characteristic of crosslinked networks and strongly suggests the existence of interchain connectivity through the metal. It is important to emphasize again that this network formation is chemically reversible since the metal-polymer composites redissolve in amide solvents. The softening temperatures of the polymeric complexes obtained from the $\tan \delta$ values (Figure 4.10) follow the same trends observed by differential scanning calorimetry.

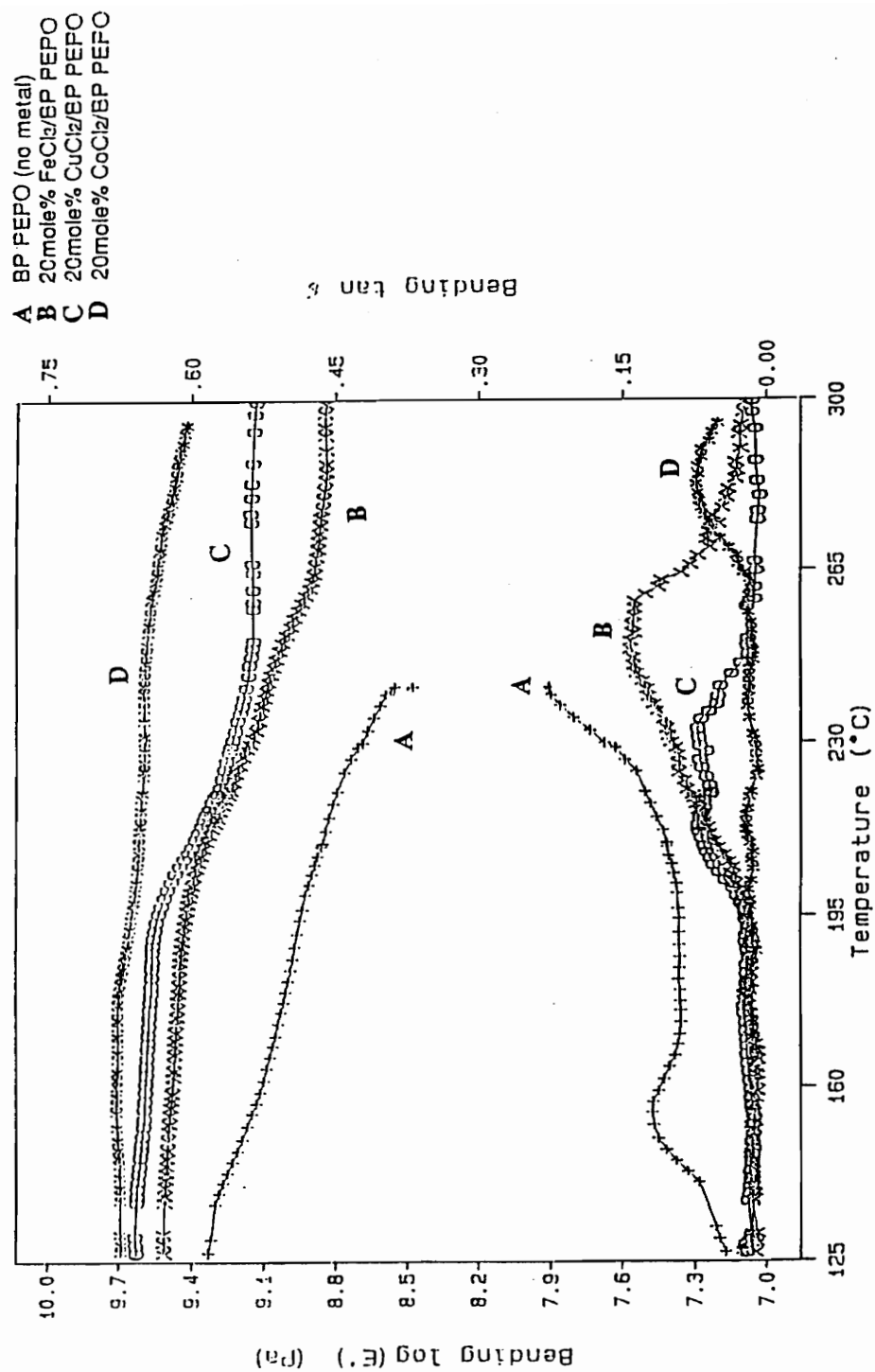


Figure 4.10 Dynamic Mechanical Analysis of BP-PEPO Composites (1Hz, 2.5°C/min)

4.2.5 FTIR Spectroscopic Studies

In order to substantiate the presence of interactions between the metal salt and the polymer matrix through the phosphine oxide linkage, thin films of the BP-PEPO modified, base materials were cast and their FTIR spectra obtained. Figure 4.1 shows the spectrum of the BP-PEPO film and peak assignments are discussed in section 4.1.1. The phosphine oxide bond stretch appears at approximately 1197 cm^{-1} . As discussed in Chapter 2, the effect of coordination upon the P-O stretch has been studied for a number of trialkyl and triaryl phosphine oxides.⁵⁷ Complex formation was found to shift the frequency of the vibration to lower energies. The infrared spectra of the unmodified BP-PEPO film along with those of the metal salt modified films are shown in Figure 4.11. A decrease in the intensity of the labeled phosphine oxide peak can be observed qualitatively. This decrease was also quantified by ratioing the absorbance of the P=O stretch separately to each of the aromatic C=C stretches at 1487 and 1589 cm^{-1} , which are assumed to be unaffected by the addition of metal salt. The results of this analysis are given graphically in Figure 4.12.

Polymeric ligands generally result in unsaturated complexes as argued in the literature review chapter. The observed intensity decrease of the phosphine oxide peak can possibly result from the complexation of a fraction of the phosphine oxide moieties in the chains. The appearance of a new peak at lower wavenumbers corresponding to the complexed moieties is not readily apparent from the spectra. It is possible that this low intensity peak is hidden beneath other peaks. Therefore, it is desirable to verify the existence of the complexation in these composite films by other methods.

A small decrease in the intensity of the C-O-C stretch was also observed. It is, therefore, likely that interaction of the metal compounds with the ether unit in the polymer may also be occurring. Again, there was no evidence of a new peak.

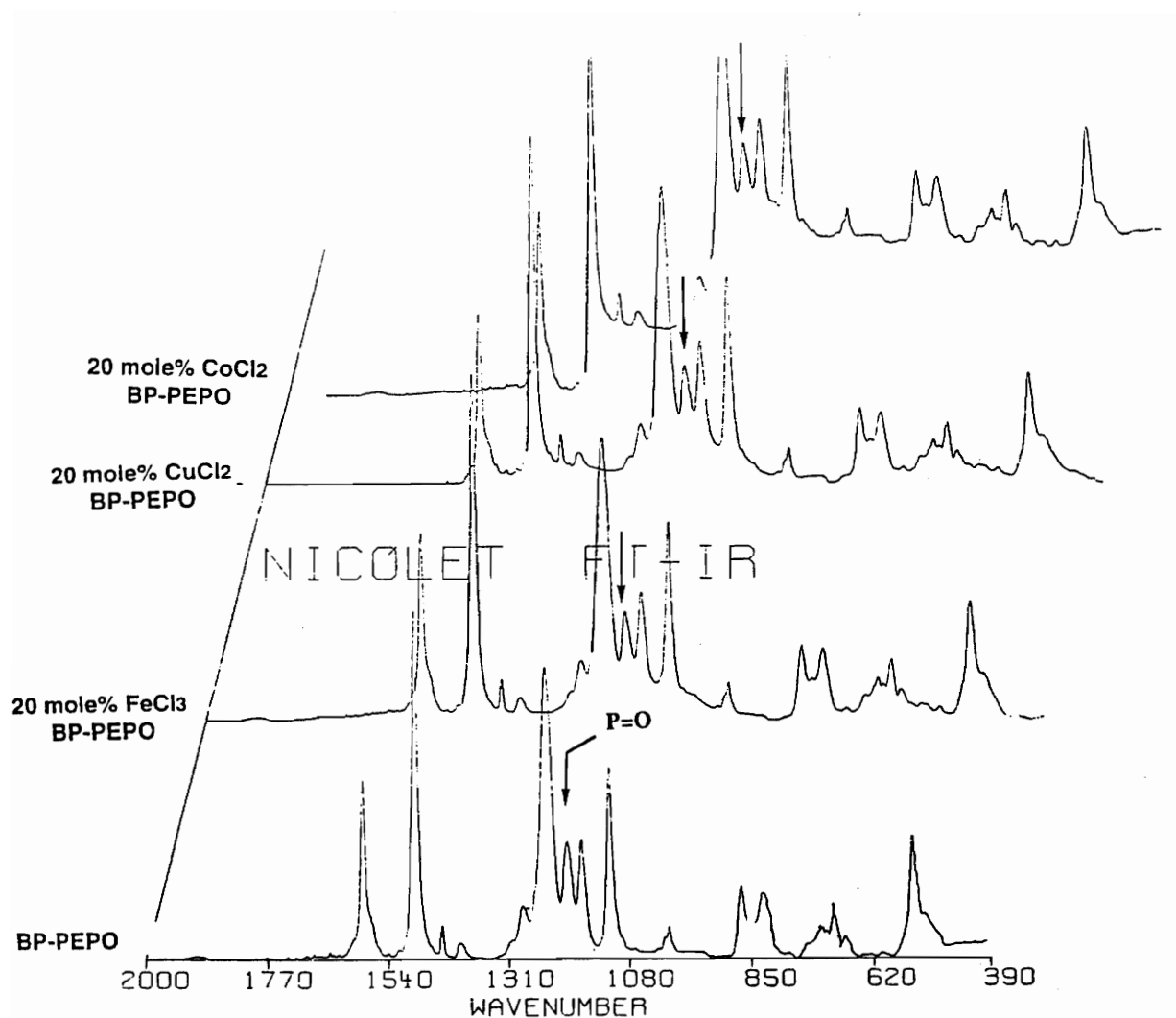


Figure 4.11 FTIR of 20 Mole % * Metal Chloride/BP-PEPO Composite Films
(mole % based on the repeat unit molecular weight, 460.28 g/mol)

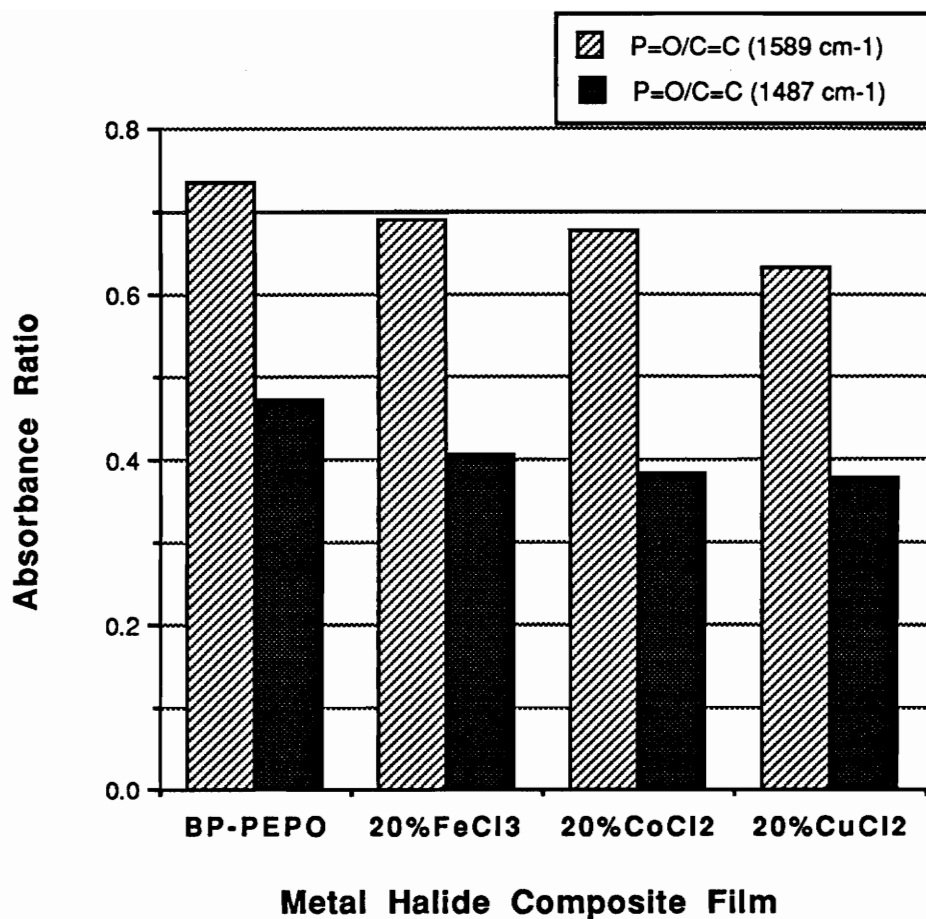


Figure 4.12 Quantitative Analysis of the Decrease in the P=O Stretch Intensity

(% = mole % based on the repeat unit molecular weight, 460.28 g/mol)

4.2.6 Phosphorus (^{31}P) NMR Studies

Phosphorus (^{31}P) studies were undertaken to further substantiate the interaction of the phosphine oxide group in the polymer with the metal salts. Solutions of Bis A-PEPO in DMAc (of approximately equal concentration) containing varying mole percents (0-20 mole % based on the repeat unit molecular weight, 502.55 g/mol) of FeCl_3 (Fe^{III} , d^5), CoCl_2 , (Co^{II} , d^7) and CuCl_2 (Cu^{II} , d^9) were prepared. The spectra of these solutions were obtained using 85% H_3PO_4 as an external reference and in the absence of a deuterated solvent. Phosphorus-31 (spin=1/2) is a 100% abundant isotope and is, therefore, an easy nucleus to observe. Comparison of chemical shifts was possible as each set of data was obtained under the same instrumental conditions and employing dichlorophenyl phosphine sulfide as a standard (76.05 ppm).

A marked downfield shift and broadening of the phosphine oxide peak is observed on binding with the metal salts. This effect is magnified with increasing metal salt content as is seen for Bis A-PEPO solutions with different CuCl_2 concentrations in Figure 4.13. The same trend is observed for FeCl_3 and CoCl_2 . The greatest shifts were observed for the CoCl_2 /Bis A-PEPO solutions with those of the CuCl_2 and FeCl_3 being smaller and of similar magnitude. The changes in chemical shift of the phosphine oxide resonance due to metal salt complexation relative to the Bis A-PEPO solution are reported in Table 4.7. The width of the peaks was measured in terms of the linewidth at half height (LWHH). The results of these measurements for the different metal salt concentrations are summarized in Table 4.8. Upon 5 and 10 mole % addition of metal salt, FeCl_3 and CuCl_2 show a greater broadening relative to the unmodified sample than the corresponding CoCl_2 solutions. However, at greater concentrations the CoCl_2 /Bis A-PEPO solutions show much greater phosphine oxide peak widths.

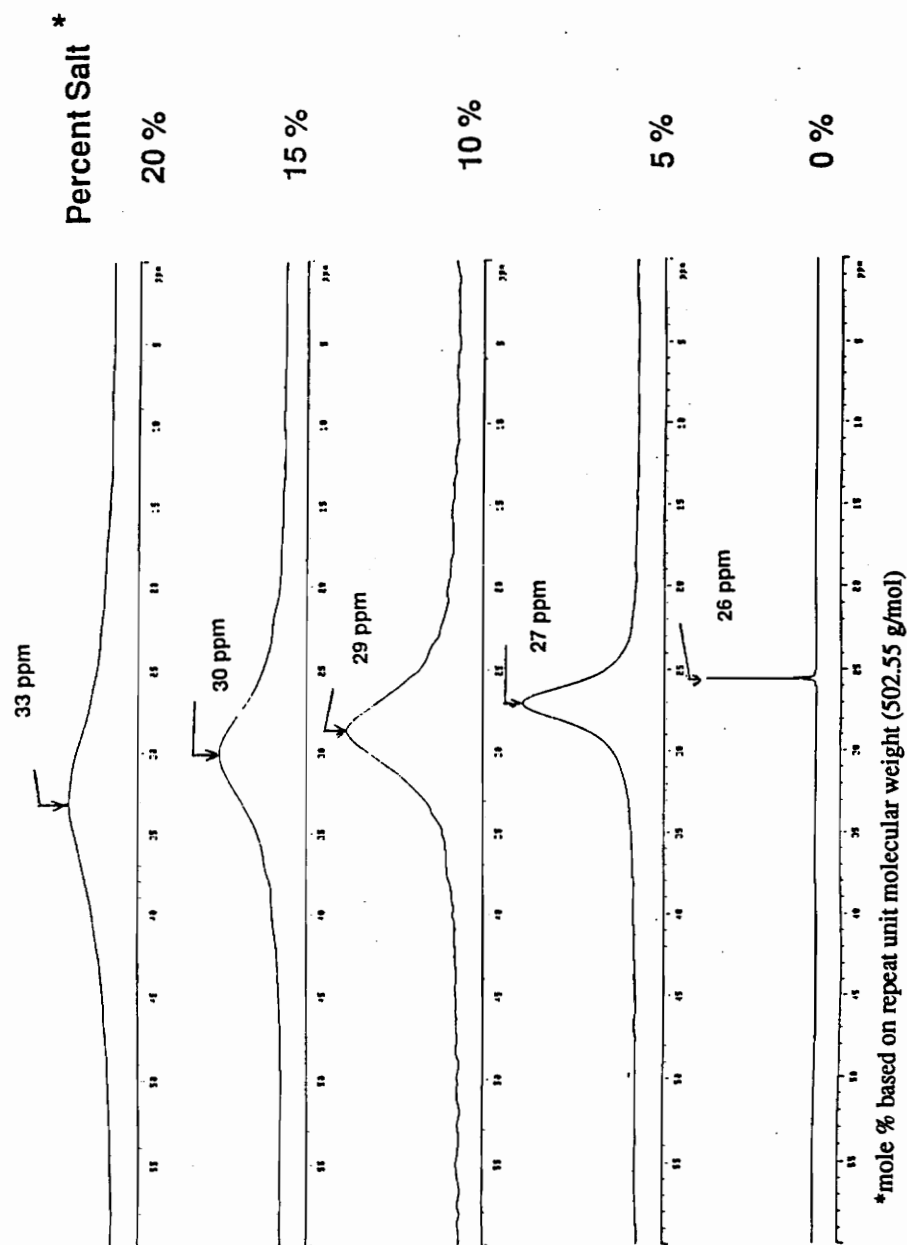


Figure 4.13 Phosphorus (^{31}P) NMR of Bis A-PEPO/ CuCl_2 in DMAc Referenced to H_3PO_4 at 0 ppm (161.9 MHz)

Table 4.7 Chemical Shift Changes Upon Metal Salt Addition

	Δ Chemical Shift (ppm)**		
Mole % salt*	CoCl₂	CuCl₂	FeCl₃
5	5	1	2
10	8	3	4
15	15	4	5
20	23	7	5

*Based on the repeat unit molecular weight, 502.55 g/mol

**Relative to a Bis A-PEPO DMAc solution

Table 4.8 Line Width at Half Height Results from ³¹P NMR Spectra of Metal Salt/Bis A-PEPO DMAc Solutions

	Line Width at Half Height (Hz)		
Mole % salt*	CoCl₂	CuCl₂	FeCl₃
0	7	7	7
5	8	8	610
10	350	830	890
15	7100	1000	1200
20	7300	1800	1600

*Based on the repeat unit molecular weight, 502.55 g/mol

The metal salts investigated thus far are all paramagnetic. Iron(III) is a d^5 transition metal, cobalt(II) is d^7 , and copper(II) is d^9 . In all three complexes of these metal chlorides with triphenyl phosphine oxide the transition metal is found to be in the tetrahedral high spin state.^{56,60} In this instance the iron has five unpaired electrons, the cobalt three, and the copper one. The presence of unpaired electrons in the polymeric complexes was verified by electron paramagnetic resonance (EPR). The spectra for the 20 mole % CuCl_2 and the FeCl_3 BP-PEPO films are shown in Figures 4.14 and 4.15, respectively. The EPR signal of the paramagnetic Co(II) could not be observed. However, spin-lattice relaxation time solid state measurements discussed later in this section confirm the existence of unpaired electrons in the polymer complexes of this salt.

The shift observed in solution due to the interaction of a paramagnetic substance with a diamagnetic reagent is a well studied phenomenon. It results from two terms: a contact interaction (Fermi contact interaction), and a through space dipolar interaction between an electron and a nucleus which is inversely proportional to the electron-magnetic nucleus distance.¹²⁰ This second term generally averages to zero in solution and can be ignored. The Fermi contact interaction results from a partially covalent bond or weak transient complex formation that causes a finite unpaired electron spin density on the nucleus. The magnitude of the contact shift in solution is a function of the concentration of the paramagnetic substance (C_1), the concentration of the substance interacting with the unpaired electrons (C_2), and the equilibrium constant for the complex formation or ligand exchange (K_C). From the experimental measurement of the paramagnetic shift for different known concentrations of the paramagnetic substance or the substrate, and using a simple linear equation one can calculate the equilibrium constant of ligand exchange as well as the hyperfine constant. This last quantity gives information about the strength of the interactions. Unfortunately, the evaluation of these parameters was not possible in our case since no specific control over the concentration was attempted during the experiments.

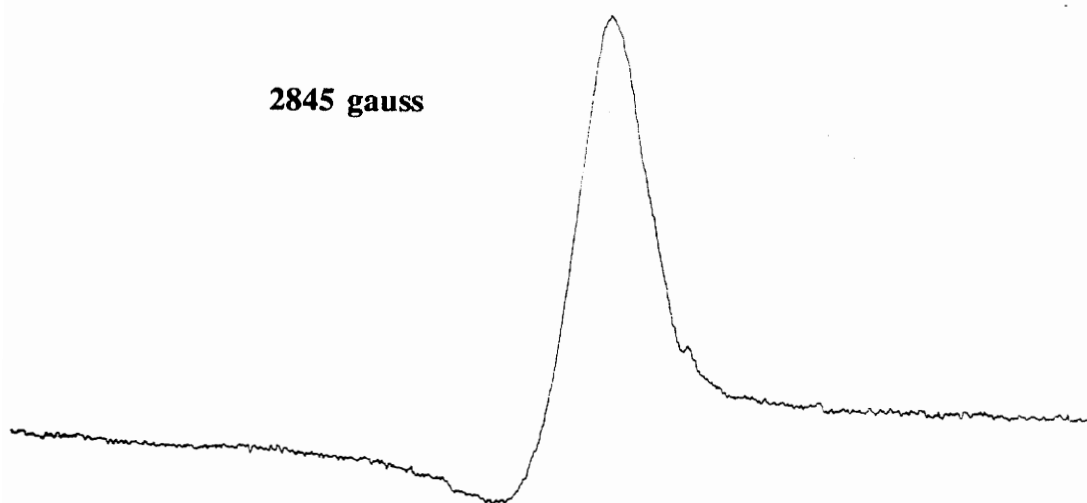


Figure 4.14 Electron Paramagnetic Resonance Spectrum of 20 Mole% CuCl_2 /BP-PEPO Film (9.55 GHz)



Figure 4.15 Electron Paramagnetic Resonance Spectrum of 20 Mole% FeCl_3 /BP-PEPO Film (9.55 GHz)

Additionally, the contact shift could not be measured accurately as the peaks were very broad. Nonetheless, the dependence of the change in the chemical shift on the metal salt concentration is a clear indication that there is an association equilibrium in solution between the metal and the phosphine oxide group in the polymer.

Ligand exchange in solution could conceivably account for the broad NMR linewidths observed. Two resonances would be predicted from the complexed and free P=O units in the polymer chain. However, if the exchange of the metal between different phosphine oxides in the solution occurs at a rate comparable with the NMR time scale (10^{-1} - 10^{-6} sec.) only one broad resonance is observed.¹²¹ This seems to be the case in our systems. In order to observe two resonances the rate of exchange can be reduced by lowering the temperature. Alternatively, warming the sample increases the rate of exchange, leading to a fully averaged spectrum in which case only one sharp peak would be seen. Dynamic NMR techniques can be very effective tools for obtaining kinetic information about the ligand exchange process and are suggested for future research.

Solvent interference with the metal salt-polymer coordination undoubtedly occurs in the DMAc solutions. Therefore, the solid state ^{31}P NMR spectra of the composite films were investigated. The paramagnetic shift and peak broadening were not observed in the solid state probably due to the restriction of motion in this state. However, ^{31}P NMR spin-lattice relaxation time (T_1) measurements at room temperature have proved useful in the study of the direct interaction of the paramagnetic salts with the phosphine oxide polymers. The relaxation times for the BP-PEPO films were determined using the inversion recovery method.¹²¹ This method involves the application of a 180° pulse which inverts the nuclear spin, followed by a delay time in which the spin partially recovers and further application of a 90° pulse placing the spin vector in the xy plane where it can be measured by the detector. The delay period is varied in a series of experiments, and the resulting signal is recorded. The T_1 is calculated from the time at which the response intensity is null. An

experimental example of the determination of the spin-lattice relaxation time using this method is given in Figure 4.16. The room temperature T_1 values of the phosphine oxide resonance measured for BP-PEPO composite films are summarized in Table 4.9. The polymer complexes of FeCl_3 , CoCl_2 , and CuCl_2 are paramagnetic. A diamagnetic ZnCl_2 /BP-PEPO composite film was used as a control. The BP-PEPO film phosphine oxide relaxation time was found to be 9.8 seconds. It is seen from Table 4.9 that the T_1 s of the paramagnetic composites are significantly lower relative to that of the unmodified BP-PEPO film.

Table 4.9 Spin-Lattice Relaxation Time Results for BP-PEPO Composites

Mole % Metal Salt*	Salt	T_1 (seconds)
0	---	9.8
20	CuCl_2	1.1
20	CoCl_2	0.9
20	FeCl_3	0.01
20	ZnCl_2	11.0

*Based on repeat unit molecular weight, 460.28 g/mol

Paramagnetic metal ions generally enhance the NMR relaxation rates, therefore, reducing the spin relaxation times. The spin-lattice relaxation is generally governed by the magnetic dipole-dipole interaction of the nucleus with the fluctuating magnetic dipoles of the surrounding spins (the lattice).¹²² The magnitude of the magnetic moments of the interacting spins determines, in part, the effectiveness of the dipole-dipole relaxation. The electron magnetic moment is considerably greater than the proton or

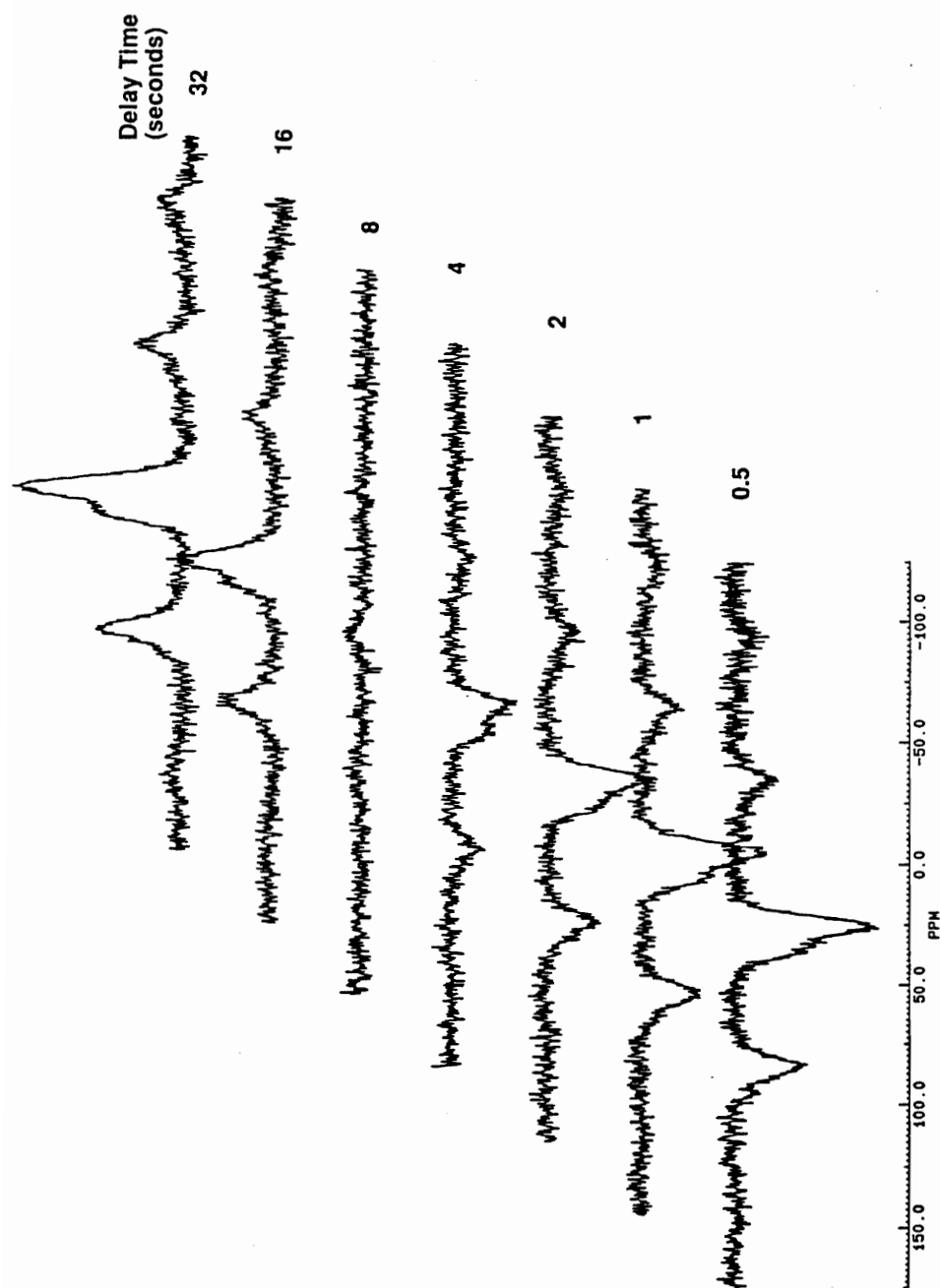


Figure 4.16 Illustration of Inversion Recovery Method for Spin-Lattice Time Determination from Solid State ^{31}P NMR of BP-PEPO Composites Referenced to H_3PO_4 at 0 ppm (121.4 MHz)

phosphorus-31 magnetic moments. Therefore, in the vicinity of unpaired electrons the relaxation process is dominated by the electron-nuclear dipole-dipole interactions.

The relaxation rates ($1/T_1$) for the direct interaction of a nuclear spin with a paramagnetic ion are related to the number of unpaired electrons as well as the separation between the electron spin and the nuclear spin (r).¹²² The relaxation rate is directly proportional to the total electron spin [$S(S+1)$, where S is the number of unpaired electrons], and increases as r^{-6} . In our study, the largest decrease in the relaxation time relative to the unmodified film was observed for the FeCl_3 composite followed by that of the CoCl_2 and, lastly, the CuCl_2 film (Table 4.9). On the other hand, within experimental error, the T_1 of the diamagnetic system was the same as for the BP-PEPO film. Assuming that the coordination geometry of the polymeric complexes is the same as that of the monomeric counterparts, the number of unpaired electrons for Fe(III) , Co(II) , and Cu(II) are five, three, and one, respectively. The trend observed in the reduction of the relaxation times for the paramagnetic salts appears to be consistent with the dependence of $1/T_1$ on the total electron spin. Additionally, this finding substantiates that the direct interaction between the metal chloride and the phosphine oxide unit in the polymer is responsible for the observed chemical shifts in solution. However, from these studies alone no conclusions can be drawn about the metal-phosphine oxide distance.

4.2.7 Microscopy Studies

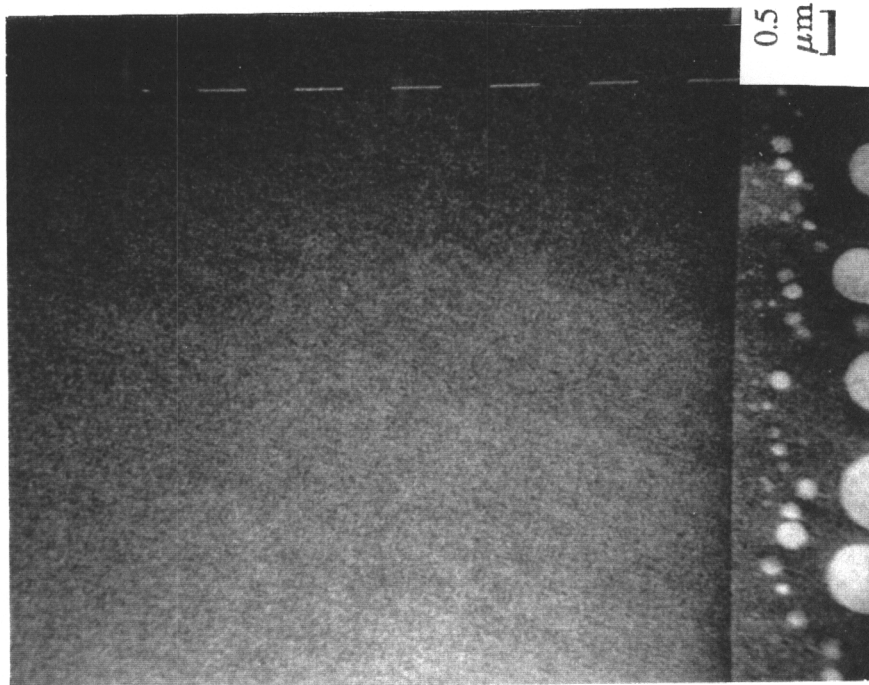
Selected electron microscopy studies were conducted to explore the bulk structural features of the metal chloride/PEPO composites. It was of interest to investigate the occurrence and extent of agglomeration of the metal salt within the composite materials. Additional information about the atomic bulk composition of these films was obtained from coupled Energy Dispersive X-Ray Analysis (EDAX).

In transmission electron microscopy a cross-section of the material is magnified and the contrast is provided by electron density differences. The high electron density of metals relative to common polymers allows for very good contrast in the case of metal halide containing polymer composites.

In order to investigate the effect of metal salt chemistry on the morphology of the metal-PEPO composites, samples of BP-PEPO films containing 20 mole % FeCl_3 , CoCl_2 , and CuCl_2 were prepared and their solid state structure was investigated by transmission electron microscopy. No structural differences were observed for the various metal chlorides. Even at high magnifications (300,000 x) there was no evidence of metal particles in these films. However, the presence of metal salt in the film was confirmed by EDAX. The phosphorus:metal:chlorine atomic ratio obtained from semi-quantitative analysis suggested the existence of the salt form of the metal in the bulk. It appears that the metal chlorides are well "dissolved" in the BP-PEPO matrix, with no detectable aggregation occurring.

The influence of the polymer matrix on the morphology of the composites was also studied. The scanning transmission electron micrographs of Bis A-PEPO and BP-PEPO films with an equal loading of CoCl_2 (20 mole %) were compared (Figure 4.17). At a magnification of 12,500, evenly distributed metal chloride particles of a 600 Å average diameter were observed in the Bis A-PEPO composite. Under the same magnification in the CoCl_2 /BP-PEPO sample no dark metal spots were found. X-ray diffraction patterns of the CoCl_2 /Bis A-PEPO film were indicative of amorphous metal halide domains. The observed differences in bulk morphology due to variations in the polymer matrix may possibly result from a combination of chain structure differences and the level of diffusion of the metal salt through the polymer matrix. The diffusion of the metal salt was discussed in section 4.2.1 in relation to film drying. It is striking how a subtle change in chain chemistry (the addition of an isopropylidene group) results in an important variation of the

A)



B)

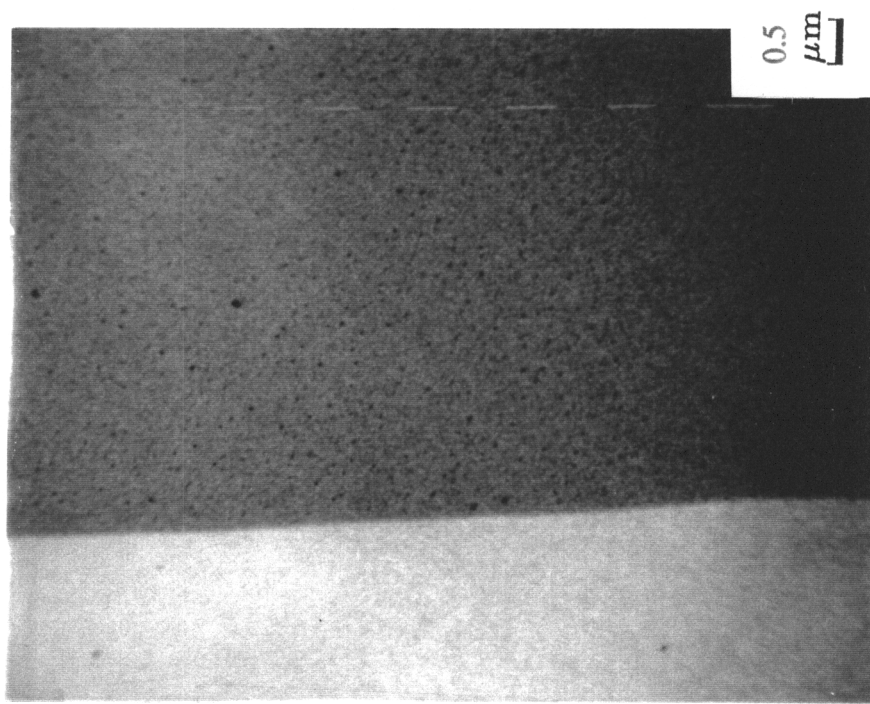


Figure 4.17 Transmission Electron Micrograph of 20 Mole % CoCl_2 Modified Films:

A) BP-PEPO Matrix, B) Bis A-PEPO Matrix

chemical structure which, in turn, influences the morphological features of the material.

To investigate the influence of a large excess of the metal salt, 50 mole % of CoCl_2 (relative to the molecular weight of the BP-PEPO repeat unit) was added. This, in effect, was an attempt at surpassing the saturation limit of the BP-PEPO matrix. The electron micrograph of the 50 mole % CoCl_2 /BP-PEPO film is shown in Figure 4.18, which reveals the existence of evenly dispersed metal chloride particles. Close to the edge of the film the average particle diameter is $\sim 0.4 \mu\text{m}$, whereas, the particle size is more than double further inside the film. As expected, a much higher metal content is obtained from the EDAX analysis of the dark particles relative to the polymer matrix. The thermal properties of the 0, 20, and 50 mole % CoCl_2 /BP-PEPO films are summarized in Table 4.10. The incorporation of 20 mole % CoCl_2 resulted in an enhancement of the thermo-oxidative stability and an increase in the glass transition temperature in relation to the BP-PEPO. However, addition of 50 mole % of this metal chloride had a detrimental effect on the thermal properties of the base polymer. The observed behavior tends to suggest that in the latter case the metal salt is at least in part plastizicing the system and decreasing the thermal stability.

Table 4.10 Thermal Properties of CoCl_2 /BP-PEPO Composites

Mole % Metal Salt*	5 % wt. Loss (°C)**	T _g (°C)***
0	518	232
20	554	266
50	506	158

*Based on repeat unit molecular weight, 460.28 g/mol

**TGA. 10°C/min. In air

***DSC. Second scan. 10°C/min

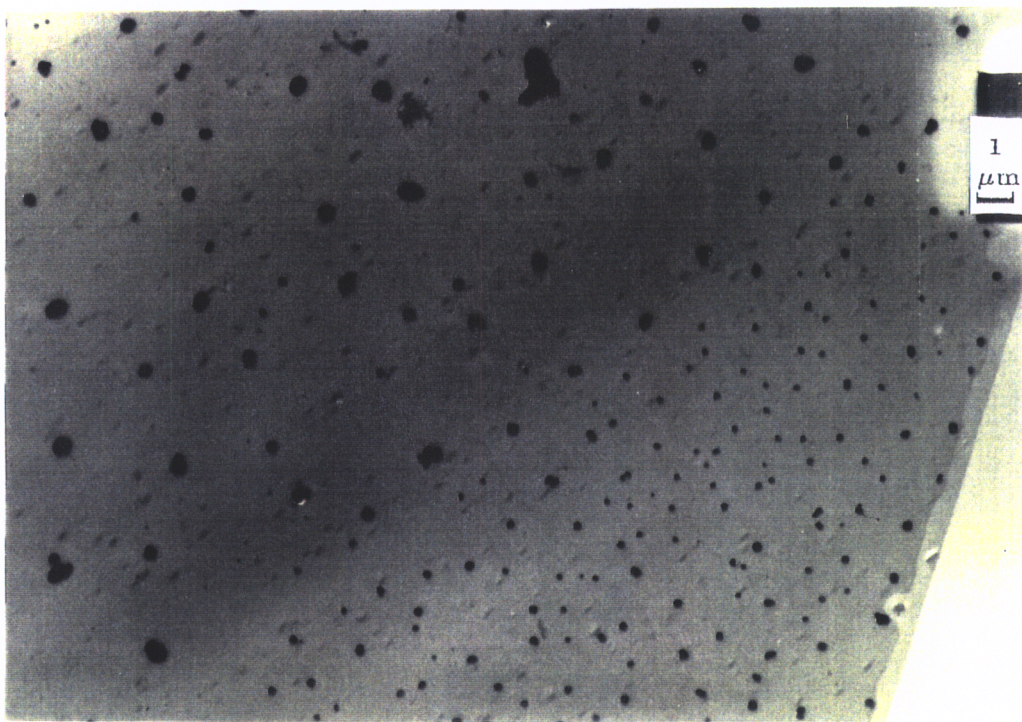


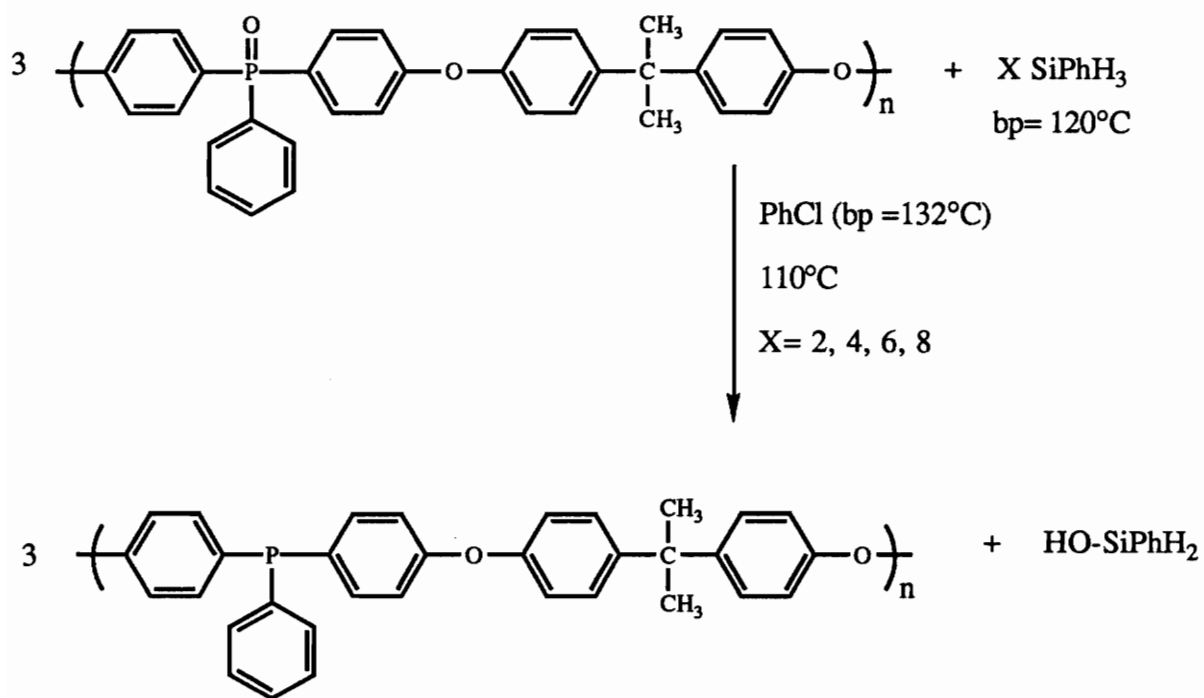
Figure 4.18 Transmission Electron Micrograph of 50 Mole % * CoCl_2 /BP-PEPO Composite (*mole % based on the repeat unit molecular weights)

4.3 Preparation and Characterization of Poly(Arylene Ether Triaryl Phosphine)s

This section reports investigations into reduction of poly(arylene phosphine oxide)s to their corresponding phosphines. It is reasonable to expect that these phosphines could serve as good ligands for metal complexation. Thus, it was of interest to investigate the formation of the novel poly(phosphine)s by reduction of the phosphine oxide polymer described above. The polymeric phosphines were synthesized via the phenylsilane reduction of BisA-PEPO (Scheme 4.1).

Silanes are commonly used for the reduction of low molecular weight phosphine oxides due to their wide scope, easy use, clean stereochemistry, and high yields.¹²³ The most frequently used silanes are trichlorosilane, hexachlorodisilane, and phenylsilane. In our case, phenylsilane was the reagent of choice since it results in the highest yields (~90%), is commercially available, and unlike trichlorosilane it does not require the use of an amine which may be difficult to remove.^{123,124} Trichlorosilane, hexachlorodisilane, and phenylsilane are often used in the synthesis of optically pure phosphines. The resulting stereochemistry depends on the reagent used, and can result in almost complete retention of configuration with phenylsilane. The proposed mechanism for the phenylsilane reduction of tertiary phosphine oxides in accordance with the observed stereochemistry is shown in Figure 4.19.¹²³

By varying the molar ratio of phosphine oxide to phenylsilane, the percent solids of the polymer solution and the reaction time, a 15 Kg/mol BisA-PEPO was reduced to different extents. The reaction was followed by phosphorus (³¹P) NMR (Figure 4.20) which permits the degree of reduction of the polymer to be determined from the integrated peak areas of the R₃P=O (25 ppm) and PR₃ (-7.5 ppm) units in the polymer. The phosphine content in the polymer can be varied by the extent of phosphine oxide reduction. A sample



Scheme 4.1 Phenylsilane Reduction of BisA-PEPO

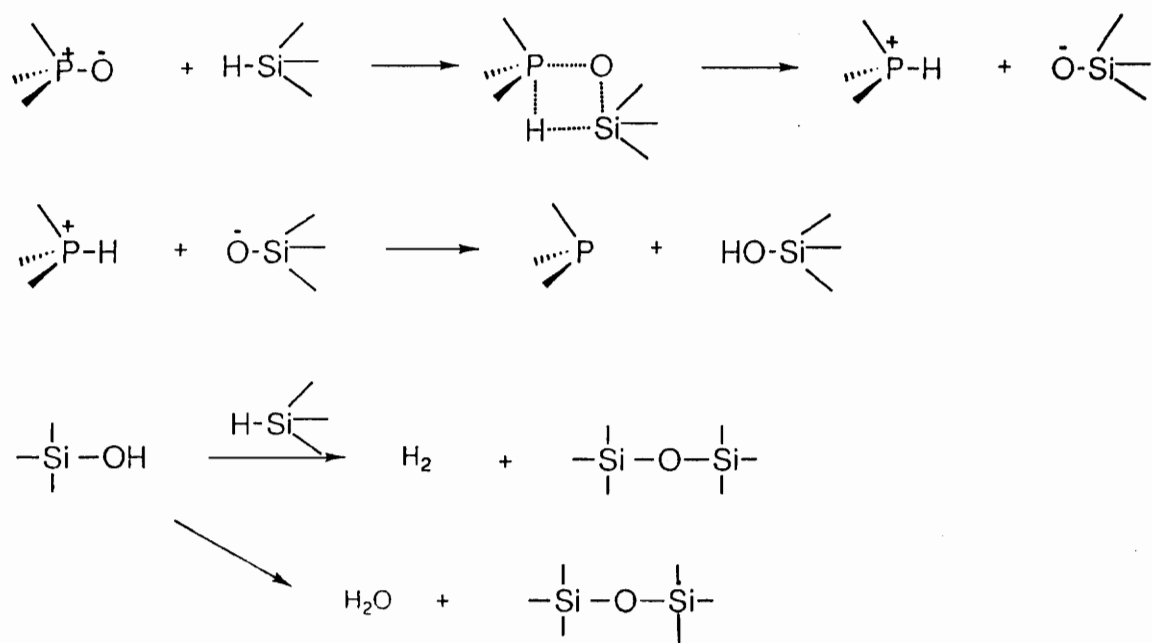


Figure 4.19 Proposed Mechanism for Phenylsilane Reduction of Tertiary Phosphine Oxides¹⁵

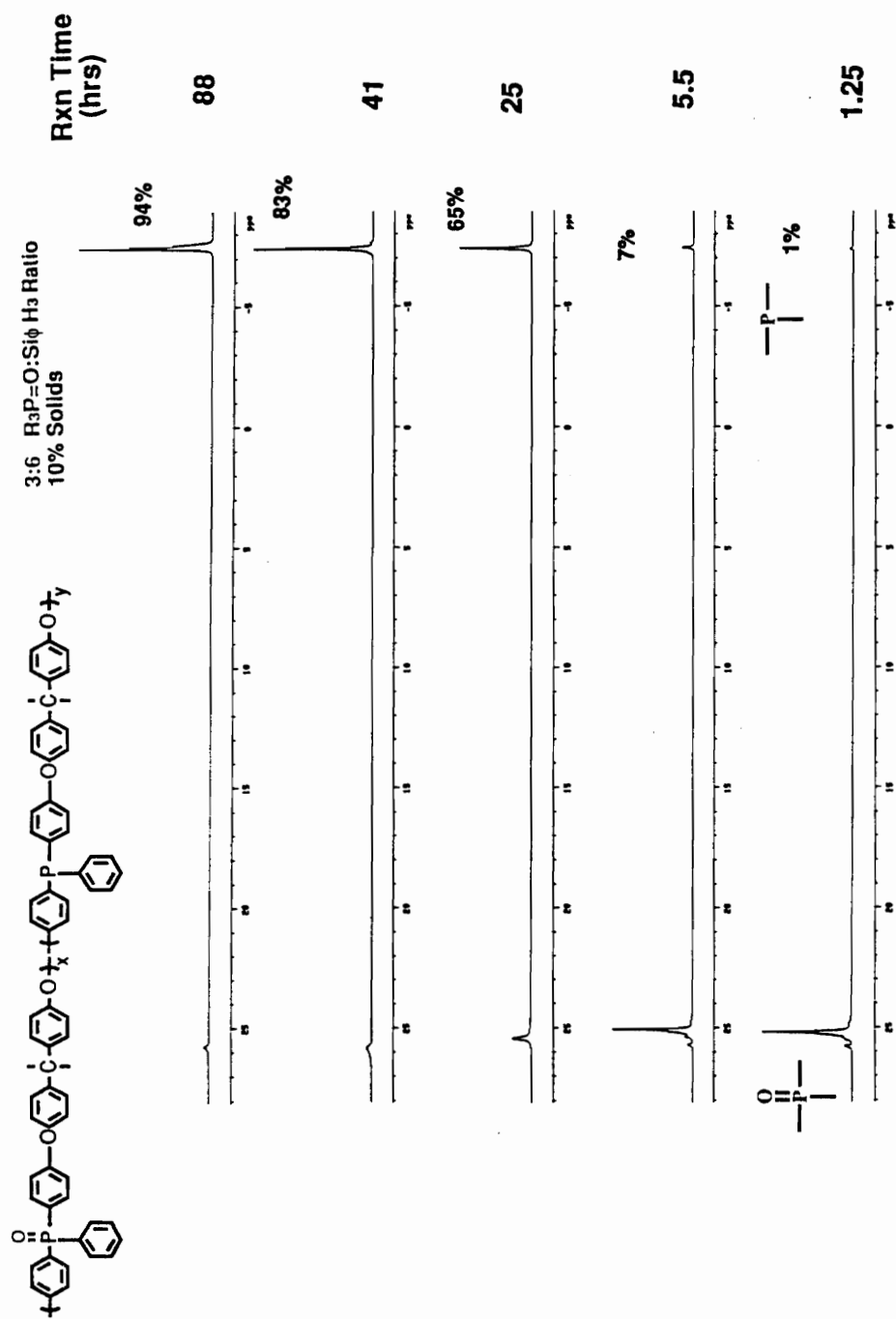


Figure 4.20 ³¹P NMR Spectra Referenced to H₃PO₄ at 0 ppm (161.9 MHz) for Different Reaction Times during the Reduction of Bis A-PEPO

proton NMR spectrum of one of these partially reduced polymers is given in Figure 4.21. The intrinsic viscosity in chloroform at room temperature, the thermo-oxidative stability, and the glass transition temperature of these triarylphosphine containing polymers were studied as a function of backbone phosphine content. These results are summarized in Table 4.11.

In general, the thermo-oxidative stability in terms of the 5% weight loss temperature was found to decrease relative to the starting poly(arylene ether phosphine oxide) with the incorporation of the phosphine unit in the chain. The room temperature intrinsic viscosity in chloroform increases with phosphine content and the 94% reduced polymer was found to be only partially soluble in the relatively polar chloroform. The glass transition temperature decreased with increasing percent phosphine as determined by differential scanning calorimetry. In the case of the 54% phosphine polymer, two distinct softening temperatures were found indicating a blocky type or at least non-random chain architecture. Transformation of the triaryl phosphine oxide to the corresponding phosphine alters both the molecular structure of the chain as well as the intermolecular interactions. The geometry of tricoordinate phosphorus is pyramidal, whereas that of pentacoordinate phosphorus is tetrahedral. This stereochemistry difference can result in very different polymer chain structures. The polarity of the chain also decreases upon reduction to the phosphine. The polymer-polymer intermolecular forces, polymer-solvent intermolecular interactions, and the intramolecular chain stiffness characteristics related to resonance possibilities are influenced by these variations. The intrinsic viscosity for a single solvent at a defined temperature, and the glass transition temperature for a given heating rate are influenced by the combination of these factors. The general decrease in the oxidative stability with increasing phosphine content is in agreement with the generally greater stability of monomeric phosphines oxides relative to the corresponding phosphines.

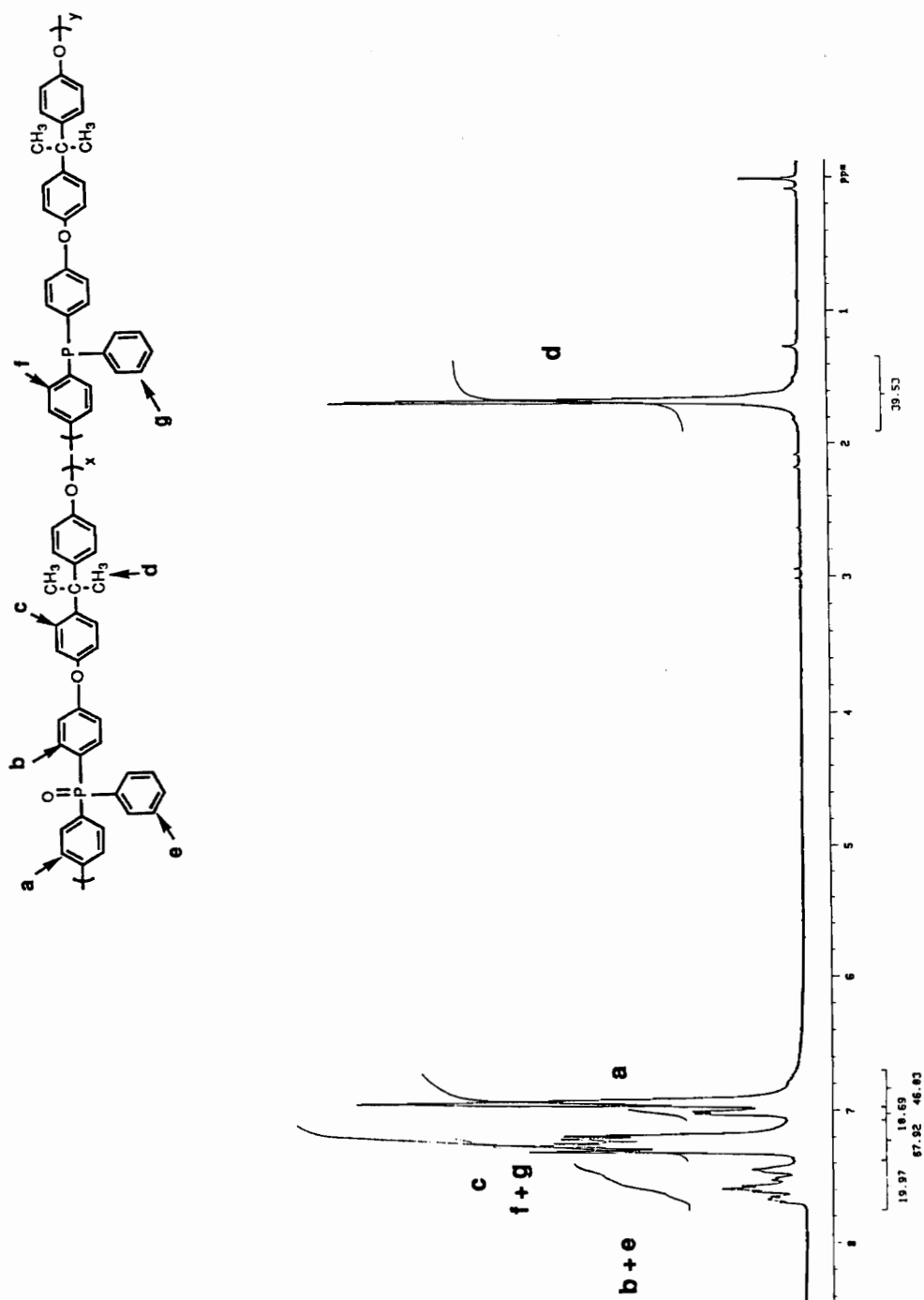


Figure 4.21 ^1H NMR Spectrum of 70% Reduced Bis A-PEPO in CDCl_3 Referenced to TMS at 0 ppm (400 MHz)

Table 4.11. Results of Phenyl Silane Reduction of 15K BisA-PEPO

POR3:SiPhH ₃	% Solids	Final mole% phosphine	Total Rxn Time(hrs)	[η] ^{25°C} (dl/g) ^{CHCl₃}	%5Wt.Loss (°C)*	Tg (°C) **
15K Bis A-PEPO	---	0	---	0.28	511	194
3:2	20	9	28	0.27	525	192
3:4	20	28	38	0.33	513	185
3:6	20	54	48	0.36	443	158/174
3:6	10	94	88	---	418	155

*Dynamic TGA. 10°C/min

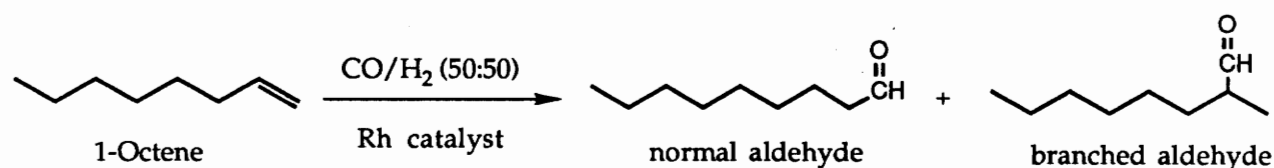
**DSC. Second scan. 10°C/min

4.4 Hydroformylation of Octene-1 over a Rhodium Complex of Poly(Arylene Ether Triaryl Phosphine)

As discussed in the literature review, triphenylphosphine is very often used as a ligand in organometallic chemistry and homogeneous catalysis due to its good reaction selectivity and activity. The large size of the ligand together with its relatively low basicity combine to make triphenylphosphine an ideal ligand. The immobilization of homogeneous catalysts, most importantly, facilitates the separation of the reaction product and the recovery of the catalyst. The preparation of polymer-anchored catalysts, generally involves the modification of an organic polymer via attachment of a ligand group such as a phosphine; onto which the soluble metal complex is bound. Phosphine modified polystyrene is the most widely used organic support. Only a few of the phosphine containing polymer anchors possess the phosphine unit in the polymer backbone,^{37,125} and those which do, generally have very low molecular weights and lack thermal as well as mechanical stability. The polymer described above is novel in that it contains the triphenylphosphine moiety in the backbone and has good thermal and mechanical properties. Another advantage of this polymeric ligand is that even though Schlenk techniques which allow one to carry out operations in an inert atmosphere were employed as a precaution, the phosphine polymers are not air-sensitive. Air and water need not be strictly excluded from the system as is required for many monomeric phosphine ligands.

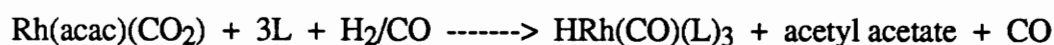
The 94% reduced BisA-PEPO polymer described in the previous section was used as a ligand in the investigation of the catalytic activity and selectivity of a rhodium complex in the hydroformylation of octene-1. This process has received considerable attention due to its industrial and commercial importance. It involves the conversion of an olefin to an aldehyde by the addition of carbon monoxide and hydrogen to a double bond. The reaction is catalyzed by a wide variety of homogeneous transition metal complexes. The hydroformylation of octene-1 in the absence of isomerization yields two products resulting

from the Markovnikov (branched aldehyde) and anti-Markovnikov (normal aldehyde) addition to the double bond (Scheme 4.2).



Scheme 4.2 Catalyzed Hydroformylation of Octene-1

Catalysts can be prepared *in situ* from $\text{Rh}(\text{acac})(\text{CO})_2$ and an appropriate ligand as shown in Scheme 4.3,^{126,127} and this was the method of choice in the present study.

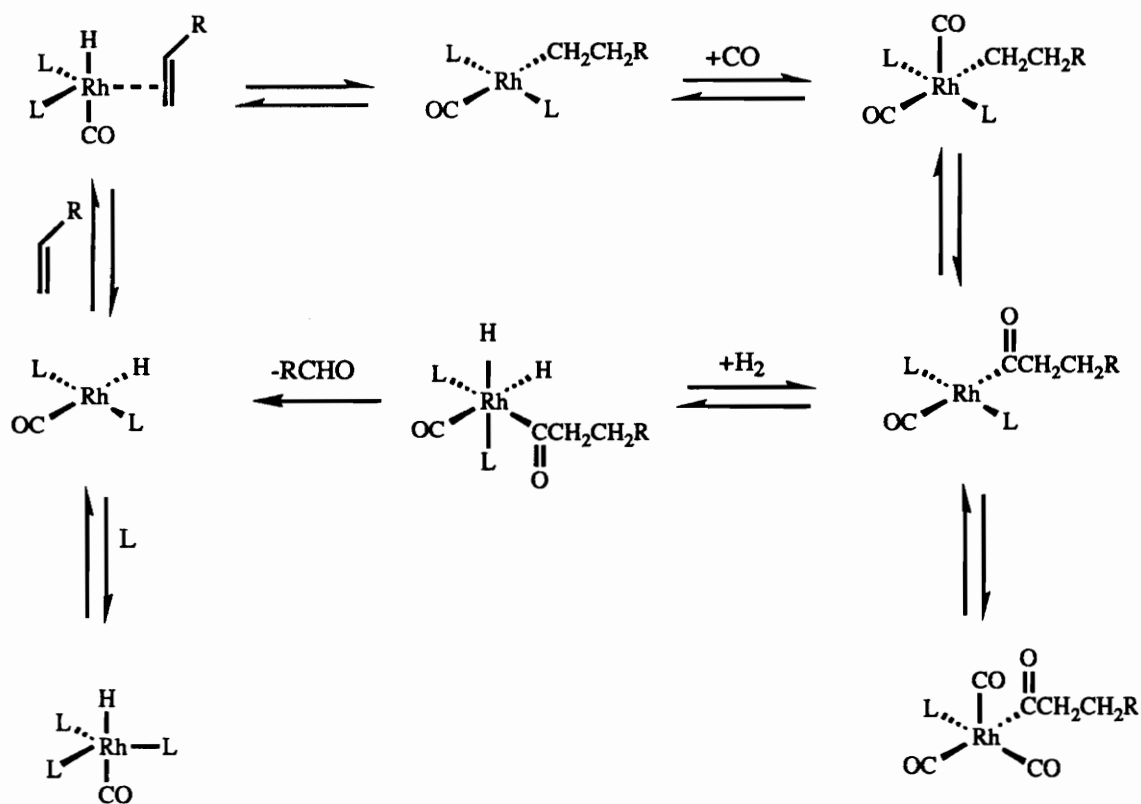


L = phosphine ligand

Scheme 4.3 *In Situ* Generation of the Active Rhodium Catalyst

The simplified catalytic cycle for hydroformylation of alkenes using rhodium complexes is shown on Figure 4.22.⁵⁰

All reactions were carried out in a stainless steel reactor at 120°C and initial pressure of 230 psi. Two separate studies were conducted, while maintaining a constant total volume inside the reactor and a fixed octene-1/rhodium ratio. Firstly, with a phosphine/rhodium ratio of two, the reaction time was varied from half an hour to fifteen hours. In a second study, the phosphine/rhodium ratio was varied from two to ten, while each reaction was



L = phosphine ligand

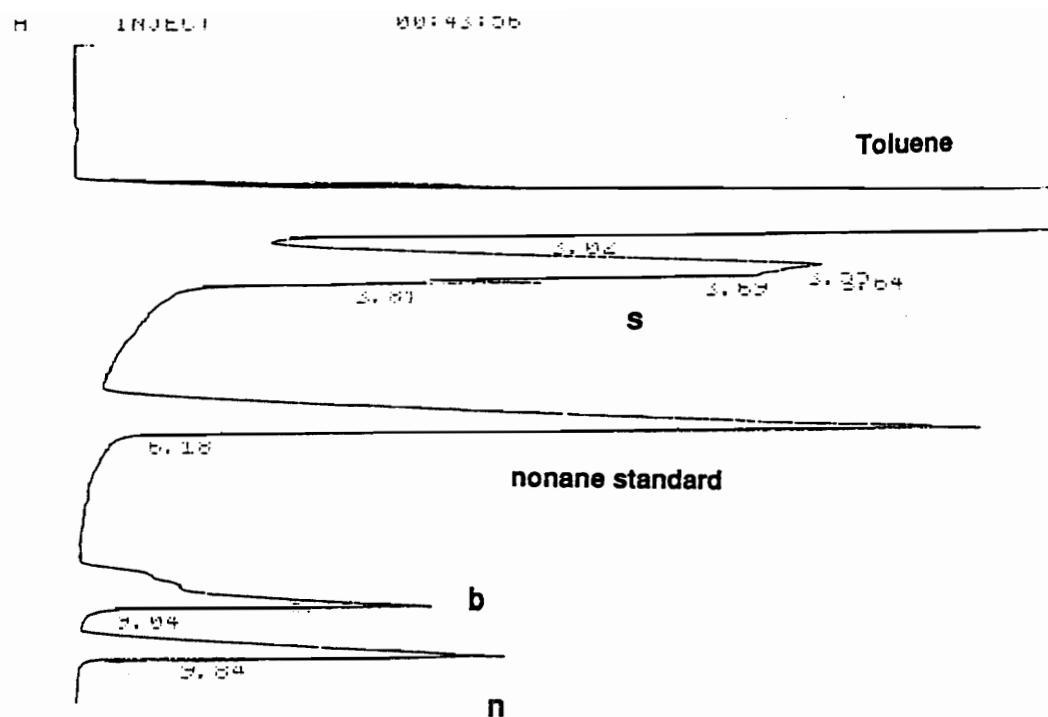
Figure 4.22 Simple Catalytic Cycle for Hydroformylation by Rhodium Catalysts⁵⁰

allowed to proceed for three hours. Gas chromatography was used for product analysis. A sample chromatogram is shown in Figure 4.23.

The catalytic activity and selectivity of the poly(arylene ether triaryl phosphine)-rhodium complex is reported as the percent yield of aldehydes and normal/branched aldehyde ratio (n/b) which includes all possible branched isomers resulting from isomerization of the double bond. The results of the time dependence and the phosphorus/rhodium variation experiments are presented graphically in Figures 4.24 and 4.25, respectively.

In the time dependence experiments in which the P/Rh ratio is 2/1 the percent conversion increases with increasing reaction time and reaches a plateau at 75% conversion after approximately fourteen hours. The n/b ratio, on the other hand, decreases with increasing reaction time as a result of a greater extent of isomerization at longer reaction times leading to the branched aldehydes. Using this low P/Rh ratio the rate of hydroformylation with this novel polymeric ligand is rather slow relative to homogeneous counterparts. However, this is not the case for higher P/Rh ratios as is seen in the phosphine/rhodium ratio variation experiments conducted at a constant reaction time of three hours. The percent conversion increases with increasing P/Rh ratio until it reaches a plateau at approximately 95% conversion, corresponding to a phosphorus/rhodium ratio of approximately 8/1. At these high P/Rh ratios the reaction is almost quantitative after only three hours. The ratio of normal to branched aldehyde products also increases with increasing phosphine ligand and attains a maximum value at ~5.5 also at a phosphorus/rhodium ratio of 10. The selectivity of this polymer supported catalyst is greatly improved compared to homogeneous counterparts.

Very comprehensive studies of microporous phosphinated styrene-divinylbenzene resins have revealed that the normal to branched aldehyde selectivity in the hydroformylation of olefins is determined by the phosphine loading of the support, the phosphine/rhodium ratio, and the crosslink density of the resin.¹²⁸ These factors alter the ligand equilibria within the swollen resin such that high phosphine loadings and high phosphine/rhodium



00:43:05

1.	METHOD	RT	INDEX
68.47	RT	68.47	02
8.732	RT	8.732	02
1.608	RT	1.608	02
1.044	RT	1.044	02
1.029	RT	1.029	03
11.342	RT	11.342	01
1.140	RT	1.140	02
2.607	RT	2.607	03
3.024	RT	3.024	01

s = starting material
n = normal aldehyde
b = branched aldehydes

Figure 4.23 Sample Gas Chromatogram of the Octene-1 Hydroformylation Product

Rxn Time=3 hrs
1-octene/Rh= 500/1

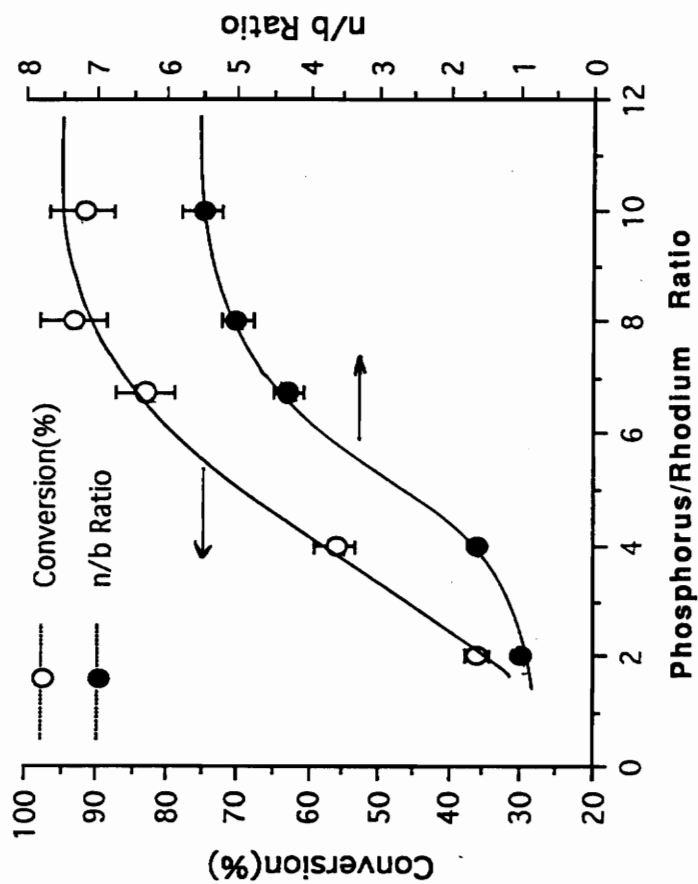
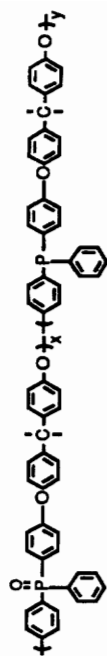


Figure 4.25 Effect of Phosphorus/Rhodium Ratio on the Hydroformylation of Octene-1

ratios promote the formation of the more crowded bisphosphine species, thus resulting in a higher yield of the normal aldehyde. In our case, the greater selectivity observed at high phosphine/rhodium ratios could, therefore, result from the steric demand of the polymeric ligand which facilitates the formation of the normal aldehyde.

The supported rhodium complex generated from the novel triarylphosphine polymeric ligand offers several important advantages over conventional homogeneous catalysts. As has been discussed, at high phosphine/rhodium ratios the selectivity and activity of the catalyst are considerably high. Additionally, the heterogeneous nature of the polymeric catalyst allows for the easy separation of the product and the recovery of the catalyst which are of considerable commercial importance. Also, the mechanical strength and thermal stability of the polymer may allow the use of this type of catalyst in reactions in which strong agitation is required and higher temperatures enhance the rate of the reaction.

5.0 Conclusions

Controlled high molecular weight poly(arylene ether phosphine oxide)s have been synthesized via the nucleophilic aromatic substitution route. These materials were subsequently used in the preparation of polymer/metal composite films. Bis A-PEPO films comprising 0-20 mole % (based on the repeat unit molecular weight, 502.55 g/mol) of FeCl_3 , CoCl_2 , or CuCl_2 were prepared to study the influence of different metal salt chemistries and concentrations on polymer properties. Additionally, BP-PEPO composite films with an equal loading of the metal salts (20 mole %) were prepared to investigate the effects of varying polymer backbone chemistry.

Homogeneous, clear, tough films were obtained with their colors varying from brown in the case of the iron and yellow for the copper to deep blue for the cobalt. The unmodified films were soluble in DMAc, N-methylpyrrolidone, and chloroform; however, the solubility of the complexed films was limited to amide solvents.

Each metal chloride/polymer pair appears to be a case unto itself regarding specific polymer properties such as thermal stability, glass transition temperature, and morphology. TGA scans revealed that the temperature related to the onset of decomposition of unmodified Bis A-PEPO was increased by the incorporation of CoCl_2 , and decreased by the addition of FeCl_3 or CuCl_2 . In the cases for which a lowering in thermal stability was observed, the decrease was generally more pronounced as the amount of metal salt added was increased. In contrast, in the case of BP-PEPO the 5 % weight loss temperature was increased by the incorporation 20 mole % of either FeCl_3 or CoCl_2 , and decreased by the addition of CuCl_2 . In general, the thermal stabilities of the metal modified polymers are influenced by the backbone structure of the polymer, the chemistry of the metal salt, and their relative concentrations.

The glass transition temperatures of the Fe(III) chloride and of the Co(II) chloride polymer films gradually increase with increasing salt content in comparison to the unmodified polymers. Whereas, all the Cu(II) chloride films exhibit a depression of the glass transition temperature relative to the base material. These trends in T_g s are influenced by factors including crosslinking through complexation, enhanced chain rigidity, decrease of preexisting intermolecular forces, and plasticizer effects.

The dynamic mechanical analysis of the biphenol PEPO films with 20 mole % concentration of CoCl_2 , FeCl_3 and CuCl_2 , respectively, showed a remarkable increase and retention of the storage modulus as a result of the incorporation of metal salt. This rise in the storage modulus may be due to cross-linking by the metal, but is possibly related to the solid state composite-like structure of the new hybrid.

Phosphorus (^{31}P) NMR studies of DMAc solutions of the different compositions of the three metal chlorides showed a gradual downfield shift and broadening of the phosphoryl peak with increasing concentration of metal salt, indicating the existence of interactions between the polymer and the metal in solution. An observed decrease in the intensity of the phosphine oxide stretch peak by infrared suggested the presence of complexation in the solid state composites. In order to substantiate this, phosphorus (^{31}P) NMR spin-lattice relaxation time measurements were performed on the composite films. A substantial lowering of the relaxation time for the paramagnetic halide containing polymer systems confirmed the interaction of the metal salts with the phosphine oxide group in the polymers.

The bulk structural features of the metal chloride/PEPO composites were explored using electron microscopy coupled with Energy Dispersive X-Ray Analysis (EDAX). The incorporation of 20 mole % of the metal salt in the BP-PEPO matrix did not result in a detectable agglomeration of the metal compound. However, the addition of 50 mole % of CoCl_2 resulted in the appearance of metal domains accompanied by a substantial decrease in the thermal stability, as well as the glass transition temperature relative to both the

unmodified polymer and the polymer with 20 mole % incorporation of this same metal chloride. This seems to indicate that the metal salt is at least in part acting as a plasticizer. The bulk morphology of the 20 mole % composites was different with the Bis A-PEPO matrix in which case metal domains were also evidenced as in the case of the 50 mole % CoCl_2 -BP-PEPO composite. A combination of chain structure differences, and the level of diffusion of the metal salt through the polymer matrix may explain the difference in morphology observed for the two matrices.

Additionally, novel poly(phosphine)s were synthesized via the reduction of linear poly(arylene ether phosphine oxide)s. Phenylsilane was employed to reduce Bis A-PEPOs to the corresponding phosphines. By varying the molar ratio of phosphine oxide to phenylsilane, the percent solids of the polymer solution, and the reaction time, varying extents of reduction were possible. The room temperature intrinsic viscosity of the starting Bis A-PEPO in chloroform increases with increasing percent phosphine. In general, the thermo-oxidative stability and the glass transition temperature of the starting polymer decreases with increasing conversion to the phosphine due to a variation in the chemistry and molecular structure of the chain as well as the intermolecular interactions.

A 94% reduced Bis A-PEPO polymer was used as a ligand in the investigation of the ability of a rhodium complex to catalyze the hydroformylation of octene-1. The catalyst activity and selectivity (percent yield of aldehydes and normal/branched ratio) were studied as functions of reaction time as well as ligand to rhodium ratio. Compared to their homogeneous counterparts, these heterogeneous catalysts suffer in terms of reaction rate at low ligand/rhodium ratios. However, at higher phosphorus/rhodium ratios the reaction is almost quantitative after three hours. At these high P/Rh ratios a great improvement in selectivity is obtained in comparison to other monomeric homogeneous catalysts.

6.0 Suggested Future Research

The investigations conducted in this thesis suggest a number of future research studies. Firstly, since several metal chlorides have been shown to complex with the triarylphosphine oxide-containing poly(arylene ether)s, it would be of interest to study the complexation of other metal compounds in an effort to impart or modify specific properties of the material. For example, it would be interesting to investigate the complexation of zirconium acetate since it has been shown to be an excellent smoke suppressor.

More research is needed to determine the metal ion geometry and coordination in these phosphine oxide polymeric complexes. UV/visible spectroscopy on the “colored” films would be very useful in this respect. Magnetic measurements as well as ^{31}P NMR would also be effective tools in the elucidation of the structure of these complexes. Additionally, information about the kinetic aspects of ligand exchange can be obtained from dynamic ^{31}P NMR techniques.

More extensive and detailed microscopy studies on the metal halide/PEPO composites would provide further information about the morphological features of these systems.

An extension of the catalyzed hydroformylation of octene-1 can be undertaken by investigating the influence of the reaction time on the percent aldehyde yield and the n/b ratio at higher phosphorus/rhodium ratios (between 8/1 and 10/1) which would give a better understanding of the catalytic activity of this polymer supported catalyst. Another possible extension of the work would be to investigate the recyclability of this polymeric catalyst which is of crucial commercial importance. Further investigation of the structure of the active catalyst using electronic spectroscopy could offer an explanation for the high n/b ratio obtained with the use of this catalyst.

7.0 References

- (1) Clagett, D. C. in *Encyclopedia of Polymer Science and Engineering*; H. F. Mark, N. M. Bikales, C. G. Overberger and G. Menges, Ed.; John Wiley and Sons: New York, 1986; Vol. 6; pp 94.
- (2) Johnson, R. N. in *Encyclopedia of Polymer Science and Technology*; N. M. Bikales, Ed.; John Wiley and Sons: New York, 1969.
- (3) Johnson, R. N.; Famham, A. G., *J. Polym. Sci., Polym. Chem. Ed.* **5**, 2415 (1967).
- (4) Searly, O. B.; Pfeiffer, R. H., *Polym. Eng. Sci.* **25** , 474 (1985).
- (5) Patai, S. in *The Chemistry of the Ether Linkage*; Interscience: London, 1967.
- (6) Carlier, V.; Devaux, J.; Legras, R.; McGrail, P. T., *Macromolecules* **25**, 6646-6650 (1992).
- (7) Finkbeiner, H. L.; Hay, A. S.; White, D. M. in *High Polymers*; C. E. Schildknecht and I. S. Skeist, Ed.; John Wiley and Sons, Inc.: New York, 1977; Vol. 29; pp 537.
- (8) Aycock, D.; Abolins, V.; White, D. M. in *Encycl. Poly. Sci. and Eng.*; J. Kroschwitz, Ed.; 1988.
- (9) Altwood, T. E.; Newton, A. B.; Rose, J. B., *Br. Polym. J.* **4**, 391 (1972).
- (10) Rose, J. B. in *Recent Advances in Mechanistic and Synthetic Aspects of Polymerization*; 1987, pp 207.

- (11) Kwiatkowski, G. T.; Colon, I.; El-Hibri, M. J.; Matzner, M., *Makromol. Chem. Macromol. Symp.* **54/55**, 199 (1992).
- (12) Stamatoff, A., *US Pat.* 228, 910 (1966).
- (13) Stamatoff, A., *French Pat.* 1, 301, 174 (1966).
- (14) Kricheldorf, H. R.; Delius, U.; Tonnes, K. U., *New Polymeric Mater.* **1**(2), 127 (1988).
- (15) Kricheldorf, H. R.; Brier, G., *Polymer* **25**, 1151 (1984).
- (16) March, J. in *Advanced Organic Chemistry: Reactions, Mechanisms, and Structure*; 4th ed.; John Wiley & Sons: 1992, pp 641.
- (17) Meisenheimer, *Liebigs Ann. Chem.* **323**, 205 (1902).
- (18) Miller, J. A. in *Aromatic Nucleophilic Substitution*; Elsevier: London, 1968, pp 61-136.
- (19) Bunnett, J. F.; Zahler, R. E., *Chem. Rev.* **49**, 273 (1951).
- (20) Beck, J. R., *Tetrahedron* **34**, 2057 (1978).
- (21) Parker, A. J., *Q. Rev.*, 163 (1962).
- (22) Johnson, R. N.; Farnham, A. G.; Clendinning, R. A.; Hale, W. F.; Merriam, C. N., *J. Polym. Sci. A-1* **5**, 2375 (1967).
- (23) Williams, F. J.; Donahue, P. E., *J. Org. Chem.* **42**, 3414 (1977).
- (24) Viswanathan, R.; Johnson, B. C.; McGrath, J. E., *Polymer* **25**, 1927 (1984).

- (25) Famham, A. G.; Robeson, L. M.; McGrath, J. E., *J. Appl. Poly. Sci.* **26**, 373 (1975).
- (26) Hartmann, L. A., *Chem. Abstr.* **91**, 75088 (1979) (*US Pat.* 4 156 068).
- (27) Mohanty, D. K.; Hedrick, J. L.; Gobetz, K.; Johnson, B. C.; Yilgor, L.; Yilgor, E.; Yang, R.; McGrath, J. E., *Polym. Prepr., Am. Chem. Soc., Div. Polym. Chem.* **23**, 284 (1982).
- (28) Blinne, G.; Cordes, C., *Chem. Abstr.* **90**, 138421 (1979) (*Ger. Pat.* 2 731 816 (1979)).
- (29) Carothers, W. H., *Trans. Faraday Soc.* **32**, 39 (1936).
- (30) Patai, S. in *The Chemistry of Organophosphorus Compounds*; John Wiley & Sons: Chichester, 1990; Vol. 1 and 2.
- (31) Corbridge, D. E. C. in *Inorganic Chemistry*; Elsevier: Amsterdam, 1985; Vol. 6.
- (32) Bailey, W. J.; Muir, W. M.; Marktscheffel, F., *J. Org. Chem.* **27**, 4404 (1962).
- (33) Gann, R. G.; Dipert, R. A.; Drews, M. J. in *Encyclopedia of Polymer Science and Engineering*; Wiley-Interscience: New York, 1987; Vol. 7, pp 154.
- (34) Maiti, S.; Banerjee, S.; Palip, S. K., *Prog. Polym. Sci.* **18**, 227-261 (1993).
- (35) Larsen, E. R.; Ludwing, R. B., *J. Fire Flammability* **10**, 69 (1979).
- (36) Aaronson, A. M. in *Phosphorus Chemistry: Developments in American Science*; American Chemical Society: New York, 1992; Vol. 486, pp 218.
- (37) Weil, E. D. in *Phosphorus-Containing Polymers*; Wiley & Sons: New York, 1984; Vol. 11, pp 96.

- (38) *Fire Retardancy of Polymeric Materials*; Marcel Dekker Inc.: New York, 1979; Vol. 5.
- (39) a) *Flame Retardant Polymeric Materials*; Plenum Publishing Corp.: New York, 1982; Vol. 3.
- b) Smith, C. D.; Grubbs, H. J.; Gungor, A.; Wescott, J.; Liptak, S. C.; Wood, P. A.; McGrath, J. E., *Proceedings of the International Conference for the Promotion of Advanced Fire Resistant Aircraft Interior Materials*, 159-174 (1993).
- (40) Korshak, V. V., *J. Polym. Sci.* (1958).
- (41) Morgan, P. W.; Herr, B. C., *J. Amer. Chem. Soc.* **74**, 4526 (1952).
- (42) Morgan, P. W., *US Pat.* 2646420 (to DuPont) (1953).
- (43) Varma, I. K.; Rao, B. S., *J. App. Polym. Sci.* **28**, 2805 (1983).
- (44) Korshak, V. V.; Frunze, T. M.; Kurashev, V. V.; Medved, T. Y.; Polikarpov, Y. M.; Hu, C. M.; Kabachnik, M. I., *Chem. Abstr.* **62**, 6507 (1965).
- (45) Medved, T. Y.; Frunze, T. M.; Mei, K. C.; Kurashev, V. V.; Korshak, V. V.; Kabachnik, M. I., *Polym. Sci. USSR* **5**, 386 (1964).
- (46) Varma, I. K.; Fohlen, G. M.; Parker, J. A., *J. Polym. Sci., Polym. Chem. Ed.* **21**, 2017 (1983).
- (47) Varma, I. K.; Fohlen, G. M.; Parker, J. A., *J. Macromol. Sci., Chem.* **A19**, 209 (1983).
- (48) Smith, C. D.; Grubbs, H.; Webster, H. F.; Gungor, A.; Wightman, J. P.; McGrath, J. E., *High Performance Polymers* **3**, 211 (1991).

- (49) Green, J. C.; King, D. I.; Eland, J. H. D., *Chem. Commun.*, 1121 (1970).
- (50) Cotton, F. A.; Wilkinson, G. in *Advanced Inorganic Chemistry*; third ed.; Interscience: New York, 1988, pp 720.
- (51) Angelici, R. J.; Ingewanson, C. M., *Inorg. Chem.* **8**, 83 (1969) .
- (52) Angelici, R. J., *J. Inorg. Nucl. Chem.* **28**, 2627 (1966).
- (53) Marynick, D. S.; Askari, S.; Nickerson, D. F., *Inorg. Chem.* **24**, 868 (1985).
- (54) Marynick, D. S., *J. Am. Chem. Soc.* **106**, 4064 (1984).
- (55) Parshall, G. W.; Ittel, S. D. *Homogeneous Catalysis*; 2nd. ed.; John Wiley & Sons, Inc.: New York, 1992.
- (56) Karayannis, N. M.; Mikulski, C. M.; Pytlewski, L. L., *Inorg. Chi. Acta, Rev.*, 69 (1971).
- (57) Cotton, F. A.; Barnes, R. D.; Barnnister, E., *J. Chem. Soc.*, 2199 (1960).
- (58) Holm, R. H.; Cotton, F. A., *J. Chem. Phys.* **32**, 1168 (1960).
- (59) Goodgame, D. M. L.; Cotton, F. A., *J. Chem. Soc.* **1961**, 2298 (1961).
- (60) Cotton, S. A.; Gibson, J. F., *J. Chem. Soc. A*, 859 (1971).
- (61) Kolawole, E. G.; Mathieson, S. M., *J. Polym. Sci. Polym. Chem. Ed.* **15**, 2291 (1977).
- (62) Dirk, C. W.; Schoch, K. F., Jr.; Marks, T. J. in *Polymer Science and Technology*; R. B. Seymour, Ed.; Plenum Press: New York, 1981; Vol. 15; pp 209.

- (63) Bigg, D. M.; Bradbury, E. J. in *Conductive Polymers*; Plenum: New York, 1981, pp 23-28.
- (64) Blythe, A. R. in *Electrical Properties of Polymers*; Cambridge University Press: Cambridge, 1979, pp 123-132.
- (65) Berlin, A. A., *Russ. Chem. Rev.* **48**, 1125 (1979).
- (66) Wohrle, D., *Adv. Polym. Sci.* **50**, 45 (1983).
- (67) Hanack, M.; Datz, A.; Fay, R.; Fischer, K.; Keppeler, U.; Koch, J.; Metz, J.; Mezger, M.; Schneider, O.; Schulze, H. in *Handbook of Conducting Polymers*; T. A. Skotheim, Ed.; Marcel Dekker, Inc.: New York, 1986; Vol. 1; pp 133.
- (68) Hatfield, W. E. in *Conductive Polymers*; Plenum: New York, 1981.
- (69) *Filled Polymers- Properties and Applications*; Marcel Dekker, Inc.: New York, 1986.
- (70) Chen, I. G.; Johnson, W. B., *J. Mater. Sci.* **26**, 1565 (1991) .
- (71) Wessling, B., *Synth. Met.* **45**, 119-149 (1991).
- (72) Wnek, G. E. in *Handbook of Conducting Polymers*; T. A. Skotheim, Ed.; Marcel Dekker, Inc.: New York, 1986; Vol. 1; pp 205.
- (73) Angelo, R. J., *US Pat.* 3,073,785 (1959) (to Dupont).
- (74) St. Clair, A. K.; Taylor, L. T., *J. Appl. Polym. Sci.* **18**, 2393-2400 (1983).
- (75) St. Clair, S. T.; Taylor, L. T., *J. Appl. Polym. Sci.* **28**, 2393-2400 (1983).
- (76) Taylor, L. T.; Rancourt, J. D. in *Inorganic and Metal-Containing Polymeric Materials*; Plenum Press: New York, 1990, pp 109.

- (77) Madeleine, D. G.; Spillane, S. A.; Taylor, L. T., *J. Vac. Sci. Technol.* **A5**, 347 (1987).
- (78) Wohlford, T. L.; Schaft, J.; Taylor, L. T.; St. Clair, A. K.; Furtch, T. A.; Khor, E. in *Conductive Polymers*; R. B. Seymour, Ed.; Plenum: New York, 1981.
- (79) Bergmeister, J. J.; Racourt, J. D.; Taylor, L. T., *Chem. Mater.* **2**, 640 (1990).
- (80) Khor, E.; Taylor, L. T. in *Metal-Containing Polymeric Systems*; C. E. Carraher Jr. and C. U. Pittman Jr., Ed.; Plenum: New York, 1985; pp 367.
- (81) Kakinoki, H.; Sumita, O.; Cho, C. S.; Higashi, F., *J. Polym. Sci. Polym. Lett. Ed.* **14**, 407 (1976).
- (82) Higashi, F.; Cho, C. S.; Kakinoki, H., *J. Polym. Sci. Polym. Chem. Ed.* **17**, 313-318 (1979).
- (83) Sumita, O.; Fukuda, A.; Kuze, E., *J. Polym. Sci. Polym. Phys. Ed.* **18**, 877-890 (1980).
- (84) Sumita, O.; Fukuda, A.; Kuze, E., *J. Appl. Polym. Sci.* **23**, 2279-2291 (1979).
- (85) Sumita, O.; Fukuda, A.; Kuze, E., *J. Polym. Sci. Polym. Phys. Ed.* **16**, 1801-1815 (1978).
- (86) Jenekhe, S. A.; Roberts, M. F., *Macromolecules* **26**, 4981-4983 (1993).
- (87) Jenekhe, S. A.; Johnson, P. O.; Agrawal, A. K., *Polym. Mater. Sci. Eng.* **60**, 404-409 (1989).
- (88) Jenekhe, S. A.; Johnson, P. O.; Agrawal, A. K., *Macromolecules* **22**, 3216-3222 (1989).

- (89) Roberts, M. F.; Jenekhe, S. A., *Chem. Mater.* **2**, 224-226 (1990).
- (90) Roberts, M. F.; Jenekhe, S. A., *Macromolecules* **24**, 3142-3146 (1991).
- (91) Bianchi, E.; Ciferri, A.; Tealdi, A.; Torre, R.; Valenti, B., *Macromolecules* **7**, 495 (1974).
- (92) Acierno, D.; Bianchi, E.; Giferri, B.; de Cindio, B.; Migliaresi, C.; Nicolais, L., *J. Polym. Sci., Polym. Symp.* **54**, 259 (1976).
- (93) Acierno, D.; La Mantia, F. P.; Titomanlio, G., *J. Polym. Sci., Polym. Phys. Ed.* **18**, 739-744 (1980).
- (94) Forsyth, M.; Shriver, D. F.; Ratner, M. A.; DeGroot, D. C.; Kannewurf, C. R., *Macromolecules* **5**, 1073-1077 (1993).
- (95) Wetton, R. E.; James, D. B.; Whiting, W., *J. Polym. Sci., Polym. Lett. Ed.* **14**, 577-583 (1976).
- (96) Rabek, J. F.; Lucki, J.; Qu, B. J.; Shi, W. F., *Macromolecules* **24**, 836-843 (1991).
- (97) Moacanin, J.; Cuddihy, E. F., *J. Polym. Sci. Polym. Phys. Ed.* **14**, 313-322 (1966).
- (98) Agnew, N. H., *J. Polym. Sci., Polym. Chem. Ed.* **14**, 2819-2830 (1976).
- (99) Card, R. J.; Neckers, D. C., *J. Amer. Chem. Soc.* **99**, 7733 (1977).
- (100) Neckers, D. C. in *Metal-Containing Polymeric Systems*; J. E. Sheats, C. E. Carraher Jr. and C. U. Pittman Jr., Ed.; Plenum Press: New York, 1985; pp 385.
- (101) Berger, M.; Manuel, T. A., *J. Polym. Sci.* **4**, 1509-1516 (1966).

- (102) Block, B. P.; Rose, S. H.; Schaumann, C. W.; Roth, E. S.; Simkin, J., *J. Amer. Chem. Soc.* **85**, 2018 (1963).
- (103) Davydova, S. L.; Plate, N. A., *Coord. Chem. Rev.* **16**, 195-225 (1975).
- (104) Carraher, C. E. in *Metal-Containing Polymeric Systems*; J. E. Sheats, C. E. Carraher Jr. and C. U. Pittman Jr., Ed.; Plenum Press: New York, 1985.
- (105) Schmuckler, G. in *Encyclopedia of Polymer Science and Technology*; Interscience: New York, 1977; Vol. Suppl. Vol. 2, pp 197.
- (106) Merrifield, R. B., *J. Am. Chem. Soc.* **85**, 2149 (1963).
- (107) Holy, N. L. in *Homogeneous Catalysis with Metal Phosphine Complexes*; L. H. Pignolet, Ed.; Plenum Press: New York, 1983.
- (108) Hartley, F. R. in *Supported Metal Complexes: A New Generation of Catalysts*; Reidel: Dordrech, 1985.
- (109) Imanaka, T.; Kaneda, K.; Teranishi, S.; Terasawa, M., *Proc. 6th Int. Congr. Catal.* **A-41**, 509 (1976).
- (110) Terasawa, M.; Kaneda, K.; Imanaka, T.; Teranishi, S., *J. Catalysis* **51**, 406 (1978).
- (111) Bergbreiter, D. E. in *Functional Polymers (Proc. Annu. IUCCP Symp.)*; D. E. Bergbreiter and C. R. Martin, Ed.; Plenum: New York, 1989.
- (112) Pittman, C. U., Jr.; Ng, Q. Y., *J. Organometal. Chem.* **153**, 85 (1978).
- (113) Pittman, C. U. in *Comprehensive Organometallic Chemistry: the Synthesis, Reactions, and Structures of Organometallic Compounds*; G. Wilkinson, E. W. Abel and F. G. A. Stone, Ed.; Pergamon Press: New York, 1982; Vol. 8.

- (114) Allum, K. G.; Hancock, R. D., *J. Organometal. Chem.* **87**, 189 (1975).
- (115) a) Smith, C. D. *et al.*, *High Performance Polymers* **4**, 211 (1991).
 b) Smith, C. D.; Gungor, A.; Wood, P. A.; Liptak, S. C.; Grubbs, H.; Yoon, T. H.; McGrath, J. E., *Makromol. Chem., Macromol. Symp.* **74**, 185 (1993).
- (116) Jurek, M. J.; McGrath, J. E., *Polymer* **30**, 1552 (1989).
- (117) Smith, C. D., Ph. D. Thesis, Virginia Polytechnic Institute and State University, 1991.
- (118) Drago, R. S.; Calson, R. L.; Purcell, K. F., *Inorg. Chem.* **4**, 15 (1965).
- (119) Waghorne, W. F.; Rubalcava, H., *J. Chem. Soc., Faraday Trans., 1*, **78**, 1199 (1982).
- (120) LaMar, G. N.; Horrocks, W. D.; Holm, R. H., Jr. in *NMR of Paramagnetic Molecules*; Academic Press: New York, 1973.
- (121) Crabtree, R. H. in *The Organometallic Chemistry of the Transition Metals*; John Wiley & Sons: New York, 1988, pp 225.
- (122) Krugh, T. R. in *Molecular Biology. An International Series of Monographs and Textbooks*; L. J. Berliner, Ed.; Academic Press: New York, 1976; pp 339.
- (123) Marsi, K. L., *J. Org. Chem.* **39**, 265 (1974).
- (124) Marsi, K. L., *J. Am. Chem. Soc.* **91**, 4724 (1969).
- (125) Steininger, E.; Sander, M., *Kunststoffe* **54**, 507 (1964).
- (126) Toth, I.; Hanson, B. E.; Davis, M. E., *Catal. Lett.* **8**, 209 (1991).

- (127) Bartik, T.; Bartik, B.; Hanson, B. E., *Mol. Catal.* **88**, 43 (1994).
- (128) Pittman, C. U., Jr.; Hanes, R. M., *J. Am. Chem. Soc.* **98**, 5402 (1976).
- (129) Yee, A. F.; Smith, S. A., *Macromolecules* **14**, 54 (1980).

Vita

Elena Bonaplata Revilla was born in Jerez de la Frontera, Spain on August 19, 1969. She entered The College of William and Mary in August, 1989 and graduated Summa Cum Laude with a Bachelor in Science in Chemistry in May 1992. The author then entered the graduate program in Chemistry at Virginia Polytechnic Institute and State University in August, 1992. Under the direction of Dr. James E. McGrath, Elena began her thesis research centered on the study of complexation of metal salts with phosphorus-containing poly(arylene ether)s. The author received her Master of Science in Chemistry with an emphasis in polymer science in May, 1994.